Study on Photoregulation of DNA Hybridization by Introducing Modified Azobenzene

(修飾アゾベンゼン導入による DNA ハイブリダイゼーションの光制御に関する研究)

NISHIOKA Hidenori
西岡　英則
2011

Table of contents

Chapter 1. General Introduction

1-1 Properties of DNA duplex

DNA, deoxyribonucleotide is composed of four nucleotides called adenosine (A), thymine (T), guanine (G) and cytosine (C) and these nucleotide bind each other by phosphodiester bound. These four nucleotides can form pairs by hydrogen bound: A-T and G-C pairs. Therefore, DNA strands which are complementary each other can form duplex. In addition, in the DNA duplex, the base pairs sited parallel each others, and inter act each other by π-π interaction (stacking effect). Therefore, DNA duplex has beautiful regularities:[1] 1) the distance between base pairs is 3.4 Å; 2) the duplex is right-handed helix; 3) the adjacent base pairs twisted 36 ^{o} each other, so every ten base pairs, the duplex turns one time; 4) the duplex is reasonable rigid more than single-stranded DNA.[1] In addition, 5) only designing the sequence, several complex strictures can be created; 6) with the development of phosphoroamidite chemistry, arbitral sequences can be made and non-natural molecule also can be introduced in DNA sequence; and 3) DNA has high affinity for biological system.

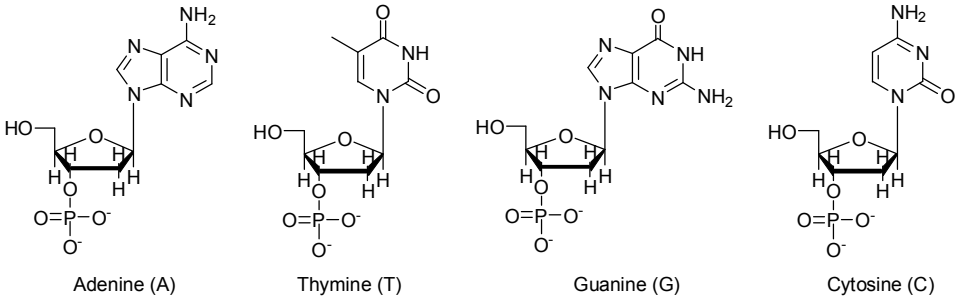

Figure 1-1. Structures of nucleotides composing DNA.

1-2 DNA applications and controlling of its functions

Recently, to focus on the advantages of DNA deceived in **1-1**, DNA has come to be regarded not only as a carrier of genetic information but as an excellent nanomaterial. The studies in which DNA was used as nanomaterial reported by several groups.[2] For example, Rothemund *et al.* reported "DNA origami" in which DNA was used as a nano material for constructing nano ordered structures.[2-a] Furthermore, some DNA nono devices which can perform mechanical motion have reported. For example, Yurke *et al.* demonstrated the first DNA machine that functioned as "tweezers" fuelled by two strands of DNA with tailored complimentarily.[2-b] As the energy for operating this DNA nanomachine is produced by a strand-exchange strategy. On the other hand, Shin *et al.* reported "walker" also fuelled by DNA. By using DNA walker, they also succeeded in transporting gold micro particle.[2-c] In both "DNA tweezers" and "DNA walker", DNA was used not only as structural materials but also as "fuel" of mechanical motion. However, for example in the case of DNA fueled tweezers, waste DNA duplexes were

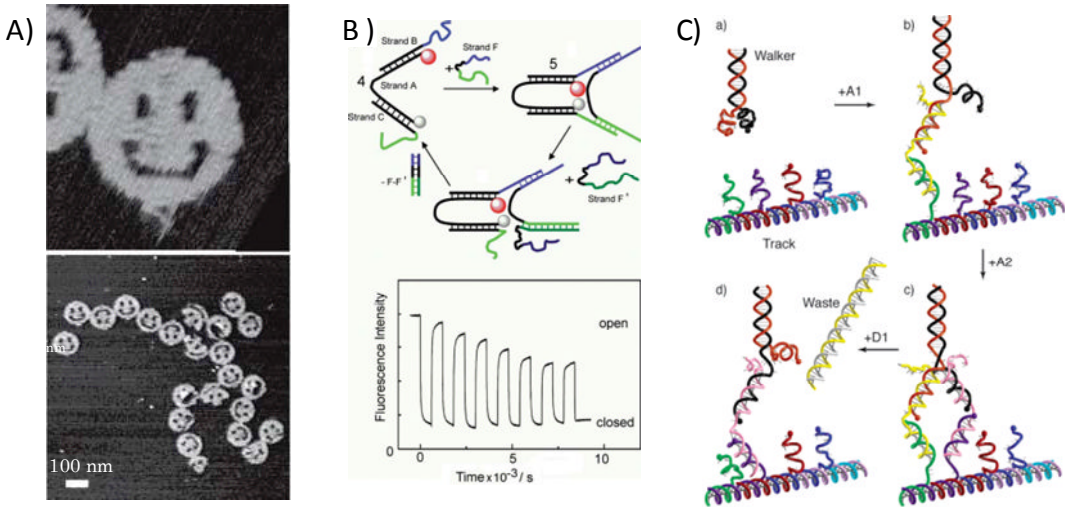

Figure 1-2. Examples of DNA nano technology. A) DNA origami[2-a] reported by Rothemund et al., B) DNA tweezers[2-b] reported by Yurke et al. and C) DNA walker[2-c] reported by Shin et al. All figures were shown in references.

accumulated in the system. Therefore, the working efficiencies decreased after several time regulations (Figure 1-2B).

Yan *et al.* also report DNA fueled structure changing.[2-d] In this study, they prepared two times crossed two DNA duplex. By selecting the added DNA strand, they succeeded in increasing the number of crossed point or not (Figure 1-3A). In addition, by strand-exchange strategy, the number of crossed point can be changed. Moreover, they also succeeded in regulating of more large structure by using this strategy. In this study, they modified the "fuel DNA" by biotin to remove the waste DNA duplex from the regulation system. The decrease of the regulation efficiency could be kept off, however, biotin labeling of DNA requires cumbersome handling.

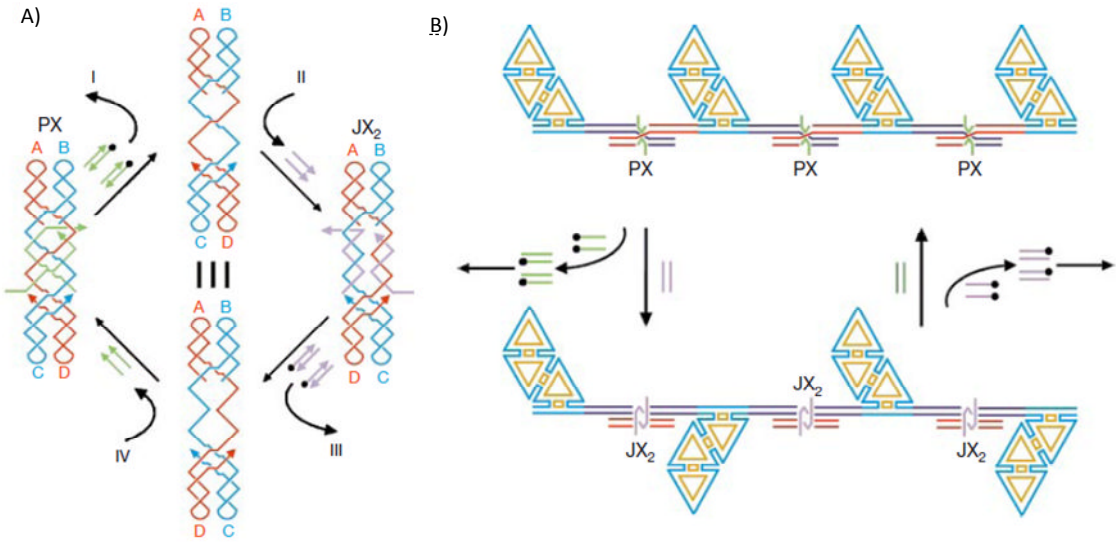

Figure 1-3. Controlling the topology of DNA and the DNA nanostructure reported by Sherman *et.al*. (A) By selecting the added DNA strand (green or blue), two conformations could be selected (PX or JX_2). (B) By changing the conformation between PX and JX_2, The DNA nanostructure could be regulated. All figures were shown in references.

Although several nano devices composed of DNA has been reported, since achievable performance is still limited with only four natural nucleotides. In order to

overcome the limit and enhanced the possibility of DNA, a variety of functional DNAs involving non-natural molecules have been proposed.[3, 4] For example, Kruger *et al.* reported Size-Expanded DNAs.[3] In this study, they synthesized size expanded nucleotides, and synthesized artificial DNA strands involving size expanded nucleotide. To hybridize these DNA strands, they get new DNA duplex in which the distance between back born of each other was longer than that of natural DNA.

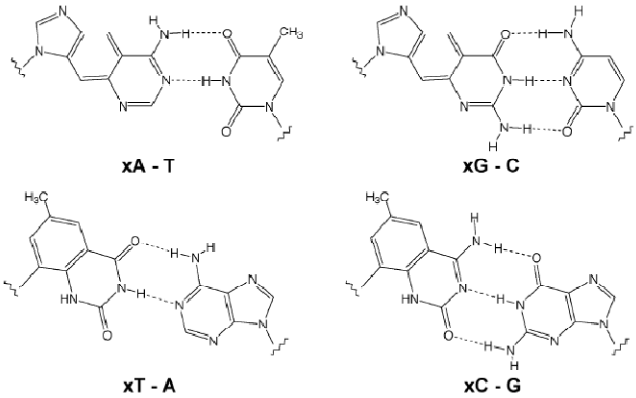

Figure 1-4. Structure of Size-Expanded nucleotides reported by Kruger et al. Figure shown in reference.

In addition, by introducing non-natural molecules in DNA, the function of DNA as genetic carrier has also regulated.[4] For example, Kröck *et al.* reported the photo activation of transcription reaction of the T7 polymerase.[4-a] In this study, they introduced caged thymine in the T7 promoter region which was recognized by the T7 polymerase. The promoter region including caged thymine, so the T7 promoters could not transcribe and synthesize mRNA. By right irradiation, the caging compound released and caged thymine turned to natural Thymine. As a result, T7 polymerase transcribed the mRNA. Another photoregulation of biological reaction was reported by Young *et al*. In this study, they used another type of caged Thymine (Figure 1-5) to

control the translation by regulate DNA/RNA hybridization.[4-b] First, antisense agent including caged thymine could not hybridize with mRNA, so the translation was occurred. On the other hand, by light irradiation, the caging compound released and caged thymine turned to natural thymine and antisense agent DNA formed duplex with mRNA. As a result, the translation was silenced.

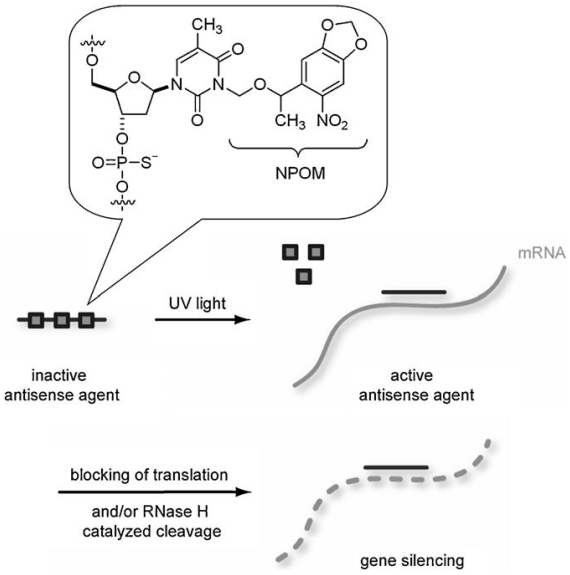

Figure 1-5. Model of photoregulation of translation in cell[4-b] reported by Young *et al*. The figure was shown in references.

1-3 Photo irradiations as external stimulus for controlling bio molecules

As external stimulus, photo irradiation has several advantages compared with another method: 1) photo irradiation can be carried out for specific position and any time we want; 2) photo irradiation does not cause contamination for the system, so several times regulations would be possible; and 3) by churning the photo responsive molecule and wavelength, a variety of regulation would be possible. Therefore, a variety of photoregulation of bio molecule or biological reaction including not only DNA but also other bio molecule were reported.[5] For example, Hiraoka *et al.* reported

photo activation of enzymatic reaction by introducing caged amino acid into active site of enzyme RNase S′.[5-a] The modified RNase S′ did not have cleavage activity. On the other hand, with light irradiation, the caging compound released so the RNase S′ recovered the cleavage activity. Furthermore, Woolley *et al.* also reported photoregulation of protein activity.[5-b, c, d,] In this study, they used azobenzene as reversible photo switch. They cross-linked the amino acid residues (cysteine) in protein to regulate the secondary or tertiary structures. By the isomerization of azobenzene induced by photoirradiation, the higher-structure formed or destroyed. In this study, they photo regulated the α-helix structure of DNA-binding protein. With UV light irradiation, azobenzene isomerizes to *cis*-form and α-helix was formed. As a result, two subunits of DNA-binding protein assembled and bound DNA duplex. On the other hand, without UV light irradiation, azobenzene took *trans*-form and α-helix was destroyed. As a result, DNA binding protein could not bind DNA duplex.

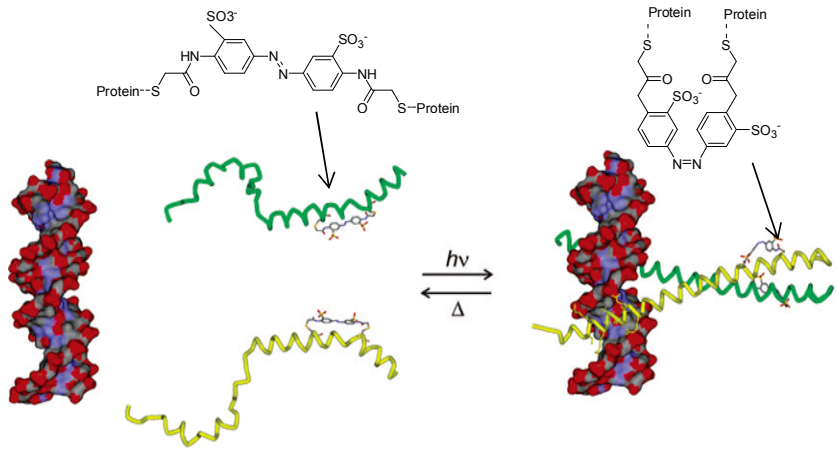

Figure 1-6. Model of photoregulation of activity of DNA binding protein[5-d] reported by Woolley *et al.* Figure was shown in reference.

Schierling *et al.* reported photoregulation of restriction enzyme by light.[5-e] They also introduced azobenzene moieties into peptides and regulated its active formation of

enzyme (Figure 1-7A, B). As a result, they succeeded in reversible photoregulation of the activity of enzyme by light irradiation (Figure 6B).

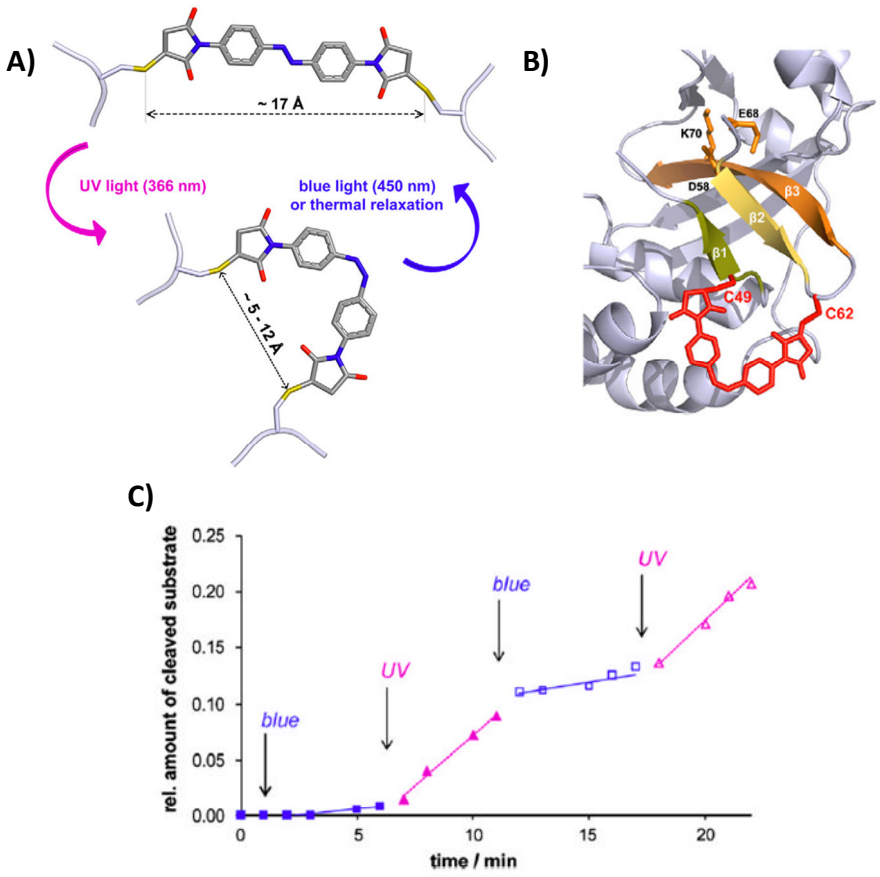

Figure 1-7. Photoregulation of restrict enzyme activity by introducing azobenzene reported by Schierling *et al.* Figure was shown in reference.

1-4 Reversible photo regulation of DNA function

In the case of using DNA as a nano material, especially for constructing DNA devices which can do mechanical motion, reversible regulation of DNA hybridization would be required. As described above, some DNA devices (DNA tweezers or DNA walker) which can do mechanical motion have reported. However, because these devices using strand exchange as energy, a DNA duplex is produced as a waste product in every working cycle, thereby, after several time working cycles, waste product

accumulates in the system. Therefore, working efficiency decreases after several times working.[2-b, c] Reversible regulation of DNA hybridization with photoirradiation would be expected to overcome this limit because photoirradiation does not cause contamination and has several advantages shown in previous section (**1-3**). For the reversible photoregulation of DNA hybridization, "photo switch" was needed because DNA itself cannot response the photo irradiation. As a photo switch, three typical molecules are widely used: A) stilben,[6] B) spiropyran[7] and C) azobenzene.[8]

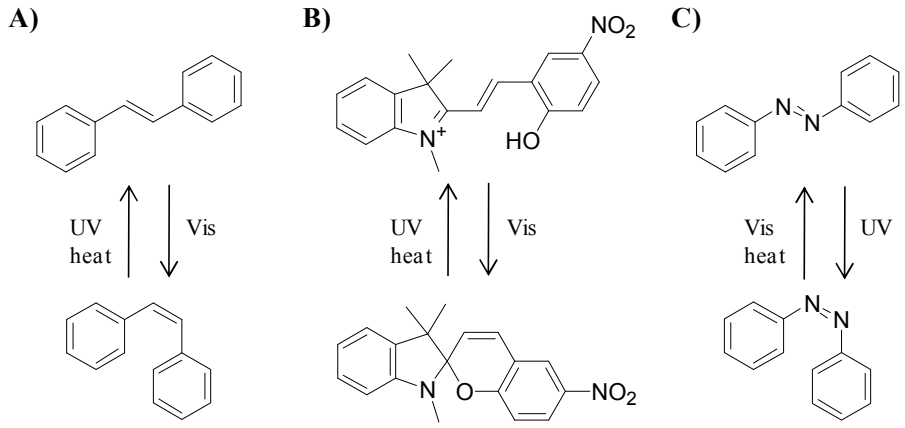

Figure 1-8. Structures and photochromism of A) stiliben, B) spiropyren and C) azobenzene.

Photoregulation of DNA hybridization by introducing these molecules has reported by several groups. For example, Ogasawara *et al.* reported reversible photoregulation of DNA hybridization with stilben derivatives.[6] In this study, they modified guanine with stilben derivatives. The modified guanine they synthesized can photo isomerize between *trans*- and *cis*-form reversible. As a result, they succeed in photoregulation of DNA hybridization. Asanuma *et al.* reported photoregulation of DNA hybridization introducing spiropyran.[7-a] In addition, Anderson et al. reported photoregulation of DNA hybridization.[7-b]

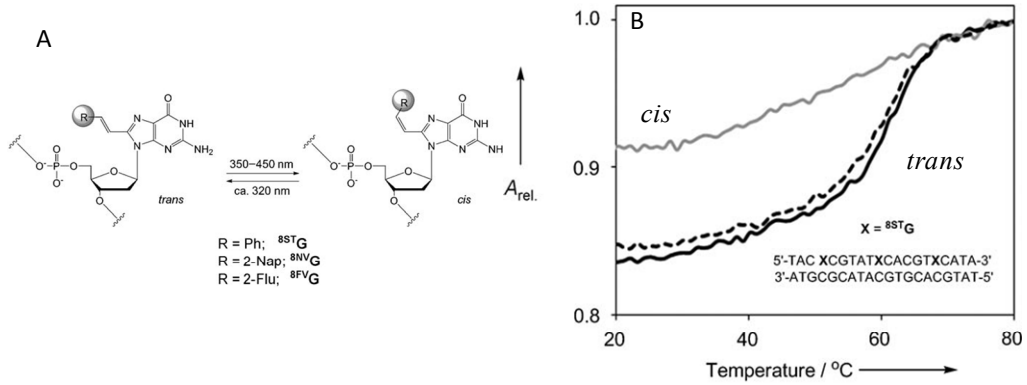

Figure 1-9. Photoregulation of DNA hybridization[6] reported by Ogasawara *et al.* A) The modified nucleotide and b) the T_m curves of duplex involving either *trans*- (black sold line) or *cis*-form (gray line) Black dot line showed the T_m curves of duplex involving *trans*-form of nucleotides isomerized *cis*- to *trans*-form again. These figures showed in reference.

In our laboratory, we focused on azobenzene as a photo switch for photoregulation of DNA or RNA functions because azobenzene has several advantage as a photo switch: 1) photoisomerization induces planar/nonplanar structural changes that crucially affect duplex stability;[8-a] 2) unlike other photoresponsive molecules such as spiropyran,[7] azobenzenes are sufficiently stable in water so that repeated photo-irradiation does not cause deterioration or unfavorable chemical reactions; and 3) facile synthetic procedures allow a variety of modifications of azobenzene that can diversify the photoswitching properties.[9]

1-5 Present study

In this study, photoregulation efficiency of DNA hybridization was improved by modifying azobenzene. Photoregulation of DNA hybridization only with visible region light was archived with newly synthesized azobenzene derivative. In addition, DNA nanomachine driven by light irradiation was constructed by using photoresponsive DNA involving azobenzene moieties. The prosperities of modified azobenzene derivatives

were also investigated. Especially, the *cis*-to-*trans* thermal isomerization was investigated.

In Chapter 2, the effect of chemical modification of azobenzene for the photoregulation efficiency of DNA hybridization was investigated. By modification of *ortho*-positions of azobenzene, the photoregulation efficiency was improved. Especially for the methylation of two *ortho*-positions of distal benzene ring of azobenzene (**2′,6′-Me-Azo**), photoregulation efficiency was dramatically improved. The dependency of photoregulation efficiency of **2′,6′-Me-Azo** on adjacent base-pairs was also investigated. In addition, the mechanism of efficient photoregulation by *ortho*-modified azobenzene was investigated from the NMR analysis and computer modeling.

In Chapter 3, the photoisomerization of modified azobenzene derivatives tethered into DNA was investigated. In the case of modification of two *ortho*-positions, *trans*-to *cis*-photoisomerization was inhibited, whereas *cis*-to-*trans* photoisomerization was not inhibited. In the case of **2′,6′-Me-Azo** tethered into DNA duplex, the rate of *cis*-form after UV light irradiation decreased compared with in single-stranded DNA. The thermal stability of *cis*-azobenzene was improved by modification of both *ortho*-positions of distal benzene ring: **2′,6′-Me-Azo** was about ten times as long as non-modified azobenzene (**Azo**). For investigating the mechanism of the improvement of thermal stability, several *ortho*-modified azobenzene derivatives were synthesized and the dependence of the half lives of *cis*-azobenzenes on the polarity of solvents.

In chapter 4, photoregulation of DNA hybridization only with visible light was archived by introducing **Thio-DMAzo** in which methylthio group was introduced at

para-position and methyl groups were introduced at the *ortho*-positions of distal benzene ring. The photoregulation efficiency of **Thio-DMAzo** was as same as that of **2′,6′-Me-Azo**. The thermal stability of **Thio-DMAzo** was as high as **Azo** although the electro donating methylthio group was introduced at the *para*-position.

In Chapter 5, photoregulation of DNA hybridization irradiated at fixed temperature was directly observed with the change of fluorescence intensity by introducing fluorescence and quencher at the end of DNA. In the case of introducing twelve **Azo** moieties into twenty bases DNA, the photoregulation efficiency was decreased compared with that of involving five **Azo** moieties because the stability of DNA involving *trans*-**Azo** moieties was decreased. On the other hand, introducing twelve **2′,6′-Me-Azo** moieties into same DNA, efficient photoregulation of DNA hybridization was archived at wide range of temperatures because the stability of DNA involving *trans*-**Azo** moieties was not decreased.

In Chapter 6, photo driven DNA nanomchine (DNA tweezers) was created by using photoresponsive DNA involving **Azo**. The tweezers worked with UV and visible light irradiation. The working efficiency of tweezers was not decreased after several times work because light irradiation did not cause any damage in the regulation system. In addition by using **Azo** and **Thio-DMAzo**, the formation and dissociation of DNA duplex could be regulated independently because theses azobenzenes can isomerize independently by selecting irradiation light wavelength.

1-6 Notes and References

[1] C. Branden, J. Tooze, (勝部幸輝, 竹中章郎, 福山恵一, 松原央 監訳), タンパク質の構造入門 第２版, *2000*, 第 7 章, 121-125, (株式会社ニュートンプレス), and references cited therein.

[2] a) P. W. K. Rothemund, *Nature*, **2006**, 440, *297-302*. b) B. Yurke, A. J. Turberfield, A. P. Mills Jr, F. C. Simmel, J. L. Neumann, *Nature*, **2000**, *406*, 605-608. c) J-S. Shin, N. A. Pierce, *J. Am Chem. Soc.*, **2004**, *126*, 10834-10835. d) H. Yan, X. Zhiyong, Z. Shen, N. C. Seeman, *Nature*, **2002**, *415*, 62-65. e) M. K. Beissenthirtz, I. Willner, *Org. Biomol. Chem.*, **2006**, *4*, 3392-3401, and references cited therein.

[3] A. T. Krueger, H. Lu, A. H. F. Lee, E. T. Kool, *Acc. Chem. Res.*, **2007**, *40*, 141-150.

[4] a) L. Kröck, A. Heckel, *Angew. Chem. Int. Ed.*, **2005**, *44*, 471-473. b) D. D. Young, H. Lusic, M.Lively, J. A. Yoder, A. Deiters, *ChemBioChem.*, **2008**, *9*, 2937-2940.

[5] a) T. Hiraoka, I. Hamachi, Bioorg. *Chem. Lett*., **2003**, *13*, 13-15. b) J. R. Kumita, O.S. Smart, G. A. Woolley, *PNAS*, **2000**, *97*, 3803-3808. c) L. Guerrero, O. S. Smart, C. J Weston, D. C. Burns, G. A. Woolley, R. K. Allemann, *Angew. Chem. Int. Ed.*, **2005**, *44*, 7778-7782. d) G. A. Woolley, A. S. I. Jasikaran, M. Berezovski, J. P. Calarco, S. N. Krylov, O. S. Smart, J. R. Kumita, *Biochemistry*, **2006**, *45*, 6075-6084. e) B. Schierling, A-J. Noel, W. Wenda, L. T. Hien, E. Volkov, E. Kubareve, T. Oreskaya, M. Kokkinidis, A. Rompp, B.Spengler, A. Pingoud, *PNAS*, **2010**, *107*, 1361-1366. f) g) G. Mayer, A. Heckel, *Angew. Chem. Int. Ed.*, **2006**, *45*, 4900-4921, and references cited therein.

[6] S. Ogasawara, M. Maeda, *Angew. Chem. Int. Ed.*, **2008**, *47*, 8839-8842.

[7] a) H. Asanuma, K. Shirasuka, T. Yoshida, T. Takarada, X. G. Liang, M. Komiyama, *Chem. Lett.*, **2001**, 108-109. b) J. Anderson, S. Li, P. Lincoln, J. Andreasson, *J. Am. Chem. Soc.*, **2008**, *130*, 11836-11837.

[8] a) H. Asanuma, T. Takarada, T. Yoshida, D. Tamaru, X. G. Liang, M. Komiyama, *Angew. Chem., Int. Ed.* **2001**, *40*, 2671-2673. b) C. Renner, L. Moroder, *ChemBioChem* **2006**, *7*, 868-878. c) S. Yagai, A. Kitamura, *Chem. Soc. Rev.* **2008**, *37*, 1520-1529, and references cited therein.

[9] a) T. Gunnlaugsson, J. M. Kelly, M. Nieuwenhuyzen, A. M. K. O'Brien, *Tetrahedron Lett.* **2003**, *44*, 8571-8575; b) Q. Wang, L. Yi, L. Liu, C. Zhou, Z. Xi, *Tetrahedron Lett.* **2008**, *49*, 5087-5089.

Chapter 2. Effect of Alkylation of Azobenzene for the Improvement of Photoregulation Efficiency

2-1 Abstract

For the improvement of photoregulation efficiency of DNA hybridization, modified azobenzene derivatives alkylated at several positions of benzene rings were synthesized and introduced into DNA strand. Modified at *ortho*-positions with respect to the azo bond, the photoregulation efficiency based on the differences of T_m between visible light irradiation (azobenzene takes *trans*-form) and UV light irradiation (azobenzene takes *cis*-form) was improved. Especially for modification at two *ortho*-positions of distal benzene ring (both 2′ and 6′-positions), photoregulation efficiency was remarkably improved.

2-2 Introduction

As described in Chapter 1, DNA attracts much attention not only as bio molecule but also as nano material. Both as bio molecule and nano material, DNA hybridization is the key feature. In previous studies, photoregulation of DNA hybridization has be attained by introducing azobenzene into DNA via D-threoninol as a linking molecule. The photoregulation mechanism is as follows: planar *trans*-azobenzene (visible light

irradiation) is intercalated between the adjacent base-pairs and thus stabilizes the duplex, whereas non-planar *cis*-azobenzene (UV light irradiation) destabilizes the duplex by steric hindrance (Figure 2-1).[1] As previous study, it has already known that D-threoninol induce right handed helix and the length of linker to the direction of main strand is as same as that of native nucleotides. Therefore, even additional introducing *trans*-azobenzene via D-threoninol stabilizes DNA duplex. By using photo responsible DNA involving azobenzene, photoregulation of primer extension, transcription, the RNase H reaction, DNA enzyme and some DNA structure have succeeded.[2]

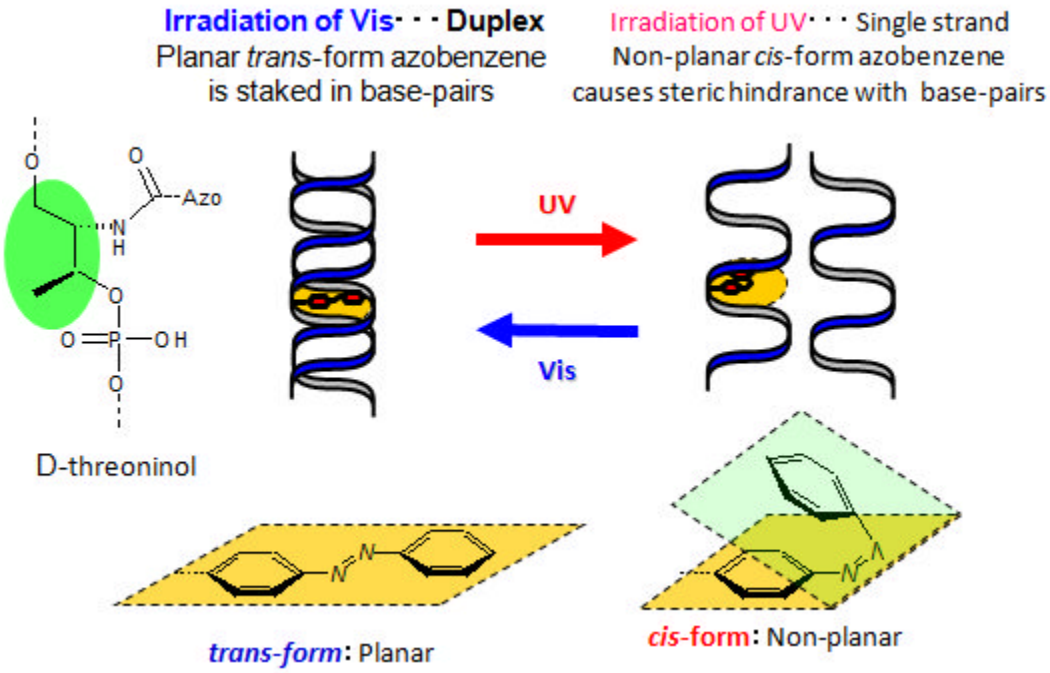

Figure 2-1. Mechanism of photoregulation of DNA hybridization by introducing azobenzene.

Since the photoregulation efficiency of one azobenzene depended on melting

temperature (ΔT_m) induced by *trans-cis* isomerization, the enhancement of ΔT_m has been crucially important in achieving still more effective photoregulation. One of the methods for raising ΔT_m is to introduce multiple azobenzene moieties.[3] For example, in previous study, by introducing nine azobenzene moieties into 20 bases DNA strand, DNA hybridization could be efficiently photoregulated. However, this causes grate change in the structure of DNA duplex far from the B-form because azobenzene moieties introduced asymmetry of DNA duplex. Such a structural change prevents the normal interaction with protein including enzyme. Therefore, improvement of photoregulation efficiency with only one azobenzene moieties is required. In order to improve the photoregulation efficiency, there are two theories: 1) further stabilizing the duplex in the *trans*-form by stacking interactions; and 2) destabilization in the *cis*-form due to steric hindrance.

In this chapter, for this purpose, several alkylated azobenzene derivatives were synthesized and photoregulation efficiencies of those azobenzene moieties based on ΔT_m was measured. In addition, in order to understand the mechanism of efficient photoregulation, NMR analysis and computer modeling were performed.

2-3 Results and Discussions

2-3-1 Photoregulation efficiency of mono-alkylation of azobenzene

Figure 2-2 showed the modified azobenzene derivatives in which one position of benzene ring was alkylated together with the DNA sequences used in this study. These azobenzene derivatives were introduced into DNA via D-threoninol as a linking molecule. The melting temperature involving both *trans*- and *cis*-azobenzene was measured by the change of absorbance at 260 nm induced by temperature change. The T_m curves DNA involving each azobenzene derivative was shown in Figure 2-3 and the values of T_m and ΔT_m were listed in Table 2-1.

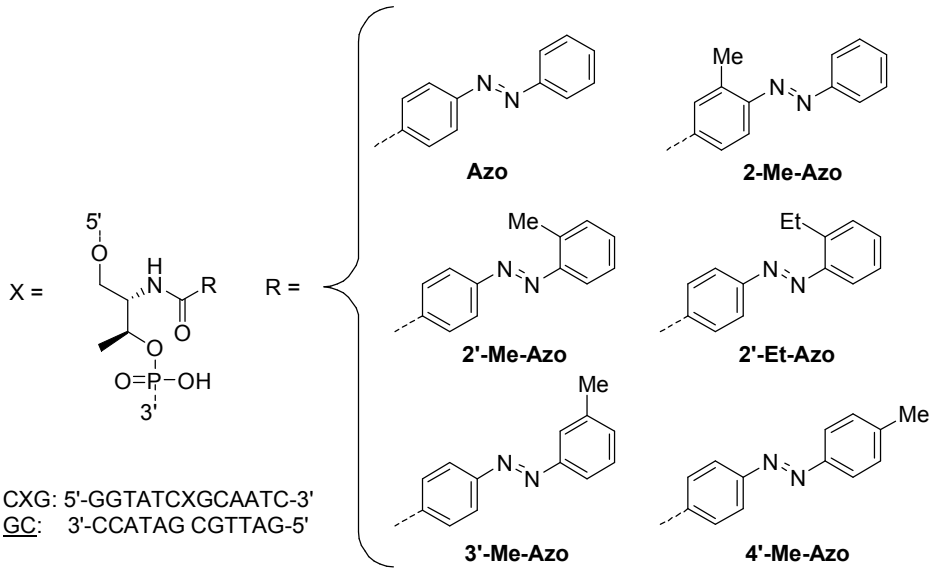

***Figure* 2-2.** Structures of mono-alkylated azobenzene derivatives and the DNA sequences. **X** indicates azobenzene and its derivatives.

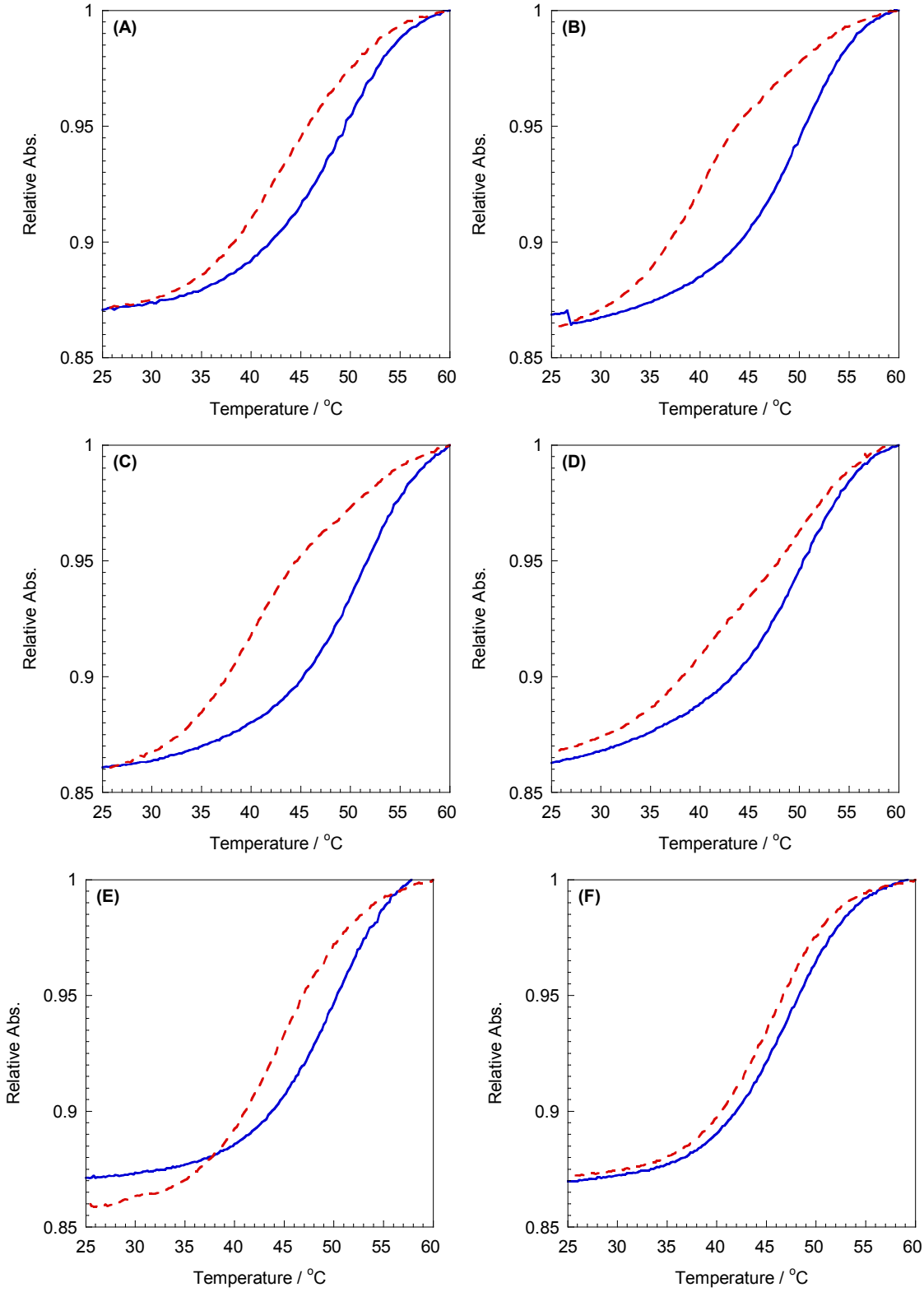

Figure 2-3. Melting curves of CXG/GC involving (A) **Azo**, (B) **2-Me-Azo**, (C) **2′-Me-Azo**, (D) **2′-Et-Azo**, (E) **3′-Me-Azo** and (D) **4′-Me-Azo** either in the *trans*-form (blue solid line) or *cis*-form (red dot line). Solution conditions: [DNA] = 5 μM, [NaCl] = 100 mM, pH 7.0 (10 mM phosphate buffer).

Table 2-1. Effect of chemical modification of azobenzene on the T_m of **CXG/GC** in *trans*- and *cis*-forms: mono-alkylation.

	T_m / °C[a]		
Azobenzene	*trans*	*cis*	ΔT_m[b]
Azo	48.9	43.2	5.7
2-Me-Azo	48.8	39.3	9.5
2′-Me-Azo	50.7	40.1	10.6
2′-Et-Azo	49.6	39.8	9.8
3′-Me-Azo	49.7	44.8	4.9
4′-Me-Azo	46.8	45.4	1.4

[a] Solution conditions: [DNA] = 5 μM, [NaCl] = 100 mM, pH 7.0 (10 mM phosphate buffer). [b] Change in Tm induced by *cis*- *trans* isomerization.

Irradiated with Visible light, the T_m of **4′-Me-Azo** was 46.8 °C, which was lower than that of non-modified azobenzene (**Azo**, 48.9 °C) and even lower than that of native DNA duplex (involving no-azobenzene moiety: 47.7 °C). The methyl group introducing at *para*-position of distal benzene ring caused steric hindrance with the back born of complementary strand.[4] On the other hand, irradiated with UV light, the T_m of **4′-Me-Azo** was 45.4 °C, which was higher than that of **Azo** (43.2 °C). As a result, the ΔT_m became 1.4 °C, which was smaller than that of **Azo**, in other world, photoregulation efficiency decreased.[5] The *meta*-substitution of (**3′-Me-Azo**) did not significantly affect the stability of the duplex; both with visible light and UV light irradiation, the T_m increased compared with those of **Azo** and so the ΔT_m became 4.9 °C, which was almost the same as that of **Azo**.

However, by alkylation of *ortho*-position of benzene ring (**2-Me-Azo**, **2′-Me-Azo** and **2′-Et-Azo**), photoregulation efficiency was increased; the ΔT_m of those azobenzene derivatives were about 10 ^oC, which was almost twice as large as that of **Azo**. In the case of ci*s*-form, the T_ms decreased efficiently compared with that of **Azo**. On the other hand, in the case of *trans*-form, the differences of alkylation benzene ring showed small but clear difference appeared; in the case of alkylation of distal benzene ring (**2′-Me-Azo** or **2′-Et-Azo**), the T_ms were about 50 ^oC, which was 1 ^oC higher than that of **Azo** whereas T_m of **2-Me-Azo** was almost same as that of **Azo**. This tendency also appeared in the case of di-alkylation of azobenzene (see the section **2-3-2**). The effect of *ortho*-alkylation will be discussed in section **2-3-4**. In contrast, the differences between methylation and ethylation did not appear. Ethyl group is larger than methyl group, however sterically effect for DNA duplex would be small because additional methyl group of ethyl group could locate far from adjacent base-pairs.

2-3-2 Photoregulation efficiency of di-methylation of azobenzene

As described in previous section, methylation at *ortho*-position of benzene ring caused improvement of photoregulation efficiency. Therefore, for more efficient photoregulation, *ortho* di-methylated azobenzene derivatives were synthesized and

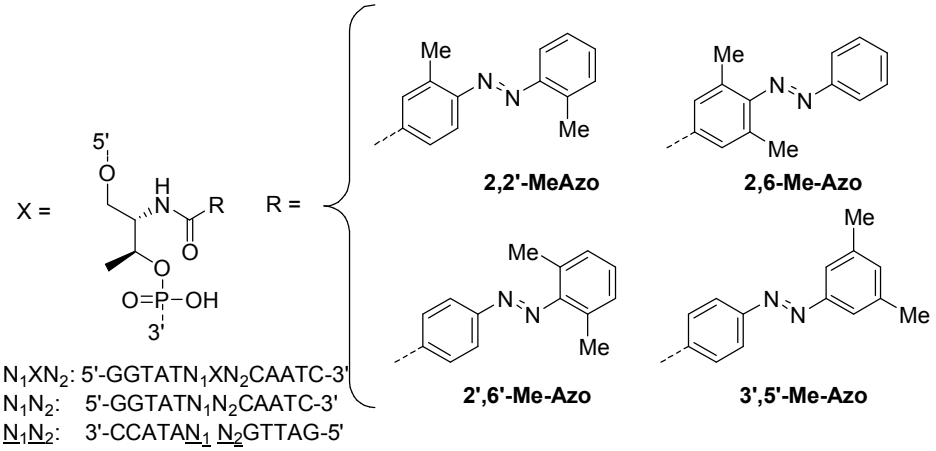

Figure 2-4. Structures of di-alkylated azobenzene derivatives and the DNA sequences. X indicates azobenzene and its derivatives. **N_1** and **N_2** represent natural nucleotides (A, G, C, T), and **$\underline{N_1}$** and **$\underline{N_2}$** do their complementary ones. **X** indicates azobenzene and its derivatives.

introduced into DNA together with *meta* di-methylated azobenzene. Figure 2-4 showed the di-methylated azobenzene derivatives together with the DNA sequences used in this study. The absorbance of DNA involving each azobenzene derivatives and that of T_m curves were shown in Figure2-5 and the values of T_m and ΔT_m were listed in Table 2-2.

In the case of *ortho* di-methylated azobenzene derivatives (**2,2′-Me-Azo**, **2,6-Me-Azo**, **2′,6′-Me-Azo**), photoregulation efficiency improved. As described in previous section **2-3-1**, in the case of *trans*-form, by methylation at *ortho*-position of distal benzene ring, the T_m increased compared with that of **Azo**; the T_ms of *trans*-**2,2′-Me-Azo** and *trans*-**2′,6′-Me-Azo** were 51.4 ^oC and 50.9 ^oC, respectively which were almost same as that of **2′-Me-Azo** (50.7 ^oC) and higher than that of **Azo**

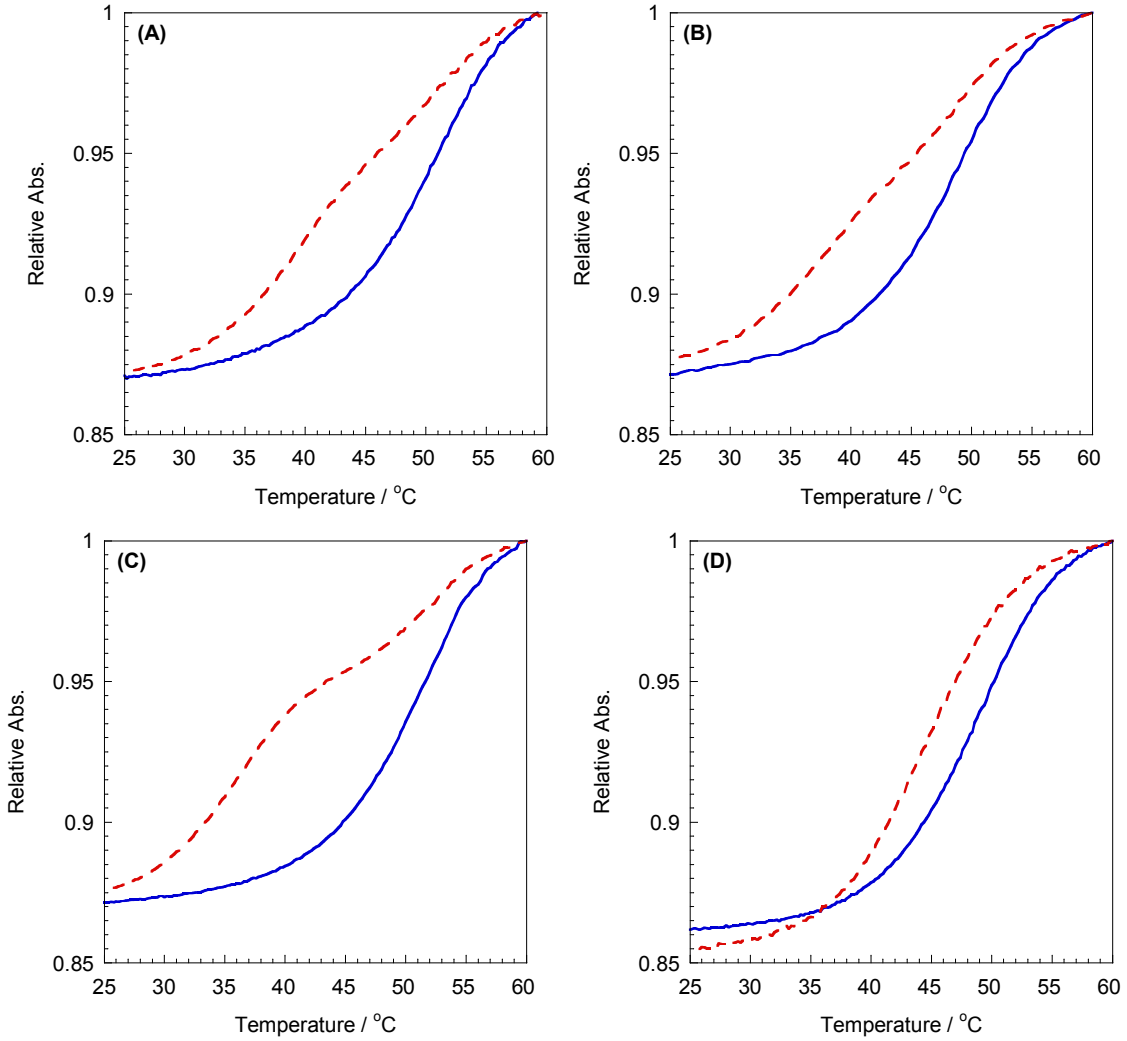

Figure 2-5. Melting curves of CXG/GC involving (A) **2,2′-MeAzo**, (B) **2,6-Me-Azo**, (C) **2′,6′-Me-Azo** and (D) **3′,5′-Me-Azo** either in the *trans*-form (blue solid line) or *cis*-form (red dot line). Solution conditions: [DNA] = 5 μM, [NaCl] = 100 mM, pH 7.0 (10 mM phosphate buffer).

(48.9 °C). In contrast, in the case of methylation of only proximal benzene ring did not cause such a stabilization; the T_m of *trans*-**2,6-Me-Azo** was 48.6 °C, which was almost same as that of **2-Me-Azo** (48.8 °C) and that of **Azo** (48.9 °C). On the other hand, in the case of *cis*-form, di-methylation of distal benzene ring (**2′,6′-Me-Azo**) caused dramatically decrease of T_m; the T_m of *cis*-**2′,6′-Me-Azo** was 36.3 °C, which was about

Table 2-2. Effect of chemical modification of azobenzene on the T_m of **CXG/GC** in *trans*- and *cis*-forms: di-alkylation.

	T_m / °C[a]		
Azobenzene	*trans*	*cis*	ΔT_m[b]
2,2′-Me-Azo	51.4	39.9	11.5
2,6-Me-Azo	48.6	40.0	8.6
2′,6′-Me-Azo	50.9	36.3	14.6
3′5′-Me-Azo	49.0	44.4	4.6

[a]Solution conditions: [DNA] = 5 μM, [NaCl] = 100 mM, pH 7.0 (10 mM phosphate buffer). [b]Change in T_m induced by *cis*- *trans* isomerization.

4 °C lower than that of **2′-Me-Azo** (40.1 °C). Interestingly, such a effective decrease of T_m was not observed in the case of di-methylation at *ortho*-positions of proximal benzene ring (**2,6-Me-Azo**) or mono-methylation at *ortho*-position of both distal and proximal benzene rings. The effect of *ortho*-alkylation will be discussed in section **2-3-4**. As a result, photoregulation efficiency was dramatically improved by di-methylation at *ortho*-positions of distal benzene ring; the ΔT_m of **2′,6′-Me-Azo** became 14.6 °C, which was almost 3-folds as large as that of **Azo**.[5]

In the case of *meta*-dimethylated azobenzene (**3′,5′-Me-Azo**), the T_ms of both *trans*- and *cis*-form were almost as same as those of **3′-Me-Azo**. As a result, the photoregulation efficiency (ΔT_m) did not improved compared with **3′-Me-Azo** and **Azo**.

2-3-3 Dependency of photoregulation efficiency of 2′,6′-Me-Azo on DNA sequence

As described in section **2-3-2**, **2′,6′-Me-Azo**, in which two *ortho*-positions of distal benzene ring were methylated, showed highest photoregulation efficiency on **CXG/GC** DNA duplex. In this section, dependency of T_m of duplex involving **2′,6′-Me-Azo** on DNA sequence was investigated because the stabilizing effect of the intercalator generally depends on the neighboring base-pairs.[6] As shown in Table 2-3, in all the possible combination of neighboring base-pairs, the T_ms of *trans*-form were 5 ^oC higher than those of native duplex (without azobenzene moiety). In contrast, the T_ms of *cis*-form were 10 -15 ^oC lower than those of native duplex. As a result, ΔT_m increased as much as 14-20 °C, clearly demonstrating that **2′,6′-Me-Azo** is a superior photoregulator of DNA hybridization. Compared with **Azo**, the dependency of T_ms of both *trans*- and *cis*-form on neighbor base-pairs were almost same, as shown in appendix section. These results indicated that di-metylation at *ortho*-positions of distal benzene ring could improve the photoregulation efficiency in any combination of neighboring base-pairs.

Table 2-3. Effect of neighboring bases on the T_ms of N_1XN_2/N_1N_2 duplexes involving *trans*- and *cis*-forms of **2′,6′-Me-Azo**.

	T_m / °C[a]			
Duplex	Native duplex[b]	*trans*	*cis*	ΔT_m [c]
AXA/TT	36.9	44.1 (+7.2)[d]	24.6 (-12.3)[d]	19.5
AXC/TG	38.3	41.3 (+3.0)	25.7 (-12.6)	15.6
AXG/TC	41.2	47.1 (+5.9)	30.3 (-10.9)	16.8
AXT/TA	36.8	42.5 (+5.7)	21.1 (-15.7)	21.4
CXA/GT	42.6	47.2 (+4.6)	28.8 (-13.8)	18.4
CXC/GG	43.6	47.8 (+4.2)	28.6 (-15.0)	19.2
CXG/GC	47.7	50.9 (+3.2)	36.3 (-11.4)	14.6
CXT/GA	41.3	46.4 (+5.1)	26.3 (-15.0)	20.1
GXA/CT	41.3	48.0 (+6.7)	29.2 (-12.1)	18.8
GXC/CG	46.1	48.0 (+1.9)	32.8 (-13.3)	15.2
GXG/CC	46.5	50.5 (+4.0)	36.3 (-10.2)	14.2
GXT/CA	42.0	47.7 (+5.7)	28.7 (-13.3)	19.0
TXA/AT	36.9	42.8 (+5.9)	24.8 (-12.1)	18.0
TXC/AG	40.3	42.2 (+1.9)	28.0 (-12.3)	14.2
TXG/AC	43.1	48.0 (+4.9)	31.9 (-11.2)	16.1
TXT/AA	38.3	43.1 (+4.8)	21.9 (-16.4)	21.2

[a] Solution conditions: [DNA] = 5 μM, [NaCl] = 100 mM, pH 7.0 (10 mM phosphate buffer). [b] Melting temperature of the corresponding native duplex without **X** residue. [c] Change in T_m induced by *trans*-to-*cis* isomerization of **2′,6′-Me-Azo**. [d] The data in parentheses show the difference of T_m between native duplex and modified duplex containing *trans* or *cis*-**2′,6′-Me-Azo**.

2-3-4 Mechanism of improvement of photoregulation efficiency by *ortho*-methylation

As described previous sections, improvement photoregulation efficiency of DNA hybridization was attained with *ortho*-methylated azobenzene. In this section, the mechanism of efficient photoregulation with *ortho*-methylated azobenzene derivatives was investigated by NMR analysis and computer modeling.

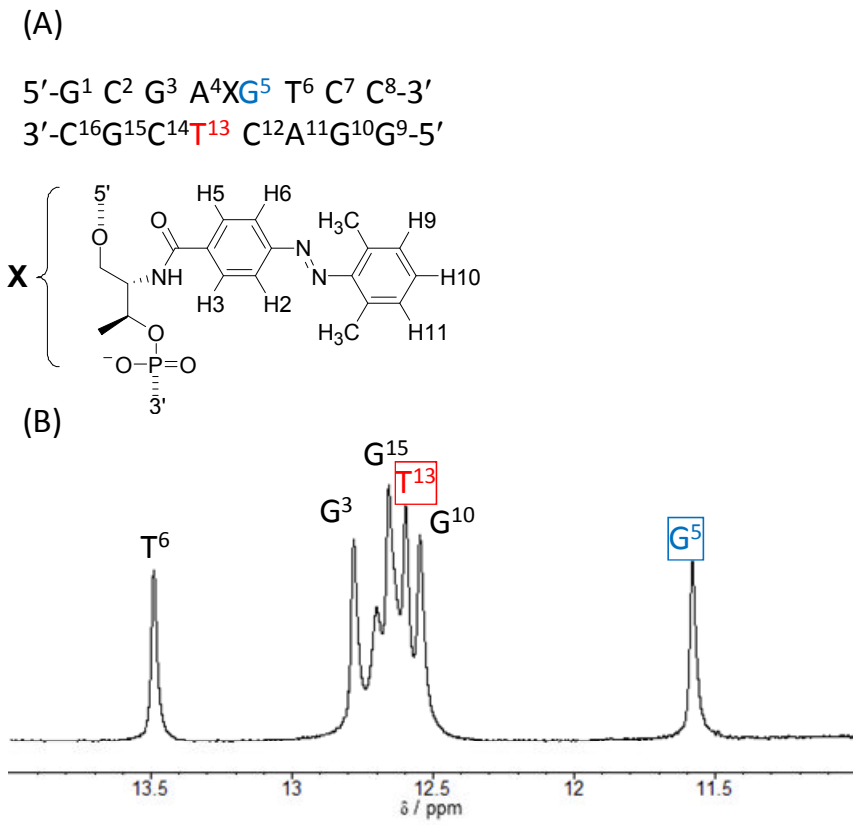

Figure 2-6. Sequence of modified DNAs used for NMR measurements and computer modeling (A) and the one-dimensional NMR spectrum at the imino region in H_2O/D_2O (9/1) at 278 K (mixing time = 150 ms), [NaCl] = 200 mM, pH 7.0 (20 mM phosphate buffer), in the presence of 200 mM NaCl (B). The concentration of each DNA was 560 μM. Assignments of the imino protons and the residue numbers are denoted at the top of the peaks.

Stabilization effect of *trans*-azobenzene derivatives: First, the position of *trans*-**2′,6′-Me-Azo** in the duplex was determined by NMR. In order to monitor the imino protons that are exchangeable with water molecules, NMR measurements were carried out in H_2O (H_2O/D_2O = 9/1) with a 3-9-19 WATERGATE for H_2O suppression. A one-dimensional spectrum at the region of the imino protons (11–14 ppm) is depicted in Figure 2-6B, which exhibited seven signals corresponding to eight base-pairs. Except for the terminal G^1 (G^1-C^{15} pair) and G^9 (C^8-G^9 pair) that broadened due to rapid exchange with water, all the internal imino protons could be assigned from NOESY, DQF-COSY, and TOCSY.[7] The signal assigned to G^5 and T^{13} adjacent to azobenzene (**X** residue) showed a distinct upfield shift compared with those to G^{15}, G^3, or T^6 that stayed distant from azobenzene. This upfield shift was attributed to the ring

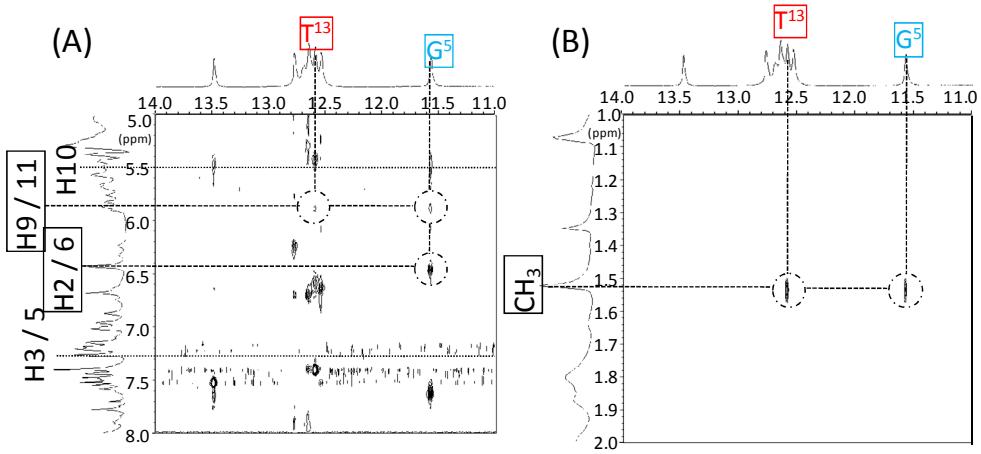

Figure 2-7. 2D NOESY spectra of the duplex involving *trans*-**2′,6′-Me-Azo** between a) aromatic protons and the imino proton, and b) methyl groups and imino proton regions. Solution conditions: [DNA] = 560 μM, [NaCl] = 200 mM, pH 7.0 (20 mM phosphate buffer).

current effect of *trans*-azobenzene, demonstrating that these protons were located at the axial position.[8] Figure 2-7A depicts the NOESY between the imino proton (11-14 ppm) and the aromatic proton (5.5-8.0 ppm) regions. Weak NOEs were observed between H9 (H11) of the distal ring of **2′,6′-Me-Azo**, and T^{13} and G^5 imino protons. In addition, the G^5 imino proton had relatively strong NOE with the H2 (H6) aromatic proton on the proximal ring. Methyl protons on **2′,6′-Me-Azo** also showed distinct NOE with imino protons as shown in Figure 2-7B; strong NOEs were observed for both T^{13} and G^5 with almost equal intensity. These NOEs clearly demonstrated that **2′,6′-Me-Azo** is intercalated between A^4-T^{13} and G^5-C^{12}. Computer modeling of this duplex involving *trans*-**2′,6′-Me-Azo** also supported an intercalated structure as depicted in Figure 2-8. Two methyl groups of the distal benzene ring were located between the hydrogen-bonded imino protons of G^5 and T^{13} as depicted in Figure 2-8B, which was consistent with the NMR results.

As described in **2-3-1** and **2-3-2**, stabilization effects of the *trans*-form of the distal benzene ring methylated derivatives such as **2′-Me-Azo**, **2,2′-Me-Azo**, and **2′,6′-Me-Azo** was more effective than at the proximal ring (**2-Me-Azo** and **2,6-Me-Azo)**; the T_m of former was about 1 ^oC higher than those of latter. NMR analysis of the duplex with *trans*-**2′,6′-Me-Azo** demonstrated that the H2 (H6) proton at the

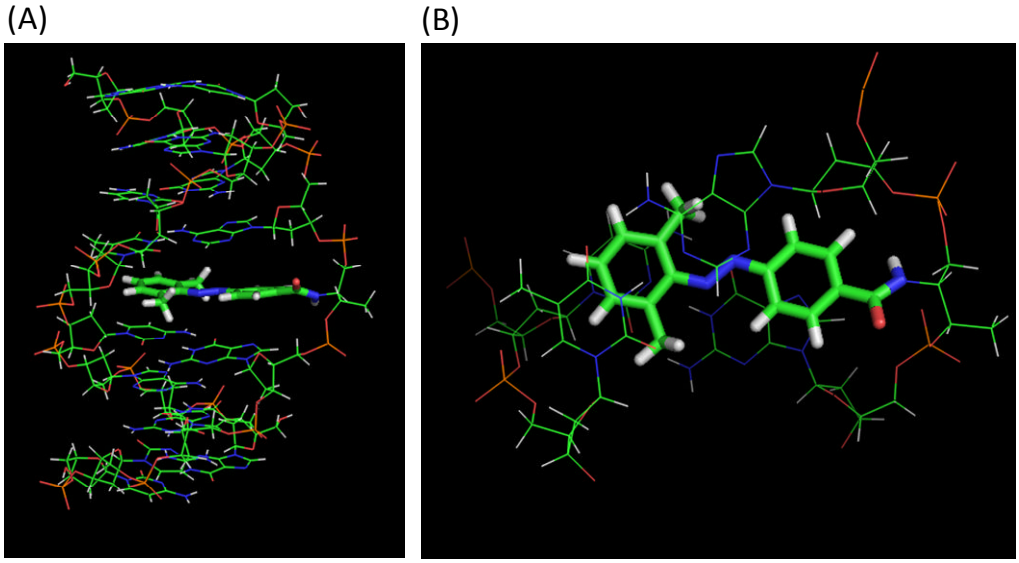

Figure 2-8. Energy-minimized structure of a modified duplex involving *trans*-**2′,6′-Me-Azo** (A) viewed from the side of azobenzene and (B) viewed from the 5'-side of the helix axis. For the top view (b), only the 5'-A^{4}**X**G^{5}-3'/3'-T^{13}C^{12}-5' part is depicted and *trans*-**2′,6′-Me-Azo** is drawn in stick form for clarity.

proximal side had NOE only with the imino proton G^{5}, whereas both G^{5} and T^{13} had distinct NOE with CH_3 protons, indicating that the *ortho*-positions on the distal side were located on the axial positions of the center of the G^{5}-C^{12} and A^{4}-T^{13} pairs. Consistently, computer modeling also showed that the distal *ortho*-methyl groups were located in close proximity to the adjacent G^{5}-C^{12} and A^{4}-T^{13} pairs whereas the proximal H2 (H6) positions were rather distant from these base-pairs and located near the *N*-glycosidic linkage between the nucleobase and deoxyribose. From the result of computer modeling of the duplex having *trans*-**2,6-Me-Azo** (Figure 2-9), it was found that two methyl groups were displaced from the bases. Thus, distal modification at the

ortho-positions made the *trans*-azobenzene a more effective intercalator which facilitated stacking or hydrophobic interactions between the adjacent base-pairs and stabilized the duplex.

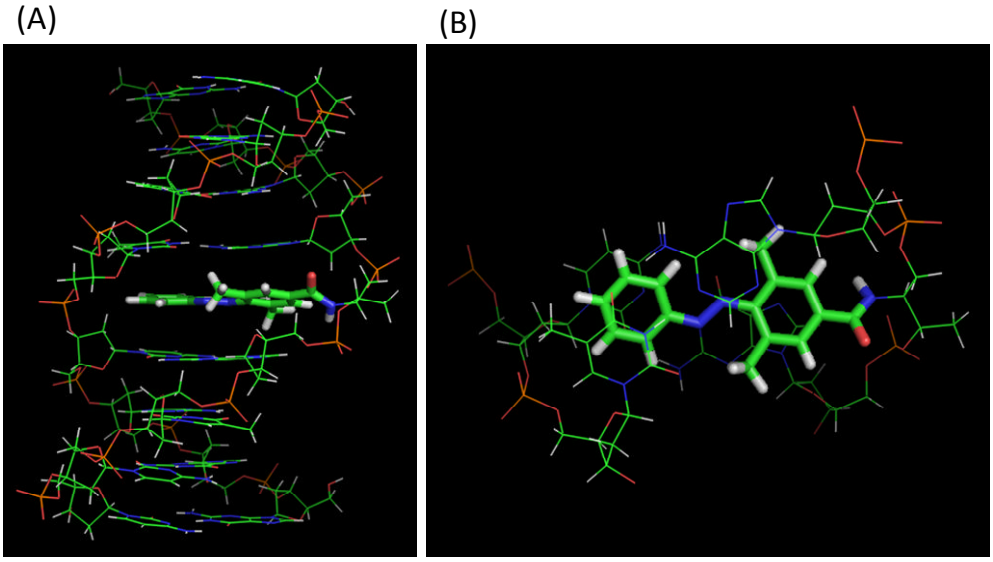

Figure 2-9. Energy-minimized structure of a modified duplex involving *trans*-**2,6-Me-Azo** (A) viewed from the side of azobenzene and (B) viewed from the 5'-side of the helix axis. For the top view (b), only the 5'-A^{4}**X**G^{5}-3'/3'-$T^{13}C^{12}$-5' part is depicted and *trans*-**2,6-Me-Azo** is drawn in stick form for clarity.

Destabilization effect of *cis*-azobenzene derivatives: In order to investigate the efficient destabilization of DNA duplex by *cis*-**2′,6′-Me-Azo**, NMR analysis was also attempted. However, in the condition of NMR analysis attempted, DNA duplex did not form even at 5 ^{o}C (278 K).[9] Therefore, the mechanism of efficient destabilization was analyzed by computer modeling. Since preliminary analysis indicated that even *cis*-azobenzene is partially intercalated,[10] the calculation was started with intercalated

cis-**2′,6′-Me-Azo** as an initial structure.

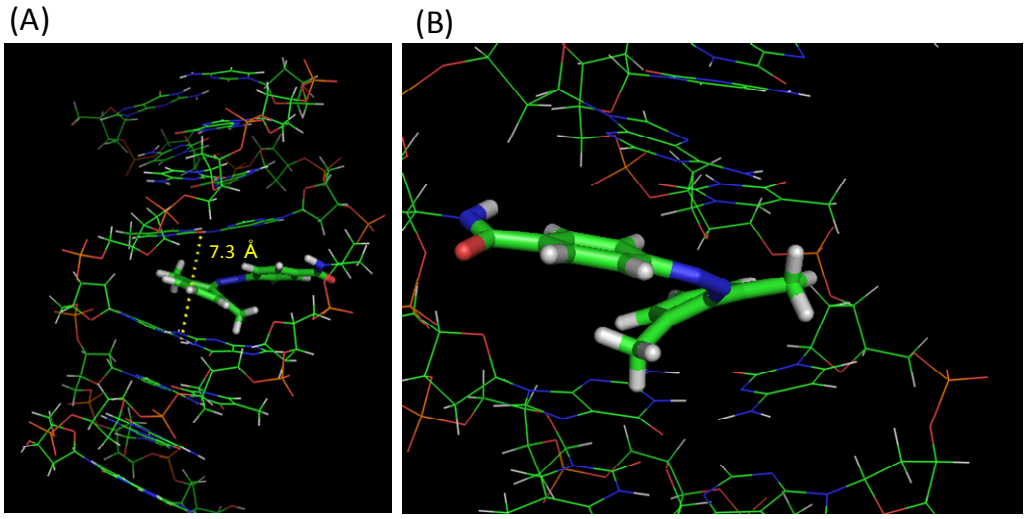

Figure 2-10. Energy-minimized structure of a modified duplex involving *cis*-**2′,6′-Me-Azo** viewed from the side of azobenzene. (A) Whole structure of the duplex. (B) Magnified around *cis*-**2′,6′-Me-Azo.** The distance of imino protons between G^5-C^{12} and A^4-T^{13}, depicted with dotted yellow line in (A), was calculated to be 7.3 Å.

Figure 2-10 showed the converged structure of the duplex with non-planar *cis*-**2′,6′-Me-Azo**, which was located between adjacent base-pairs. The proximal benzene ring covalently bound to the main chain of threoninol was largely parallel to the A^4-T^{13} base-pair while the distal ring was twisted in the duplex and the two methyl groups protruded to both adjacent base-pairs. Since the proximal ring was directly bound to the main chain of threoninol through the rigid amide bond, its orientation might be restricted in the duplex. In contrast, the distal ring was flexible enough to be twisted with respect to the -N=N- bond by *cis*-isomerization. Consequently, the two *ortho*-positions protruded close to the base-pairs (G^5-C^{12} and A^4-T^{13}) so that they had to

be separated to accept the twisted benzene ring with two methyl groups; the distance of imino protons between G^5-C^{12} and A^4-T^{13} was calculated to be 7.3 Å as shown with dotted yellow line in Figure 2-10A, which should significantly hinder their base-pairing and thus destabilize the duplex as shown in Figure 2-10.

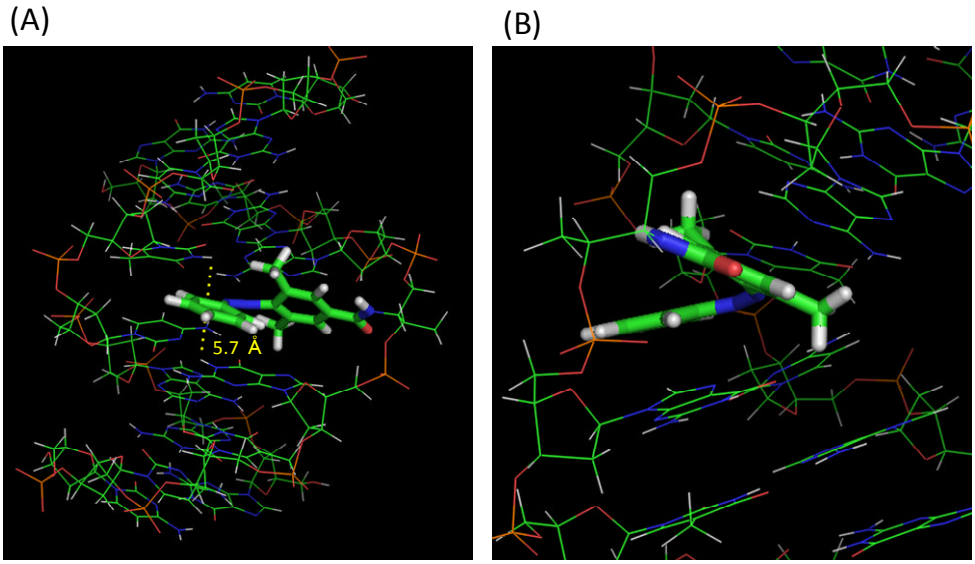

Figure 2-11. Energy-minimized structure of a modified duplex involving *cis*-**2,6-Me-Azo** viewed from the side of azobenzene. (A) Whole structure of the duplex. (B) Magnified around *cis*-**2,6-Me-Azo.** The distance of imino protons between G^5-C^{12} and A^4-T^{13}, depicted with dotted yellow line in (A), was calculated to be 5.7 Å

In the case of other *ortho*-methylated azobenzene derivatives, computer modeling showed a twisted conformation similar to *cis*-**2′,6′-Me-Azo**. However, the steric effect of introduced methyl groups was limited. For example, in the case of **2′-Me-Azo**, there is only one methyl group on the distal benzene ring, so the twisted distal benzene ring allowed for a smaller space between the G^5-C^{12} and A^4-T^{13} pairs (the distance was 5.6

Table 2-4. Distance between the G^5-C^{12} and A^4-T^{13} pairs in the computer modeling DNA sequence including *ortho*-methylated azobenzene derivatives.

Azobenzene	Distance / Å[a]
Azo	5.8
2-Me-Azo	5.6
2′-Me-Azo	5.6
2,2′-Me-Azo	5.6
2,6-Me-Azo	5.7
2′,6′-Me-Azo	7.3

[a] Distance between imino protons of G^5-C^{12} and A^4-T^{13}.

Å). In the case of methylation on proximal benzene ring (**2-Me-Azo** and **2,6-Me-Azo**), the absence of methyl group on the twisted distal benzene ring allowed for a smaller space between the G^5-C^{12} and A^4-T^{13} pairs. The distances between the G^5-C^{12} and A^4-T^{13} pair imino protons was 5.7 Å (**2,6-Me-Azo** Figure 2-11 and Table 2-4). In the case of methylation of one *ortho*-position of distal and proximal benzene rings (**2, 2′-Me-Azo**), the steric effect was same as **2′-Me-Azo** and **2-Me-Azo** (**2,6-Me-Azo**); the distance between the G^5-C^{12} and A^4-T^{13} pairs were 5.6 Å, the distances between the G^5-C^{12} and A^4-T^{13} pairs were almost same as that of *cis*-**Azo** (non-modified azobenzene: 5.8 Å). However, modified azobenzenes could locate other conformations; in those cases, the distances became longer than that of *cis*-**Azo**. Therefore, all *ortho*-methylated azobenzene would destabilize DNA duplex, in *cis*-form. In conclusion, even in energy-minimized structure *cis*-**2′,6′-Me-Azo** cause large steric hindrance with

neighboring base-pairs and destabilized DNA duplex efficiently.

2-4 Conclusions

(1) By using *ortho*-alkylated azobenzene derivatives, efficient photoregulation of DNA hybridization with visible and UV light was attained. In the case of **2′,6′-Me-Azo**, in which two *ortho*-position of distal benzene ring were methylated, the photoregulation efficiency based on ΔT_m induced by *trans*-to *cis*- photo isomerization of azobenzene became 3-folds as large as that of non modified azobenzene (**Azo**). In the case of other *ortho*-methylated azobenzenes, the ΔTm became twice as large as that of **Azo**.

(2) By NMR analysis and computer modeling, efficient photoregulation mechanism of *ortho*-methylated azobenzene derivatives was investigated. In the case azobenzenes took *trans*-form, they intercalated between neighboring base-pairs and methyl groups introduced at *ortho*-positions of benzene ring facilitated stacking or hydrophobic interactions between the adjacent base-pairs and stabilized the duplex. According to the NMR analysis, the effect of or methyl groups at distal benzene ring were larger than that of proximal benzene ring. In the case of azobenzenes took *cis*-form, introduced methyl group increased the steric hindrance with adjacent base-pairs. In particular, in the case of **2′,6′-Me-Azo**, in which two *ortho*-positions of distal benzene ring were methylated,

the methyl groups caused effective steric hindrance and destabilized DNA duplex.

2-5 Experimental section

2-5-1 Synthesis of DNAs involving alkylated azobenzene derivatives

The modified DNAs containing modified azobenzenes were synthesized on an automated DNA synthesizer (ABI-3400, Applied Biosystems) using conventional and azobenzene-carrying phosphoramidite monomers. The DNAs containing only native bases were supplied by Integrated DNA Technologies, Inc. (Coralville, IA. U.S.A.).

Materials: Mesitylene, fuming nitric acid, absolute ethanol, sodium hydrate, hydrochloric acid and chromic acid were purchased from Kishida Chemical Co., Ltd. (Osaka, Japan). Nitrosobenzene, 4,4-dimethoxytrityl chloride, 2-methyl aniline, 2-ethyl aniline, 3-methyl aniline, 4-methyl aniline, 2,6-dimethyl aniline, 3,5-dimethyl aniline, 4-nitrobenzoic acid ethyl ester and 3-Methyl 4-nitrobenzoic acid were purchased from Tokyo Chemical Industry (Tokyo, Japan). D-Threoninol and 1-hydroxy 1H-benzotriazol (HOBt) were purchased from Sigma-Aldrich (St. Louis, MO, U.S.A.). N, N′-dicyclohexylcarbodiimde (DCC) was purchased from WATANABE CHEM. IN., LTD. (Hiroshima, Japan). 2-Cyanoethyl *N,N,N′,N′*-tetraisopropylphosphordiamidite was purchased from ChemGenes (Wilmington, MA, U.S.A.).

2-5-1-1 Synthesis of carboxylic acid of modified azobenzene derivatives

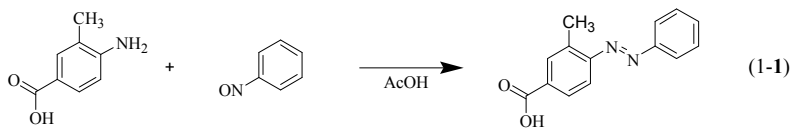

Scheme 1. Synthesis of carboxylic acid of **2-Me-Azo**.

Synthesis of carboxylic acid of 2-Me-Azo: 2-methyl 4-(2-methyl phenylazo) benzoic acid[11] (Carboxyl acid of **2-Me-Azo**) (compound 1-**1**) was synthesized as follow: 0.50 g (3.31 mmol) of 4-amino-3-methylbenzoic acid and 0.30 g (2.80 mmol) of nitosobenzene were dissolved in 30 ml of acetic acid under nitrogen. The mixture was stirred at room temperature over night under dark, and was poured into water followed by the extraction with ethyl acetate. The organic layer was washed with distilled water (once), saturated solution of NaCl, and dried over $MgSO_4$. After the removal the solvent, the crude mixture was subjected to silica gel column chromatography. (Hexane : AcOEt = 5 : 1) to afford 0.30 g (1.26 mmol) of **2-Me-Azo** (yield: 44.8%).

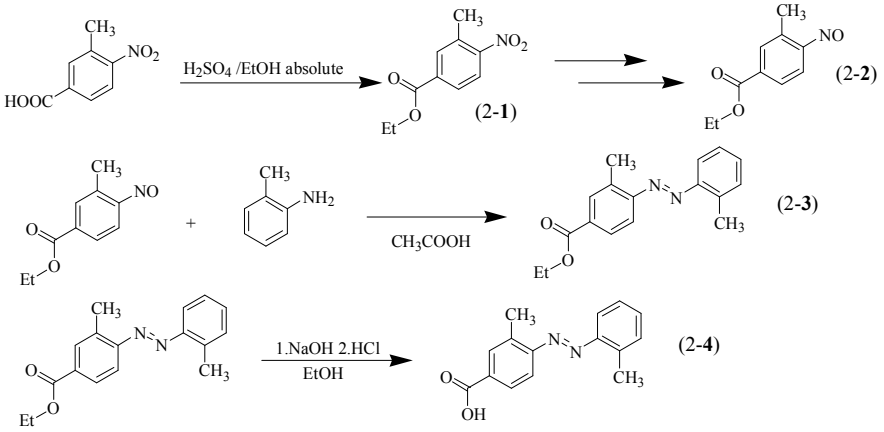

Scheme 2. Synthesis of carboxylic acid of **2,2′-Me-Azo**.

Synthesis of carboxylic acid of 2,2′-Me-Azo: 3-Methyl 4-nitrobenzoic acid ethyl ester[12] (Compound 2-**1**) was synthesized as follows:4.00 g (0.022 mol) of 3-methyl 4-nitrobenzoic acid were dissolved in 40 ml of absolute ethanol treated with 2.5 ml of concentrated sulfuric acid in two-necked flask under nitrogen. The mixture was heated to reflux for 24 hours with stirring. After removal the solvent, the crude mixture was dissolved in ethyl acetate. The solvent was washed with distilled water and saturated solution of $NaHCO_3$ and saturated solution of NaCl and dried over $MgSO_4$. After

removal the solvent, 4.41 g (0.021 mol) of 3-methyl 4-nitrobenzoic acid ethyl ester was obtained without further purification (yield: 95.9 %).

3-Methyl 4-nitrosobenzoic acid ethyl ester[13] (Compound 2-**2**) was synthesized as follows: After 4.41 g (0.021 mol) of 3-methyl 4-nitrobenzoic acid ethyl ester was dissolved in 56 ml of 2-methoxy ethanol, solution of 1.7 g (0.032 mol) of ammonium chloride in 13.5 ml of water was added and the mixture was warmed to 30 ^{o}C. With vigorous stirring, 3.6 g (0.055 mol) of powdered zinc dust was added in small potion over 30 minutes and the temperature held 33-35 ^{o}C. The stirring was continued until the reaction mixture became colorless. Then, the reaction mixture was suction filtrated, and the filter cake was washed by 2-methoxy ethanol. The filtrated and washing solvent was added dropping funnel, under nitrogen with rapid stirring, to solution of 8.4 g (0.031 mol) of ferric chloride 6-hydrate in 95 ml of distilled water and 24 ml of ethanol maintained -5 ^{o}C with ice-sodium chloride bath. After the additional was completed, stirring at -5 ^{o}C was continued for an additional 30 minutes, the reaction mixture was poured into 200 ml of cold water and suction filtered. After being washed with water, the cake was collected. 2.72 g (0.014 mol) of 3-Methyl 4-nitrosobenzoic acid ethyl ester was recrystallized from ethanol (yield: 66.7 %).

2-methyl 4-(2-methyl phenylazo) benzoic acid ethyl ester (Ethyl ester of **2,2′-Me-Azo**)[11] (Compound 2-**3**) was synthesized as follows: 2.72 g (0.014 mol) of 3-methyl 4-nitrosobenzoic acid ethyl ester and 2.21 g (0.020 mol, 2.21 ml) of 2-methyl aniline were dissolved in 30 ml of acetic acid under nitrogen. The mixture was stirred and warmed 45 ^{o}C overnight under dark. Then the solution was poured into water and extracted with ethyl acetate. The organic layer was washed with distilled water,

saturated solutions of $NaHCO_3$ and saturated solutions of NaCl, and dried over $MgSO_4$. After removal the solvent, the crude mixture was subjected to silica gel column chromatography (hexane : AcOEt = 15 : 1) to afford 2.15 g (7.61 mmol) of ethyl ester of 2-methyl 4-(2-methyl phenylazo) benzoic acid (yield: 54.4 %).

2-methyl 4-(2-methyl phenylazo) benzoic acid (Carboxyl acid of **2,2′-Me-Azo**)[11] (Compound **2-4**) was synthesized as follows: 2.15 g (7.61 mmol) of ethyl ester of **2,2′-Me-Azo** was dissolved in 20 ml of ethanol. Then 4 ml of aqueous NaOH solution (2 N) was added and the mixture was stirred overnight under dark. After the hydrolysis was completed, 10 ml of aqueous HCl solution (1N) was added to the mixture and extracted with ethyl acetate. The organic layer was washed with distilled water and saturated solution of NaCl and dried over $MgSO_4$. After removal the solvent, the crude product was used in the next step without further purification (1.94 g (7.61 mmol), yield: quant.).

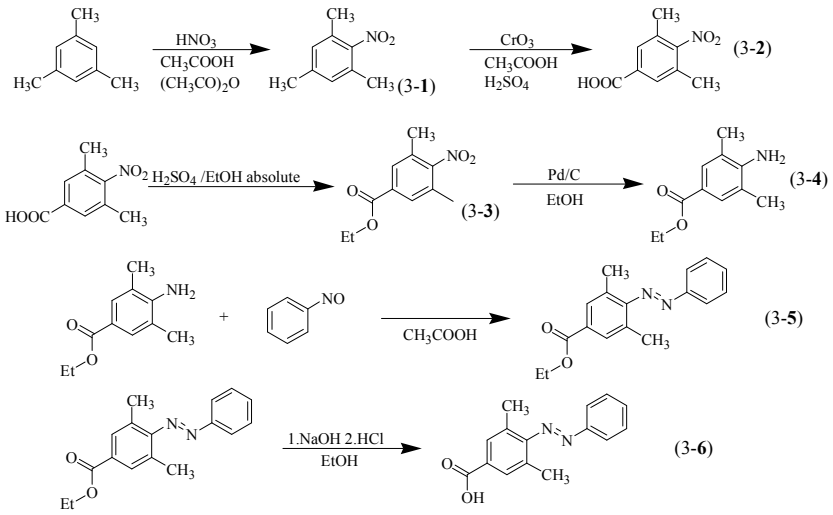

Scheme 3. Synthesis of carboxylic acid of **2,6-Me-Azo**.

Synthesis of carboxylic acid of 2,6-Me-Azo: Nitromesitylene[14] (Compound 3-**1**)

was synthesized as follows: 19.9 g (0.17 mol, 23.0 ml) of mesitylene and 30.0 g (0.29 mol, 27.8 ml) of acetic anhydride were added in two-necked flask and cooled with ice bath. A solution of 10.4 ml of fuming nitric acid (SG: 1.52) in 9.98 g (0.17 mol, 9.51 ml) of glacial acetic acid was added in mixture of mesitylene-acetic anhydride solution by using of dropping funnel. The reaction mixture was stirred and kept under 10 ^{o}C while dropping. After the dropping was completed, the flask was removed from ice bath and allowed to stand at room temperature for two hours. Then, the reaction mixture was warmed to 50 ^{o}C on a water bath with stirring for 10 minutes. The reaction mixture was poured into beaker, then, $NaHCO_3$ and aqueous NaOH solution was added in the reaction mixture to adjust the pH over 7.0. The aqueous layer of reaction mixture was decanted and extracted with ethyl acetate. The extracted ethyl acetate was added to the residual, and the solvent was washed with distilled water, saturated solutions of $NaHCO_3$ and saturated solution of NaCl and dried over $MgSO_4$. After removal the solvent, 24.9 g (0.15 mol) of nitromesitylene was recrystallized from methanol (yield: 88.6 %).

3,5-Dimethyl 4-nitrobenzoic acid[15] (Compound 3-**2**) was synthesized as follows: In a three-neck flask fitted dropping funnel and condenser, 20.7 g (0.13 mol) of nitromesitylene, 104g (1.73 mol, 98.9 ml) of glacial acetic acid and 27.6 ml of concentrated sulfuric acid were added. The mixture was heated to reflux and 38.5g (0.39 mol) of chromium (VI) oxide in 140 ml of water was added at such a rate that a moderate reflux was maintained, with stirring. After the additional was completed, stirring at reflux was continued for an additional 30 minutes, and then the reaction mixture was poured onto ice. The crystals were suction filtered from solution, washed well with water, and transferred to a beaker containing 150 ml of aqueous NaOH

solution (2N) to dissolve the acidic components. Filtration gave unreacted nitromesitylene. Concentrated aqueous HCl solution was added into filtrated solution, then, corrected the precipitate. 5.55 g (0.028 mol) of 3,5-dimethyl 4-nitrobenzoic acid was recrystallized from ethanol (yield: 21.9 %).

3,5-Dimethyl 4-nitrobenzoic acid ethyl ester[12] (Compound 3-**3**) was synthesized as follows: 5.55 g (0.028 mol) of 3,5-dimethyl 4-nitrobenzoic acid were dissolved in 50 ml of absolute ethanol treated with 1 ml of concentrated sulfuric acid in two-necked flask under nitrogen. The mixture was heated to reflux for 24 hours with stirring. After removal the solvent, the crude mixture was dissolved in ethyl acetate. The solvent was washed with distilled water and saturated solution of $NaHCO_3$ and saturated solution of NaCl and dried over $MgSO_4$. After removal the solvent, 5.92 g (0.027 mol) of ethyl ester of 3,5-dimethyl 4-nitrobenzoic acid was obtained without further purification (yield: 94.7 %).

3,5-Dimethyl 4-aminobenzoic acid ethyl ester (Compound 3-**4**) was synthesized as follows: 5.92 g (0.027 mol) of 3,5-dimethyl 4-nitrobenzoic acid ethyl ester was dissolved in 200 ml of ethanol in two-necked flask. After additional of moderate of palladium carbon, the flask was displacement with hydrogen and stirred vigorously for 72 hours. After filtrated the reaction mixture, the solvent was removed and then the crude mixture was subjected to silica gel column chromatography (Hexane : AcOEt = 5 : 1) to afford 3.47 g (0.018 mol) of 3,5-Dimethyl 4-aminobenzoic acid ethyl ester (yield: 66.5 %).

3,5-Dimethyl 4-phenylazo benzoic acid ethyl ester (Ethyl ester of **2,6-Me-Azo**)[11] (Compound 3-**5**) was synthesized as follows: 1.23 g (6.37mmol) of 3,5-Dimethyl

4-aminobenzoic acid ethyl ester and 0.76g (7.10 mmol) of nitrosobenzene were dissolved in 20 ml of acetic acid under nitrogen. The mixture was stirred at room temperature overnight under dark. Then the solution was poured into water and extracted with ethyl acetate. The organic layer was washed with distilled water, saturated solutions of $NaHCO_3$ and saturated solutions of NaCl, and dried over $MgSO_4$. After removal the solvent, the crude mixture was subjected to silica gel column chromatography (hexane : AcOEt = 20 : 1) to afford 0.52 g (1.84 mmol) of ethyl ester of 3,5-dimethyl 4-phenylazo benzoic acid (yield: 28.9 %).

3,5-Dimethyl 4-phenylazo benzoic acid (Carboxyl acid of **2,6-Me-Azo**)[11] (Compound 3-**6**) was synthesized as follows: 0.52 g (1.84 mmol) of ethyl ester of **2,6-Me-Azo** was dissolved in 20 ml of ethanol. Then 4 ml of aqueous NaOH solution (2 N) was added and the mixture was stirred overnight under dark. After the hydrolysis was completed, 10 ml of aqueous HCl solution (1N) was added to the mixture and extracted with ethyl acetate. The organic layer was washed with distilled water and saturated solution of NaCl and dried over $MgSO_4$. After removal the solvent, the crude product was used in the next step without further purification (0.46 g (1.84 mmol) yield: 97.9 %).

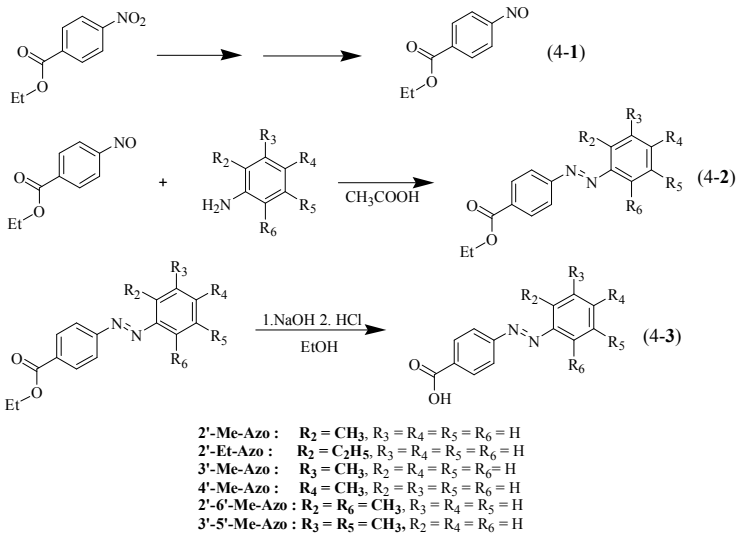

Scheme 4. Synthesis of carboxylic acid of **2′-Me-Azo**, **2′-Et-Azo**, **3′-Me-Azo**, **4′-Me-Azo, 2′,6′-Me-Azo** and **3′,5′-Me-Azo**.

Synthesis of carboxylic acid of 2′-Me-Azo, 2′-Et-Azo, 3′-Me-Azo, 4′-Me-Azo, 2′,6′-Me-Azo and 3′,5′-Me-Azo: Carboxylic acid of **2′-Me-Azo**, **2′-Et-Azo**, **3′-Me-Azo**, **4′-Me-Azo, 2′,6′-Me-Azo** and **3′,5′-Me-Azo** were synthesized according to the Scheme 4. Typical procedures are described by taking **3′-Me-Azo** as an example as follows.

Ethyl *p*-nitrosobenzoate (compound 4-**1**) was synthesized as follows[13]: 2.00 g (10.2 mmol) of ethyl *p*-nitrobenzoate was dissolved in 35 ml of 2-methoxyethanol and the solution of 1.08 g (20.2 mmol) of ammonium chloride in 10 ml of water was added and the solution was warmed to 30 ^{o}C, with vigorous stirring, 2.3 g (35.2 mmol) of zinc powder was added in small potions and the temperature kept under 35 ^{o}C by cooling ice bath. The stirring was kept until the solution became colorless (the stirring was stopped to cheek the solution color). Then, the reaction mixture was suction filtered and the filtered cake was washed with 2-methoxyethanol. The filtered solution was then added dropwise, with rapid stirring, to a solution of 8.90 g (32.9 mmo) of hexa hydrate ferric chloride in50 ml of water and 15 ml of ethanol maintained -5 ^{o}C. After additional 30

minutes stirring, the reaction mixture was poured in to 100 ml of cold water and suction filtered. After washing with water, the precipitate was drying in vacuum. The crude mixture was subjected to silica gel column chromatography (hexane: AcOEt = 10 :1) to afford 1.02 g (5.69 mmol) of Ethyl *p*-nitrosobenzoate (yield: 55.4 %).

4-(3-methyl phenylazo) benzoic acid ethyl ester (Ethyl ester of **3′-Me-Azo**) (Compound 4-**2**)[11] was synthesized as follows: 0.33 g (3.08 mmol) of *m*-tolidine and 0.50g (2.79 mmol) of ethyl *p*-nitrosobenzoate were dissolved in 30 ml of acetic acid under nitrogen. The mixture was stirred at room temperature over night under dark. Then the solution was poured into water and extracted with ethyl acetate. The organic layer was washed with distilled water, saturated solutions of $NaHCO_3$ and NaCl, and dried over $MgSO_4$. After the removal the solvent, the crude mixture was subjected to silica gel column chromatography (hexane: AcOEt = 20 :1) to afford 0.38 g (1.42 mmol) of ethyl ester of **3′-Me-Azo** (yield: 50.7%).

4-(3-methyl phenylazo) benzoic acid (Carboxyl acid of **3′-Me-Azo**) (Compound 4-**3**)[11] was synthesized as follows: 0.38 g (1.42 mmol) of ethyl ester of **3′-Me-Azo** was dissolved in 15 ml of ethanol. Then 4 ml of aqueous NaOH solution (2 N) was added and the mixture was stirred overnight under dark. After the hydrolysis was completed, 10 ml of aqueous HCl solution (1M) was added to the mixture and extracted with ethyl acetate. The organic layer was washed with distilled water and saturated solution of NaCl and dried over $MgSO_4$. After removal the solvent, the crude product was used in the next step without further purification (0.33 g (1.37 mmol) yield: 97.1%).

NMR assignment

Compound 1-1: Silica gel column chromatography (Hexane : AcOEt = 5 : 1), (yield 44.8%), ^{1}H NMR (500 MHz, [D$_6$]DMSO): δ = 8.01 – 7.59 (m, 8H, aromatic protons of azobenzene), 2.72 (s, 3H, -NC$_6$H$_3$-C*H$_3$*).

Compound 2-1: (yield: 95.9 %), ^{1}H NMR (500 MHz, [D$_6$]DMSO): δ = 8.09 – 7.97 (m, 3H; aromatic protons of benzene), 4.38 (q, ^{3}J(H,H) = 7.0 Hz, 2H; -O-C*H$_2$*-CH$_3$), 3.34 (s, 3H; C$_6$H$_3$-C*H$_3$*), 1.36 (t, ^{3}J(H,H) = 7.0Hz, 3H; -O-CH$_2$-C*H$_3$*).

Compound 2-2: (yield: 66.7 %), ^{1}H NMR (500 MHz, [D$_6$]DMSO): δ = 8.29 – 8.27 (m, 3H; aromatic protons benzene), 4.38 (q, ^{3}J(H,H) = 7.0 Hz, 2H; -O-C*H$_2$*-CH$_3$), 3.37 (s, 3H; C$_6$H$_3$-C*H$_3$*), 1.36 (t, ^{3}J(H,H) = 7.0Hz, 3H; -O-CH$_2$-C*H$_3$*).

Compound 2-3: Silica gel column chromatography (hexane : AcOEt = 15 : 1), (yield: 54.4 %), ^{1}H NMR (500 MHz, [D$_6$]DMSO): δ = 8.02 – 7.34 (m, 7H; aromatic protons of azobenzene), 4.37 (q, ^{3}J(H,H) = 7.0 Hz, 2H; -O-C*H$_2$*-CH$_3$), 2,72 and 2.71 (s, 6H; C$_6$H$_3$-C*H$_3$* and C$_6$H$_4$-C*H$_3$*), 1.37 (t, ^{3}J(H,H) = 7.0 Hz, 3H; -O-CH$_2$-C*H$_3$*).

Compound 2-4: (yield: quant.), ^{1}H NMR (500 MHz, [D$_6$]DMSO): δ = 8.00 – 7.34 (m, 7H; aromatic protons of azobenzene), 2.72 and 2.71 (s, 6H; C$_6$H$_3$-C*H$_3$* and C$_6$H$_4$-C*H$_3$*).

Compound 3-1: (yield: 88.6 %), ^{1}H NMR (500 MHz, [D$_6$]DMSO): δ = 7.09 (s, 2H; aromatic protons of benzene), 2.29 (s, 3H; C$_6$H$_2$(CH$_3$)$_2$-C*H$_3$* (4-position)), 2.21 (s, 6H; C$_6$H$_2$CH$_3$-C*H$_3$* (2-and 6-position)).

Compound 3-2: (yield: 21.9 %), ^{1}H NMR (500 MHz, [D$_6$]DMSO): δ = 7.84 (s, 2H;

aromatic protons of benzene), 2.30 (s, 6H; C_6H_2-(CH_3)$_2$).

Compound 3-3: (yield: 94.7 %). ^{1}H NMR (500 MHz, [D$_6$]DMSO): δ = 7.88 (s, 2H; aromatic protons of benzene), 4.37 (q, ^3J(H,H) = 7.0 Hz, 2H; -O-CH_2-CH$_3$), 2.31 (s, 6H; C_6H_2-(CH_3)$_2$), 1.35 (t, ^3J(H,H) = 7.0 Hz, 3H; -O-CH$_2$-CH_3).

Compound 3-4: Silica gel column chromatography (Hexane : AcOEt = 5 : 1), (yield: 66.5 %), ^{1}H NMR (500 MHz, [D$_6$]DMSO): δ = 7.45 (s, 2H; aromatic protons of benzene), 4.21 (q, ^3J(H,H) = 7.0 Hz, 2H; -O-CH_2-CH$_3$), 2.10 (s, 6H; C_6H_2-(CH_3)$_2$), 1.28 (t, ^3J(H,H) = 7.0 Hz, 3H; -O-CH$_2$-CH_3).

Compound 3-5: Silica gel column chromatography (hexane : AcOEt = 20 : 1) (yield: 28.9 %), ^{1}H NMR (500 MHz, [D$_6$]DMSO): δ = 7.92 – 7.63 (m, 7H; aromatic protons of azobenzene), 4.36 (q, ^3J(H,H) =7.0 Hz, 2H; -O-CH_2-CH$_3$), 2.27 (s, 6H; -NC$_6H_2$-(CH$_3$)$_2$), 1.36 (t, ^3J(H,H) = 7.0 Hz, 3H; -O-CH$_2$-CH_3).

Compound 3-6: (yield: 97.9 %), ^{1}H NMR (500 MHz, [D$_6$]DMSO): δ = 7.91 - 7.62 (m, 7H; aromatic protons of azobenzene), 2.27 (s, 6H; C_6H_2-CH_3).

Compound 4-1: Silica gel column chromatography (hexane: AcOEt = 10 :1), (yield: 55.4 %), ^{1}H NMR (500 MHz, [D$_6$]DMSO): δ = 8.34 - 8.11 (d, 4H, ^3J(H,H) = 8.0 Hz, aromatic protons), 4.44 (q, 2H, ^3J(H,H) = 7.0 Hz, -CH_2-CH$_3$), 1.41 (d, 3H, ^3J(H,H) = 7.0 Hz, -CH$_3$-CH_2).

Compound 4-2 of 2′-Me-Azo: Silica gel column chromatography (hexane: AcOEt = 20 :1), (yield 53.3%), ^{1}H NMR (500 MHz, [D$_6$]DMSO): δ = 8.17 – 6.94 (m, 8H, aromatic protons of azobenzene), 4.38 (q, ^3J(H,H) = 7.0, 2H, -O-CH_2-CH$_3$), 2.70 (s,3H,

-NC_6H_4-CH_3), 1.36 (t.$_3J$(H,H) = 7.0 Hz, 3H, -O-CH_2-CH_3).

Compound 4-3 of 2′-Me-Azo: (yield quant), ^{1}H NMR (500 MHz, [D_6]DMSO): δ = 8.16 – 6.93 (m, 8H, aromatic protons of azobenzene), 2.71 (s, 3H, -NC_6H_4-CH_3).

Compound 4-2 of 2′-Et-Azo: Silica gel column chromatography (hexane: AcOEt = 20 :1) (yield 64.6%): ^{1}H NMR (500 MHz, [D_6]DMSO): δ = 8.18 – 6.96 (m, 8H, aromatic protons of azobenzene), 4.38 (q, $_3J$(H,H) = 7.00, 2H, -O-CH_2-CH_3), 3,17 (q, ^3J(H,H) = 7.5 Hz, 2H, -NC_6H_4-CH_2-CH_3) 1.37 (t, ^3J(H,H) = 7.00 Hz, 3H, -O-CH_2-CH_3), 1.26 (t, ^3J(H,H) = 7.5 Hz, 3H, -NC_6H_4-CH_2-CH_3).

Compound 4-3 of 2′-Et-Azo: (yield quant): ^{1}H NMR (500 MHz, [D_6]DMSO): δ = 8.17 – 7.35 (m, 8H, aromatic protons of azobenzene), 3.17 (q, ^3J(H,H) = 7.5 Hz, 2H, -NC_6H_4-CH_2-CH_3), 1.27 (t, ^3J(H,H) = 7.5 Hz, 3H, -NC_6H_4-CH_2-CH_3)

Compound 4-2 of 3′-Me-Azo: Silica gel column chromatography (hexane: AcOEt = 20 :1) (yield 50.7%): ^{1}H NMR (500 MHz, [D_6]DMSO): δ = 8.18 – 6.95 (m, 8H, aromatic protons of azobenzene), 4.39 (q, ^3J(H,H) = 7.0, 2H, -O-CH_2-CH_3), 2.44 (s, 3H, -NC_6H_4-CH_3), 1.37 (t, ^3J(H,H) = 7.0 Hz, 3H, -O-CH_2-CH_3).

Compound 4-2 of 4′-Me-Azo: Silica gel column chromatography (hexane: AcOEt = 5 :1) (yield 41.5%) 1H NMR (500 MHz, [D_6]DMSO) δ = 8.17 – 7.43 (m, 8H, aromatic protons of azobenzene), 4.39 (q, ^3J(H,H) = 7.0, 2H, -O-CH_2-CH_3), 2.43 (s, 3H, -NC_6H_4-CH_3), 1.37 (t,^3J(H,H) = 7.0 Hz, 3H, -O-CH_2-CH_3).

Compound 4-3 of 4′-Me-Azo: Silica gel column chromatography (chloroform : MeOH = 20 : 1) (yield 99.1%), ^{1}H NMR (500 MHz, [D_6]DMSO) δ = 8.15 – 7.43 (m,

8H, aromatic protons of azobenzene), 2.43 (s, 3H, -NC_6H_4-CH_3).

Compound 4-2 of 2′,6′-Me-Azo: Silica gel column chromatography (hexane: AcOEt = 20 :1) (yield 26.6%), 1H NMR (500 MHz, [D_6]DMSO) δ = 8.22 – 7.24 (m, 7H, aromatic protons of azobenzene), 4.43 (q, ^3J(H,H) = 7.0, 2H, -O-CH_2-CH_3), 2.39 (s,6H, -NC_6H_3(CH_3)$_2$), 1.41 (t, ^3J(H,H) = 7.0 Hz, 3H, -O-CH_2-CH_3).

Compound 4-3 of 2′,6′-Me-Azo: (yield 94.7%), 1H NMR (500 MHz, [D_6]DMSO) δ = 8.20 – 7.00 (m, 7H, aromatic protons of azobenzene), 2.38 (s, 6H, -NC_6H_3(CH_3)$_2$).

Compound 4-2 of 3′,5′-Me-Azo: Silica gel column chromatography (hexane: AcOEt = 20 :1) (yield 30.4%), ^{1}H NMR (500 MHz $CDCl_3$,] δ = 8.20 – 7.14 (m, 7H, aromatic protons of azobenzene), 4.43 (q, ^3J(H,H) = 7.0, 2H, -O-CH_2-CH_3), 2.41 (s ,6H, -NC_6H_3(CH_3)$_2$), 1.43 (t.^3J(H,H) = 7.0 Hz, 3H, -O-CH_2-CH_3).

Compound 4-3 of 3′,5′-Me-Azo: (yield 74.4%), ^{1}H NMR (500 MHz $CDCl_3$) δ = 8.28 – 7.17 (m, 7H, aromatic protons of azobenzene), 2.44 (s, 6H, -NC_6H_3(CH_3)$_2$).

2-5-1-2 Synthesis of phosphoramidite monomers of azobenzene derivatives

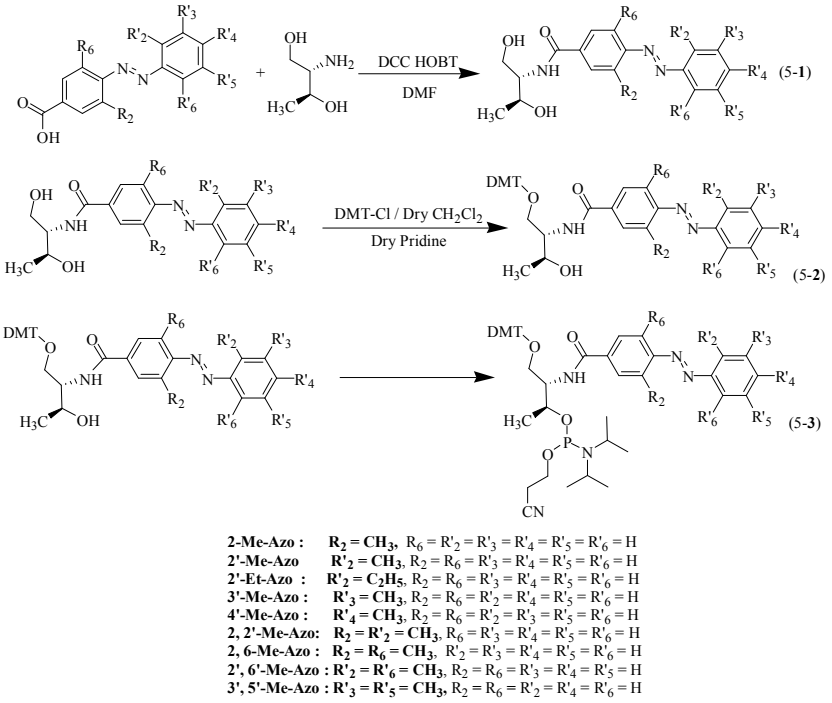

Scheme 5. Synthesis of phosphoramidite monomers of azobenzene derivatives.

Phosphoramidite of **2,-Me-Azo, 2′-Me-Azo**, **2′-Et-Azo**, **3′-Me-Azo**, **4′-Me-Azo, 2,2′-Me-Azo, 2′,6′-Me-Azo** and **3′,5′-Me-Azo** were synthesized according to the Scheme 5. Typical procedures are described by taking **3′-Me-Azo** as an example as follows.

Compound 5-1 of **3′-Me-Azo** was synthesized as follows: 0.13 g (1.24 mmol) of D-threoninol was coupled with 0.33 g (1.37 mmol) of compound 4-**3** (**3′-Me-Azo)** in the presence of 0.28 g (1.36 mmol) of dicyclohexylcarbodiimide and 0.19 g (1.41 mmol) of 1-hydroxybenzotriazole in 40ml of DMF. After the reaction mixture was stirred at room temperature for 24 h under dark, the solvent was removed and the remained oil was subjected to silica gel column chromatography (chloroform : MeOH = 20 : 1) to afford 0.39 g (1.19 mmol) of **1** (yield 97.5%).

Compound 5-2 of **3′-Me-Azo** was synthesized: Dry pyridine solution (10 ml) containing 0.39g (1.19 mmol) of compound 5-**1** (**3′-Me-Azo**) was cooled on ice under nitrogen, and 0.44 g (1.30 mmol) of 4,4-dimethoxytrityl chloride in 10 ml of dichloromethane was added to the above mixture. After 6 h of stirring, the solvent was removed, followed by silica gel column chromatography (Hexane : AcoEt : Et_3N = 50 : 50 : 3) to afford 0.34 g (0.54 mmol) of **2** (yield 45.3%).

Compound 5-3 of **3′-Me-Azo** was synthesized as follows: In dry acetonitrile (4 ml) under nitrogen, 0.17 g (0.27 mmol) of compound 5-**2 (3′-Me-Azo)** and 0.09 g (0.30 mmol) of 2-cyanoethyl *N,,N,,N′,N′* -tetraisopropylphosphordiamidite were reacted with 0.021 g (0.35 mmol) of 1*H*-tetrazole. Prior to the reaction, compound 5-**2 (3′-Me-Azo)** and 1*H*-tetrazole were dried by coevaporation with dry acetonitrile (twice). After 2 h, the solvent was removed by evaporation then the crude mixture was dissolved in ethyl acetate. The solvent was washed with distilled water and saturated solution of $NaHCO_3$ and NaCl and dried over $MgSO_4$. After removal the solvent, the oily product **3** was directly used for the DNA synthesis.

NMR assignment

Compound 5-1 of 2-Me-Azo: Silica gel column chromatography (ethyl acetate), (yield 88.9%), ^{1}H NMR(500 MHz, [D_6]DMSO) δ = 7.96 - 7.60 (m, 9H, aromatic protons of azobenzene, -N*H*CO-), 4.66 (m, 2H, $CH_3CH(OH)$-, -(NH)$CHCH_2(OH)$), 3.96 (m, 2H, -CH_2(OH)C*H*(NH)CO-)-, C*H*(OH)CH_3), 3.64 and 3.57 (m, 2H, HOCH_2CH(NH)CO), 2.73 (s,3H, -NC_6H_3-CH_3), 1.08 (d, ^3J(H,H) = 6.5 Hz, CH(OH)CH_3).

Compound 5-2 of 2-Me-Azo: Silica gel column chromatography (hexane : AcOEt : Et_3N = 60 : 40 : 3), (yield 42.6%), ^{1}H NMR ($CDCl_3$, 500 MHz) δ = 7.97 – 6.78 (m, 22H, aromatic protons of azobenzene, DMT, -N*H*CO-), 4.26 (m, 1H, -C*H*(OH)CH_3), 4.16 (m, 1H, -CH_2(ODMT)C*H*(NHCO-)-), 3.77 and 3.76 (s, 6H, -C_6H_4-OCH_3), 3.62 and 3.40 (dd, ^2J(H,H) = 9.5 Hz, ^3J(H,H) = 4.0 Hz, 2H, CH_2-ODMT), 2.78 (s, 3H, -NC_6H_3-CH_3), 1.24 (d, ^3J(H,H) = 6.5 Hz 3H, -CH(OH)CH_3) m/z 630 $(MH)^+$ (calcd. 630).

Compound 5-1 of 2′-Me-Azo: Silica gel column chromatography (chloroform : MeOH = 20 : 1), (yield quant.), ^{1}H NMR (500 MHz, [D_6]DMSO) δ = 8.10- 6.92 (m, 9H, aromatic protons of azobenzene, -N*H*CO-), 4.70 (m, 2H, CH_3CH(O*H*)-, -(NH)CHCH_2(O*H*)), 3.98 (m, 2H, -CH_2(OH)C*H*(NH)CO-)-, C*H*(OH)CH_3), 3.66 and 3.59 (m, 2H, HOCH_2CH(NH)CO), 2.71 (s,3H, -NC_6H_4-CH_3), 1.10 (d, ^3J(H,H) = 6.0 Hz, CH(OH)CH_3).

Compound 5-2 of 2′-Me-Azo: Silica gel column chromatography (hexane : AcOEt : Et3N = 50 : 50 : 3), (yield 36.5%), ^{1}H NMR ($CDCl_3$, 500 MHz) δ = 8.00 – 6.77 (m, 22H, aromatic protons of azobenzene, DMT, -N*H*CO-), 4.26 (m, 1H, -C*H*(OH)CH_3), 4.16 (m, 1H, -CH_2(ODMT)C*H*(NHCO-)-), 3.77 and 3.76 (s, 6H, -C_6H_4-OCH_3), 3.63 and 3.42 (dd, ^2J(H,H) = 9.5 Hz, ^3J(H,H) = 4.0 Hz, 2H, CH_2-ODMT), 2.76 (s, 3H, -NC_6H_4-CH_3), 1.24 (d, ^3J(H,H) = 6.5 Hz, 3H, -CH(OH)CH_3), MS(FAB): m/z 630 $(MH)^+$ (calcd. 630).

Compound 5-1 of 2′-Et-Azo: Silica gel column chromatography (ethyl acetate only), (yield 91.9%), ^{1}H NMR (500 MHz, [D_6]DMSO) δ = 8.10- 7.35 (m, 9H, aromatic protons of azobenzene, -N*H*CO-), 4.67 (m, 2H, CH_3CH(O*H*)-, -(NH)CHCH_2(O*H*)), 3.96 (m, 2H, -CH_2(OH)C*H*(NH)CO-)-, C*H*(OH)CH_3), 3.64 and 3.54 (m, 2H, HOCH_2CH(NH)CO), 3.17 (q, ^3J(H,H) = 7.5 Hz, 2H, -NC_6N_4-CH_2-CH_3), 1.27 (t,

^{3}J(H,H) = 7.5 Hz, 3H, -NC_6H_4-CH_2-CH_3), 1.09 (d, ^{3}J(H,H) = 6.5 Hz, CH(OH)CH_3).

Compound 5-2 of 2′-Et-Azo: Silica gel column chromatography (hexane : AcOEt : Et_3N = 60 : 40 : 3), (yield 66.4%), ^{1}H NMR ($CDCl_3$, 500 MHz) δ = 8.00 – 6.78 (m, 22H, aromatic protons of azobenzene, DMT, -N*H*CO-), 4.25 (m, 1H, -C*H*(OH)CH_3), 4.16 (m, 1H, -CH_2(ODMT)C*H*(NHCO-)-), 3.77 and 3.76 (s, 6H, -C_6H_4-OCH_3), 3.63 and 3.42 (dd, ^{2}J(H,H) = 10 Hz, ^{3}J(H,H) = 4.0 Hz, 2H, CH_2-ODMT), 3.22 (q, ^{3}J(H,H) = 7.5 Hz, 2H, -NC_6N_4-CH_2-CH_3), 1,34 (t, ^{3}J(H,H) = 7.5 Hz, 3H, -NC_6H_4-CH_2-CH_3) 1.24 (d, ^{3}J(H,H) = 6.5 Hz 3H, -CH(OH)CH_3), m/z 644 $(MH)^+$ (calcd. 644).

Compound 5-1 of 3′-Me-Azo: Silica gel column chromatography (chloroform : MeOH = 20 : 1), (yield 97.5%), ^{1}H NMR (DMSO, 500 MHz) δ = 8.10- 7.42 (m, 9H, aromatic protons of azobenzene, -N*H*CO-), 4.67 (m, 2H, CH_3CH(O*H*)-, -(NH)CHCH_2(O*H*)), 3.97 (m, 2H, -CH_2(OH)C*H*(NH)CO-)-, C*H*(OH)CH_3), 3.64 and 3.53 (m, 2H, HOCH_2CH(NH)CO), 2.44 (s,3H, -NC_6H_4-CH_3), 1.09 (d, ^{3}J(H,H) = 6.0 Hz, CH(OH)CH_3).

Compound 5-2 of 3′-Me-Azo: Silica gel column chromatography (hexane : AcOEt : Et_3N = 50 : 50 : 3), (yield 45.3%), ^{1}H NMR ($CDCl_3$, 500 MHz) δ = 8.00 – 6.78 (m, 22H, aromatic protons of azobenzene, DMT, -N*H*CO-), 4.26 (m, 1H, -C*H*(OH)CH_3), 4.16 (m, 1H, -CH_2(ODMT)C*H*(NHCO-)-), 3.77 and 3.76 (s, 6H, -C_6H_4-OCH_3), 3.62 and 3.42 (dd, ^{2}J(H,H) = 9.5 Hz, ^{3}J(H,H) = 4.0 Hz, 2H, CH_2-ODMT), 2.48 (s, 3H, -NC_6H_4-CH_3), 1.24 (d, ^{3}J(H,H) = 6.5 Hz 3H, -CH(OH)CH_3), m/z 630 $(MH)^+$ (calcd. 630).

Compound 5-1 of 4′-Me-Azo: Silica gel column chromatography (chloroform : MeOH = 20 : 1), (yield 99.1%), ^{1}H NMR (500 MHz, [D_6]DMSO) δ = 8.08- 7.42 (m, 9H,

aromatic protons of azobenzene, -N*H*CO-), 4.66 (m, 2H, $CH_3CH(OH)$-, -(NH)$CHCH_2(OH)$), 3.96 (m, 2H, -CH_2(OH)C*H*(NH)CO-)-, C*H*(OH)CH_3), 3.64 and 3.53 (m, 2H, HOCH_2CH(NH)CO), 2.42 (s,3H, -NC_6H_4-CH_3), 1.08 (d, ^3J(H,H) = 6.5 Hz, CH(OH)CH_3).

Compound 5-2 of 4′-Me-Azo: Silica gel column chromatography (hexane : AcOEt : Et3N = 50 : 50 : 3), (yield 32.2%), ^{1}H NMR ($CDCl_3$, 500 MHz) δ = 7.99 – 6.79 (m, 22H, aromatic protons of azobenzene, DMT, -N*H*CO-), 4.25 (m, 1H, -C*H*(OH)CH_3), 4.14 (m, 1H, -CH_2(ODMT)C*H*(NHCO-)-), 3.77 and 3.76 (s, 6H, -C_6H_4-OCH_3), 3.62 and 3.42 (dd, ^2J(H,H) = 9.5 Hz, ^3J(H,H) = 4.0 Hz, 2H, CH_2-ODMT), 2.46 (s, 3H, -NC_6H_4-CH_3), 1.24 (d, ^3J(H,H) = 6.0 Hz 3H, -CH(OH)CH_3), MS(FAB): m/z 630 $(MH)^+$ (calcd. 630).

Compound 5-1 of 2,6-Me-Azo: (yield: quant). ^{1}H NMR (500 MHz, [D_6]DMSO): δ = 7.90 – 7.51 (m, 8H; aromatic protons of azobenzene, -N*H*CO-), 4.63 (m, 2H; $CH_3CH(OH)$-, -(NH)$CHCH_2(OH)$), 3.95 (m, 2H; -CH_2(OH)C*H*(NH)CO-)-, C*H*(OH)CH_3), 3.63 and 3.52 (m, 2H; HOCH_2CH(NH)CO), 2.31 (s,6H; -C_6H_2-(CH_3)$_2$-NC_6H_5), 1.08 (d, ^3J(H,H) = 6.0 Hz, 3H; CH(OH)CH_3).

Compound 6-2 of 2,6-Me-Azo: ^{1}H NMR for Compound **3-2** of **2,6-Me-Azo** (500 MHz, $CDCl_3$): δ = 7.94 - 6.79 (m, 21H; aromatic protons of azobenzene and DMT, -N*H*CO-), 4.25 (m, 1H; -C*H*(OH)CH_3), 4.15 (m, 1H; -CH_2(OH)C*H*(NHCO-)-), 3.78 and 3.77 (s, 6H; -C_6H_5-OCH_3), 3.62 and 3.38 (dd, ^2J(H,H) = 10 Hz, ^3J(H,H) = 4.0 Hz, 2H; CH_2-ODMT), 2.37 (s, 6H; -NC_6H_4(CH_3)$_2$), 1.23 (d, ^3J(H,H) = 6.0 Hz 3H; -CH(OH)CH_3). MS (FAB): m/z 644 $(MH)^+$ (calcd. 644).

Compound 5-1 of 2,2′-Me-Azo: (yield: quant), ^{1}H NMR (500 MHz, [D_6]DMSO): δ

= 7.94 – 7.33 (m, 8H; aromatic protons of azobenzene, -N*H*CO-), 4.64 (m, 2H; $CH_3CH(OH)$-, -(NH)$CHCH_2(OH)$), 3.96 (m, 2H; -CH_2(OH)C*H*(NH)CO-)-, C*H*(OH)CH_3), 3.64 and 3.53 (m, 2H; HOCH_2CH(NH)CO), 2.73 and 2.71 (s,6H; -C_6H_3-C*H*$_3$-NC_6H_4-C*H*$_3$), 1.08 (d, ^3J(H,H) = 4.0 Hz, 3H; CH(OH)C*H*$_3$).

Compound 6-2 of 2,2′-Me-Azo: (yield 64.5 %), ^{1}H NMR (500 MHz, $CDCl_3$): δ = 7.80 - 6.76 (m, 21H; aromatic protons of azobenzene and DMT, -N*H*CO-), 4.24 (m, 1H; -C*H*(OH)CH_3), 4.15 (m, 1H; -CH_2(OH)C*H*(NHCO-)-), 3.77 and 3.76 (s, 6H; -C_6H_5-OC*H*$_3$), 3.62 and 3.40 (dd, ^2J(H,H) = 10 Hz, ^3J(H,H) = 4.0 Hz, 2H; CH_2-ODMT), 2.79, 2.77 (s, 6H; -C_6H_3-C*H*$_3$-NC_6H_4-C*H*$_3$), 1.24 (d, ^3J(H,H) = 6.5 Hz, 3H; -CH(OH)C*H*$_3$). MS (FAB): m/z 644 $(MH)^+$ (calcd. 644).

Compound 5-1 of 2′,6′-Me-Azo: Silica gel column chromatography (chloroform : MeOH = 10 : 1), (yield 95.5%), ^{1}H NMR ($CDCl_3$, 500 MHz) δ = 8.00 – 6.97 (m, 8H, aromatic protons of azobenzene, -N*H*CO-), 4.35 (m, 1H, CH_3C*H*(OH)-), 4.12 (m, 1H, -CH_2(OH)C*H*(NH)CO-)-), 4.00 (m, 2H, HOCH_2CH(NH)CO-), 2.39 (s, 6H, -NC_6H_3(C*H*$_3$)$_2$), 1.31 (d, ^3J(H,H) = 6.5 Hz, CH(OH)C*H*$_3$).

Compound 5-2 of 2′,6′-Me-Azo: Silica gel column chromatography (hexane : AcOEt : Et_3N = 50 : 50 : 3), (yield 53.2%), ^{1}H NMR ($CDCl_3$, 500 MHz) δ = 7.96 – 6.76 (m, 21H, aromatic protons of azobenzene, DMT, -N*H*CO-), 4.25 (m, 1H, -C*H*(OH)CH_3), 4.16 (m, 1H, -CH_2(ODMT)C*H*(NHCO-)-), 3.77 and 3.76 (s, 6H, -C_6H_4-OC*H*$_3$), 3.63 and 3.42 (dd, ^2J(H,H) = 9.5 Hz, ^3J(H,H) = 4.0 Hz, 2H, CH_2-ODMT), 2.41 (s, 6H, -NC_6H_3(C*H*$_3$)$_2$), 1.24 (d, ^3J(H,H) = 6.5 Hz 3H, -CH(OH)C*H*$_3$), MS(FAB): m/z 644 (MH)+ (calcd. 644).

Compound 5-1 of 3′,5′-Me-Azo: Silica gel column chromatography (chloroform : MeOH = 20 : 1), (yield quant), ^{1}H NMR ($CDCl_3$, 500 MHz) δ = 7.98 - 6.99 (m, 7H, aromatic protons of azobenzene), 4.34 (m, 1H, $CH_3CH(OH)$-), 4.11 (m, 1H, -CH_2(OH)C*H*(NH)CO-)-), 3.99 (m, 2H, HOCH_2CH(NH)CO-), 2.43 (s, 6H, -$NC_6H_3(CH_3)_2$), 1.31 (d, ^{3}J(H,H) = 6.5 Hz, CH(OH)CH_3).

Compound 5-2 of 3′,5′-Me-Azo: Silica gel column chromatography (hexane : AcOEt : Et3N = 50 : 50 : 3), (yield 28.5%), ^{1}H NMR ($CDCl_3$, 500 MHz) δ = 7.99 – 6.78 (m, 21H, aromatic protons of azobenzene, DMT, -N*H*CO-), 4.26 (m, 1H, -C*H*(OH)CH_3), 4.16 (m, 1H, -CH_2(ODMT)C*H*(NHCO-)-), 3.77 and 3.76 (s, 6H, -C_6H_4-OCH_3), 3.62 and 3.42 (dd, ^{2}J(H,H) = 9.5 Hz, ^{3}J(H,H) = 4.0 Hz, 2H, CH_2-ODMT), 2.43 (s, 6H, -$NC_6H_3(CH_3)_2$), 1.24 (d, ^{3}J(H,H) = 6.5 Hz 3H, -CH(OH)CH_3).

2-5-1-3 Synthesis of DNA

The modified DNAs containing modified azobenzenes were synthesized on an automated DNA synthesizer (ABI-3400, Applied Biosystems) using conventional and azobenzene-carrying phosphoramidite monomers as described in previous section. All the modified DNAs were purified by reversed-phase HPLC and characterized by MALDI-TOFMS (Autoflex Linear, Bruker Daltonics). The DNAs containing only native bases were supplied by Integrated DNA Technologies, Inc. (Coralville, IA. U.S.A.).

MALDI-TOFMS for **CXG** with **Azo**: obsd. 4021 (calcd. for protonated form: 4020), **2-Me-Azo**: obsd. 4032 (calcd. 4034), **2′-Me-Azo**: obsd. 4035 (calcd. 4034), **2′-Et-Azo**: obsd. 4048 (calcd. 4048), **3′-Me-Azo**: obsd. 4035 (calcd.: 4034), 4′-Me-Azo: obsd. 4035

(calcd. 4034), **2,6-Me-Azo**: obsd. 4047 (calcd. 4048), **2,2′-Me-Azo**: obsd. 4048 (calcd. 4048), **2′,6′-Me-Azo**: obsd. 4049 (calcd. 4048). **3′,5′-Me-Azo**: obsd. 4049 (calcd. 4048).

MALDI-TOFMS for DNAs containing **2′,6′-Me-Azo**: **AXA**: obsd. 4057 (calcd. for protonated form: 4056), **AXC**: obsd. 4034 (calcd. 4032), **AXG**: obsd. 4072 (calcd. 4072), **AXT**: obsd. 4048 (calcd. 4047), **CXA**: obsd. 4031 (calcd. 4032), **CXC**: obsd. 4009 (calcd. 4008), **CXG**: obsd. 4049 (calcd. 4048), **CXT**: obsd. 4021 (calcd. 4023), **GXA**: obsd. 4070 (calcd. 4072), **GXC**: obsd. 4050 (calcd. 4048), **GXG**: obsd. 4091 (calcd. 4088), **GXT**: obsd. 4062 (calcd. 4063), **TXA**: obsd. 4051 (calcd. 4047), **TXC**: obsd. 4023 (calcd. 4023), **TXG**: obsd. 4063 (calcd. 4063), **TXT**: obsd. 4037 (calcd. 4038), $\mathbf{D_{NMR}}$: obsd. 2814 (calcd. for protonated form: 2814).

2-5-2 Calculation of the concentration of DNA involving azobenzene moieties

Generally, the concentration of DNA was calculated from the absorbance at 260 nm because the extinction coefficient at260 nm can be obtained from the DNA sequence in theory.[16] However, the azobenzene derivatives also have large absorbance at 260 nm. Therefore, the extinction coefficient of azobenzene derivatives at 260 nm and the accurate concentration of DNA involving azobenzene derivatives were calculated from two different DNA sequences involving same number of azobenzene derivatives.

Two DNA strand **CXG** which was composed of 12 nucleotides and 1 azobenzene derivative, and $\mathbf{D_S}$ which was compose of 6 native nucleotides and azobenzene were used for calculation. Here, the extinction coefficient at 260 nm of native nucleotides **CXG** and $\mathbf{D_S}$ were called α and β, respectively (both of them can calculated theoretically). In addition the absorbance at340 nm which was based on azobenzene

derivatives were called $A_{340\mathbf{CXG}}$ and $A_{340\mathbf{DS}}$, and those of 260 nm were called $A_{260\mathbf{CXG}}$ and $A_{260\mathbf{DS}}$, respectively (see Figure 2-12).

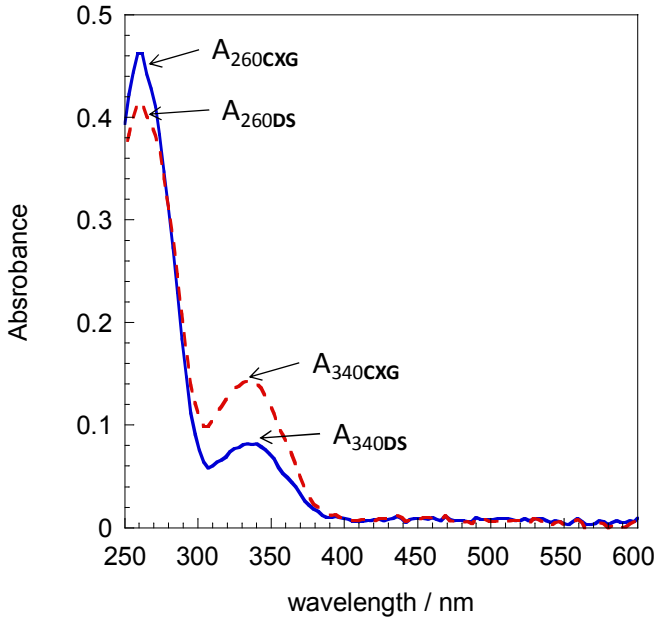

Figure 2-12. Example figures of measurement of concentration DNA involving azobenzene moiety.

If the concentration of both **CXG** and $\mathbf{D_S}$ were equal,the absorbance at 340 nm should be equal. Therefore, if the concentration of $\mathbf{D_S}$ was equal to that of **CXG**, the absorbance of $\mathbf{D_S}$ at 260 nm in the concentration of **CXG** ($Cal\_A_{260\mathbf{CXG}}$) can be calculated as expression **(1)**.

$$Cal\_A_{260\mathbf{DS}} = A_{260\mathbf{DS}} * A_{340\mathbf{CXG}} / A_{340\mathbf{DS}} \qquad \mathbf{(1)}$$

Here, the absorbance of azobenzene derivative at 260 in the concentration of $\mathbf{D_{CXG}}$ called X, the expression **(2)** is realized.

$$(Cal\_A_{260\mathbf{DS}} - X) / (A_{260\mathbf{CXG}} - X) = \beta / \alpha \qquad \mathbf{(2)}$$

Substituting (1) into the (2), X can be described as follows.

$$X = (\beta / \alpha * A_{260\mathbf{CXG}} - A_{260\mathbf{DS}} * A_{340\mathbf{CXG}} / A_{340\mathbf{DS}}) * \{1 / (\beta / \alpha - 1)\} \qquad \mathbf{(3)}$$

The concentration of **CXG** ($C_{\mathbf{CXG}}$) can be calculated as follows.

$$C_{\mathbf{CXG}} = (A260_{\mathbf{CXG}} - X) / \alpha \qquad \mathbf{(4)}$$

The extinction coefficient of azobenzene at 260 nm also can be calculated from expression **(3)** and **(4)**.

The concentration **CXG** involving azobenzene moieties were calculated in this way. The extinction coefficient of **2′,6′-Me-Azo** at 260 nm was calculated as 0.245 *10^5 mol / cm and that of Azo was 0.07 *10^5 mol / cm.

2-5-3 T_m measurements

T_m values were determined from the maximum in the first derivative of the melting curve, which was obtained by measuring the absorbance at 260 nm with a JASCO V-530 UV-Vis spectrophotometer as a function of temperature. The temperature ramp was 1.0 °C/min. Both the heating and cooling curves were measured, and obtained T_m values agreed within 2.0 °C. Conditions of the sample solutions: [NaCl] = 100 mM, pH 7.0 (10 mM phosphate buffer), [DNA] = 5 μM.

2-5-4 Photoisomerization of azobenzene

The light source for photo-irradiation was a 150 W Xenon lamp. For the *trans* → *cis* isomerization, a UV-D36C filter (Asahi Tech. Co.) was used, and UV light (λ = 300-400

nm) was used to irradiate the duplex solution at 60 °C for 5 min. The *cis* → *trans* isomerization was carried out by irradiation with visible light (λ > 400 nm) through an L-42 filter (Asahi Tech. Co.) at 60 °C for 1 min. In both cases, a water filter was used to cut off infrared light.

2-5-5 NMR analysis of DNA tethering 2′,6′-Me-Azo

NMR samples were prepared by dissolving three times lyophilized DNAs to a concentration of 560 μM duplex in H_2O/D_2O (9/1) solution containing 20 mM sodium phosphate (pH 7.0). NaCl was added to a final concentration of 200 mM. NMR spectra were measured on a Varian INOVA (700 MHz) equipped triple resonance at a prove temperature of 278 K. Resonance was assigned with the standard method using a combination of 1D, TOCSY (60 ms of mixing time), DQF-COSY, and NOESY (150 ms of mixing time) experiments. All spectra in the H_2O/D_2O solution were recorded using a 3-9-19 WATERGATE pulse sequence for water suppression.

2-5-6 Molecular modeling

The insight II/Discover 98.0 program package was used for molecular modeling to obtain energy-minimized structures by conformation-energy minimization. The azobenzene residue was built-up using a graphical program. The results of the NMR analyses served as a starting point for the modelling. For the analysis, the duplex was prepared by positioning the modified azobenzene in *trans*- or *cis*- form between the adjacent base-pairs. The effect of water and counter ions was simulated by a sigmoidal, distance-dependent, direct function. The B-type duplex was used and AMBER force filed was used for calculation. Computation was carried out on a Silicon Graphics O2

workstation with the operating system IRIX64 Release 6.5.

2-6 Note and References

[1] H. Asanuma, T. Takarada, T. Yoshida, D. Tamaru, X. G. Liang, M. Komiyama, *Angew. Chem., Int. Ed.* **2001**, *40*, 2671-2673.

[2] a) H. Asanuma, D. Tamaru, A. Yamazawa, M. Liu, M. Komiyama, *ChemBioChem*, **2002**, *8*, 786-789.b) D. Matsunaga, H. Asanuma, M. Komiyama, *J. Am. Chem. Soc.* **2004**, *126*, 11452-11453. c) X. G. Liang, T. Mochizuki, H. Asanuma, *Small*, **2009**, *15*, 1761-1768.

[3] H. Asanuma, D. Matsunaga, M. Komiyama, *Nucleic Acids Symp Ser.*, **2005**, *49*, 35-6.

[4] Modification at *para*-position led to the reversed photoswitch with the combination of L-threoninol. See X. G. Liang, N. Takenaka, H. Nishioka, H. Asanuma, *Chem. Asian. J.* **2008**, *3*, 553-560

[5] Note that di-methylation of *ortho*-positions of one benzene ring, the *trans*-to *cis*-photoisomerization was decreased because of steric hindrance. After UV light irradiation, the rates of *cis*-**2,6-Me-Azo** and *cis*-**2′,6′-Me-Azo** were about 65 % whereas those of other modified or non-modified azobenzenes were over 80 % (The absorbance spectra showed in Appendix section). Therefore, as shown in Figure 2-5B and C, in the T_m curve of *cis*-**2,6-Me-Azo** and *cis*-**2′,6′-Me-Azo**, especially for latter one, there were two sigmoid could be found. The upper one would correspond remained *trans*-**2′,6′-Me-Azo** and lower one would correspond *cis*-**2′,6′-Me-Azo** (photoisomerization of modified azobenzene derivatives were discussed in Chapter 3).

[6] R. E. Holmlin, E. D. A. Stemp, J. K. Barton, *Inorg. Chem.* **1998**, *37*, 29-34.

[7] Weak signal at 12.7 ppm was assignable to one of the terminal base-pairs (G^1 or G^9). Other terminal imino proton signal might be overlapped with the signal at 12.8 ppm.

[8] X. G. Liang, H. Asanuma, H. Kashida, A. Takasu, T. Sakamoto, G. Kawai, M. Komiyama, *J. Am. Chem.* **2003**, *125*, 16408-16415.

[9] As described above, DNA duplex contained *cis*-**2′,6′-Me-Azo** was much more unstable than that of *trans*-form.

[10] M. Liu, H. Asanuma, M. Komiyama, *J. Am. Chem. Soc*. **2006**, *128*, 1009-1015.

[11] H. Kagechika, T. Himi, K. Namikawa, E. Kawachi, Y. Hashimoto, K. Shudo, *J. Med. Chem.* **1989**, *32*, 1098-1108.

[12] H. D. H. Showalter, L. Sun, A. D. Sercel, Winters, R. T. W. A. Denny, B. D. Palmer, *J. Org. Chem.*, **1996**, *61*, 1155-1158.

[13] W. H.Hutting, R. A. Jewell, H. Rapoport, *J. Org. Chem.*, **1970**, *35*, 505-508.

[14] G. Powell, F. R. Johnson in *Organic Syntheses*, Vol. 2 (Eds.: W. W. Hartman, J. B. Dickey), Wiley and Sons: New York, **1943**, pp 449-450.

[15] J. P. Schaefer, T. J. Miragla, *J. Am. Chem. Soc.* **1964**, *86*, 64-67.

[16] C. R. Cantor, *Bioplymers*, **1970**, *9*, 1059-1077.

2-7 Appendixes

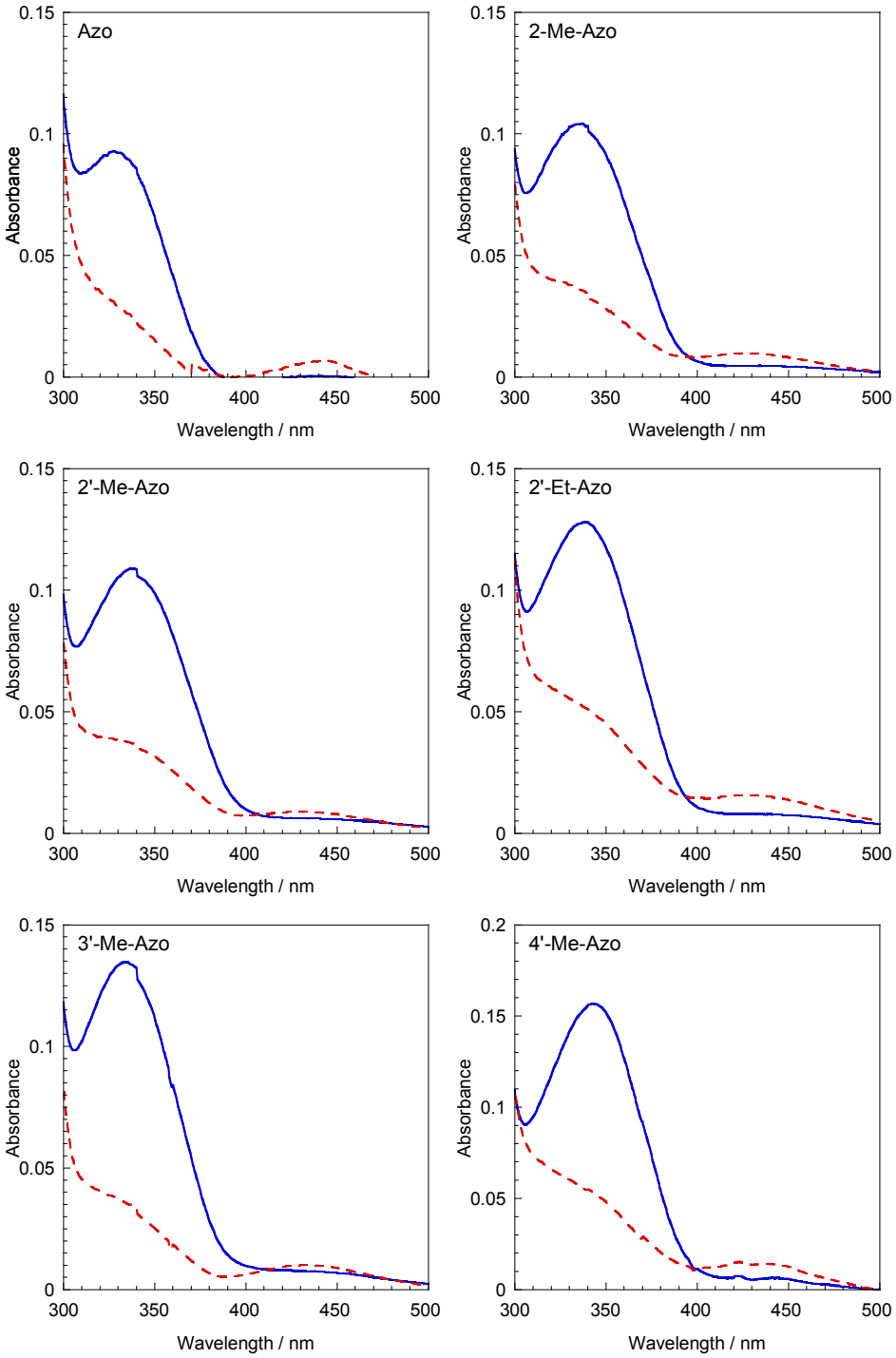

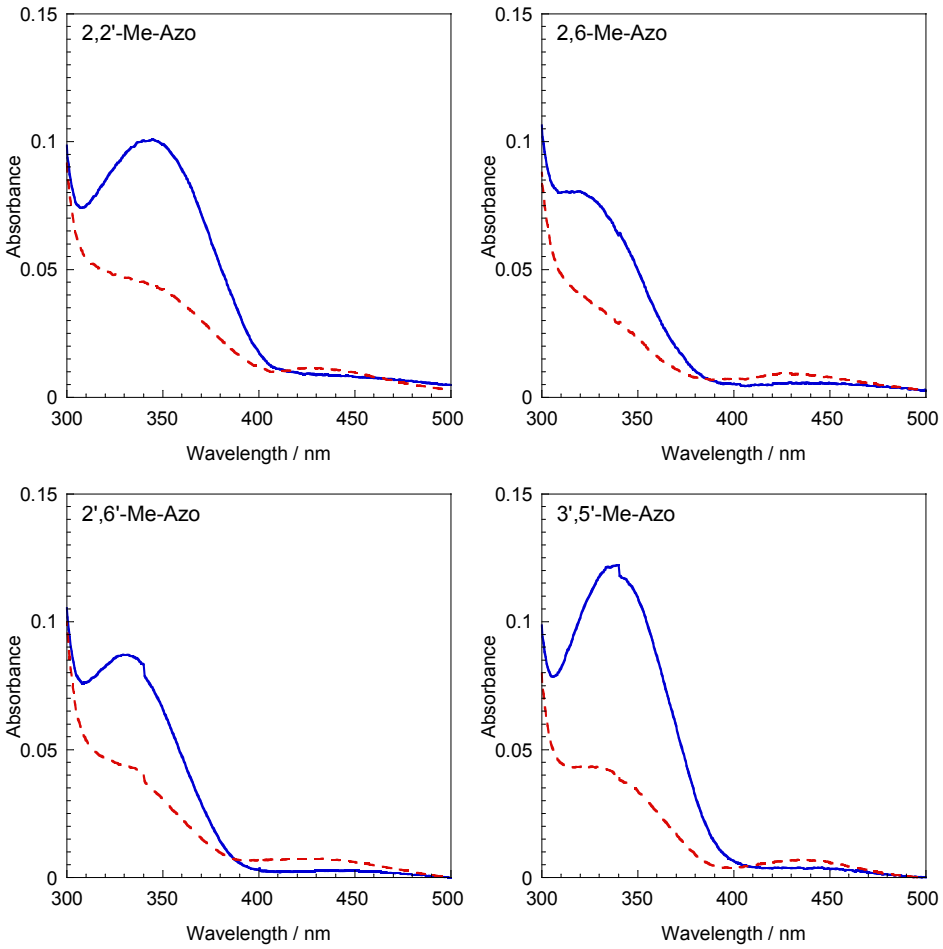

Appendix Figure 2-1. Absorbance spectra of azobenzene derivatives either *trans*- (blue solid line) or *cis*-form (red dot line) tethered into CXG strand together with GC. Azo and 3′-Me-Azo were at 65 °C and others were at 60 °C. Solution conditions: [DNA] = 5 μM, [NaCl] = 100 mM, pH 7.0 (10 mM phosphate buffer).

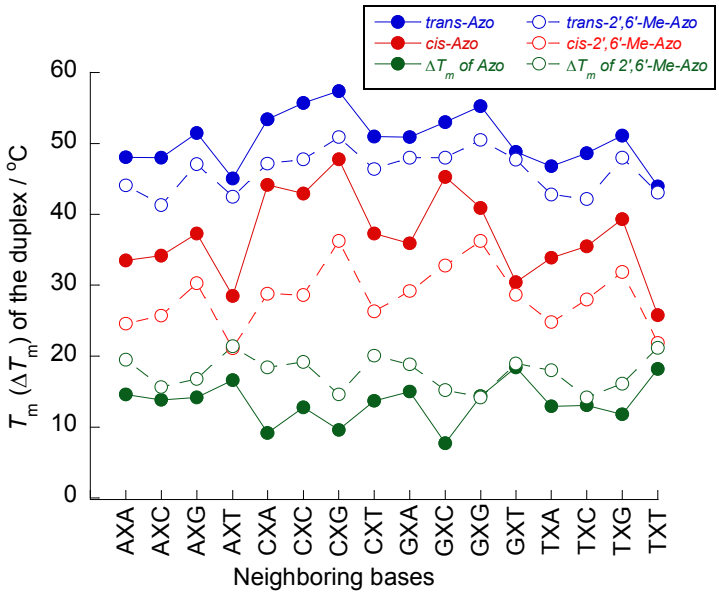

Appendix Figure 2-2. Plots of T_ms in *trans*- (blue) and *cis*-form (red), and ΔT_ms (green) of the duplexes involving **Azo** (closed circles) or **2′,6′-Me-Azo** (open circles) with respect to neighboring bases.

The sequence of DNA involving **Azo**: 5′-GCG**N**$_1$**X****N**$_2$TCG-3′ where **N**$_1$, **N**$_2$, and **X** represent natural nucleotides (A, G, C, T) and **Azo** residue, respectively. Solution conditions for **Azo**: [DNA] = 4 μM, [NaCl] = 1 M, pH 7.0 (10 mM phosphate buffer). The data for **Azo** were quoted from *Nucleic Acids Symp. Ser.*, **2005**, *49*, 283-284.

The duplex involving **Azo** showed almost the same dependency of T_m on adjacent base-pairs as that of **2′,6′-Me-Azo** in both *trans* and *cis*-form. In addition, although the length of the present sequence involving **2′,6′-Me-Azo** was 4-bases longer than that of **Azo** which our group previously used, the ΔT_m of **2′,6′-Me-Azo** was higher than that of **Azo** with all the sequences , demonstrating the superiority of **2′,6′-Me-Azo.**

(A) (B)

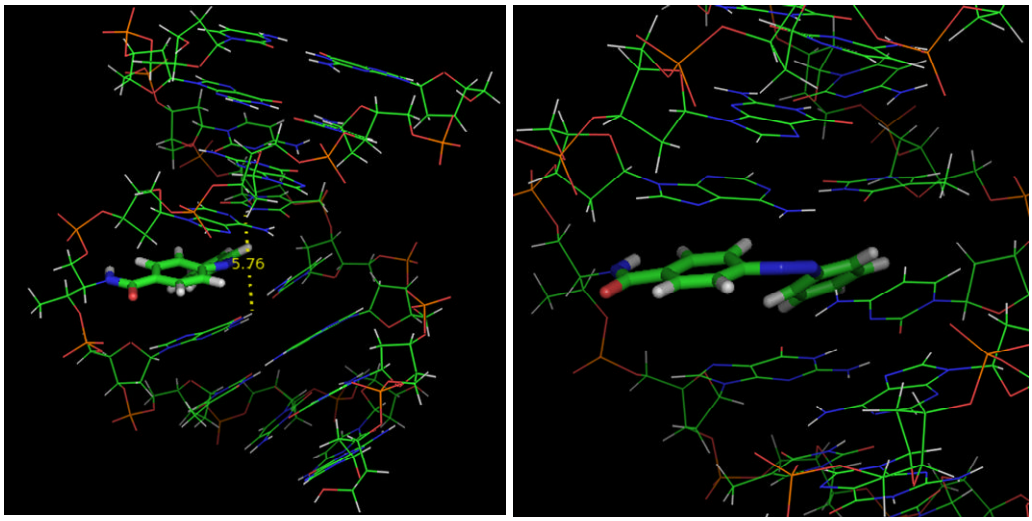

Azo

(A) (B)

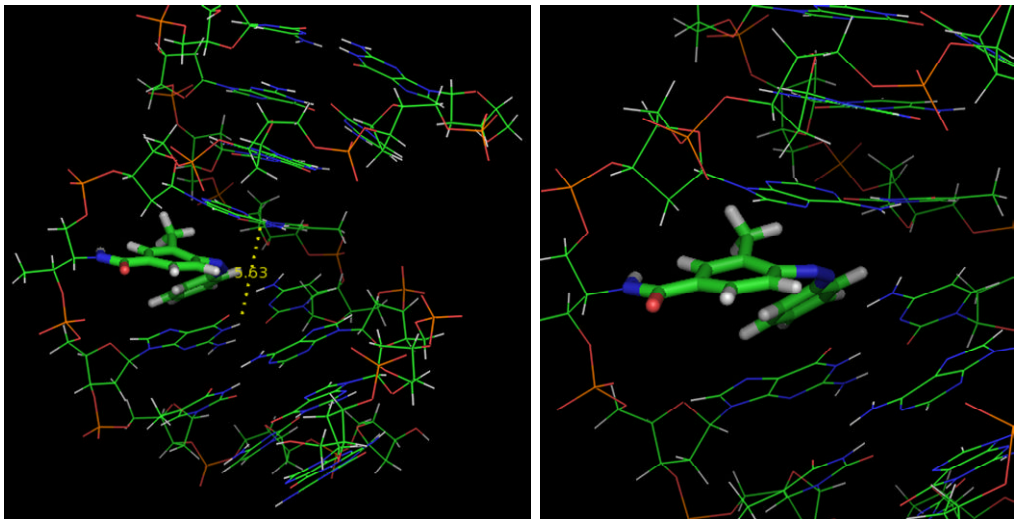

2-Me-Azo

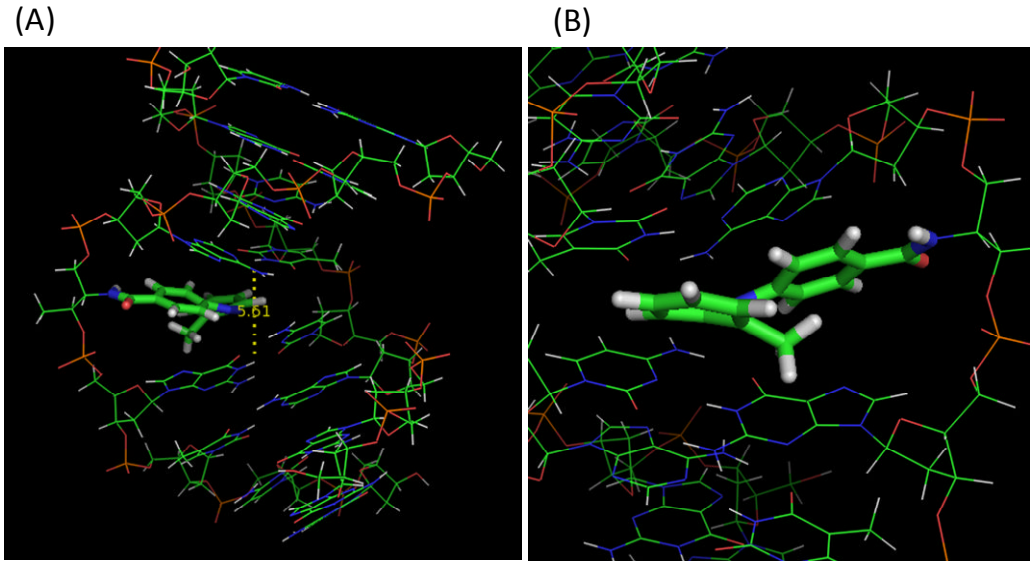

2′-Me-Azo

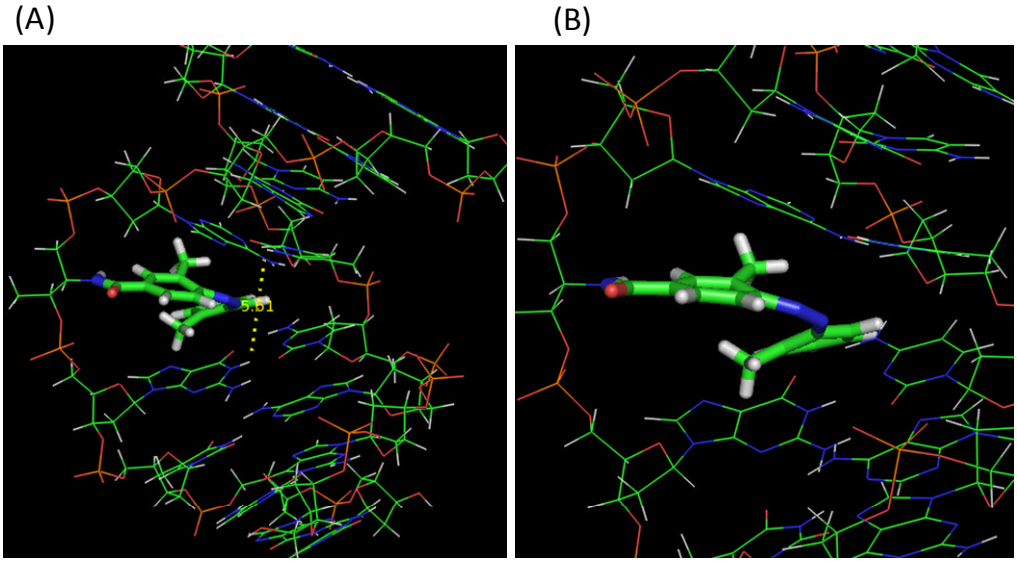

2,2′-Me-Azo

Appendix Figure 2-3. Energy-minimized structure of a modified duplex involving *cis*-azobenzene moieties viewed from the side of azobenzene. (A) Whole structure of the duplex. (B) Magnified around azobenzene moiety**.** The distances of imino protons between G^{5}-C^{12} and A^{4}-T^{13}, depicted with dotted yellow line in (A), were shown in Table 2-4.

Chapter 3. Photo and Thermal isomerization of Azobenzene Derivatives

3-1 Abstract

Photoisomerization and thermal stability of azobenzene derivatives which were used for photoregulation of DNA hybridization were investigated. By methylation at two ortho-positions of benzene ring decreased the *trans*-to *cis*- photoisomerization in single-stranded DNA. The thermal stability of *cis*-**2′,6′-Me-Azo** in which two ortho-positions of distal benzene ring were methylated was greatly improved, but not that of *cis*-**2,6-Me-Azo** in which two *ortho*-positions of proximal benzene ring were methylated. By measurement of thermal stability of several newly synthesized *ortho*-methylated *cis*-azobenzene derivatives, it was cleared that the improvement of thermal stability of *cis*-**2′,6′-Me-Azo** but not that of *cis*-**2,6-Me-Azo** was attributed to the retardation of the inversion process due to steric hindrance between lone-pair electrons of the π orbital of the N atom and the methyl group on the distal benzene ring.

3-2 Introduction

Azobenzene and its derivatives is excellent photo responsive molecule which can be isomerized *trans*- to *cis*-form and *cis*-to *trans*-form by selecting the irradiation

wavelength (Figure 3-1). However, only with photo irradiation, it is impossible to isomerize all azobenzene molecules neither only *trans*-form nor only *cis*-form and the rate of *cis*-or *trans*-form after light irradiation was influenced by chemical modifications on azobenzene derivatives.[1] In this study, azobenzene derivatives were used as a switch of regulation, so the ratio of *trans*- and *cis*-azobenzene moieties after photo irradiation affects the photoregulation efficiency, especially for multiple introduction of azobenzene moieties (discussed in Chapter 4).

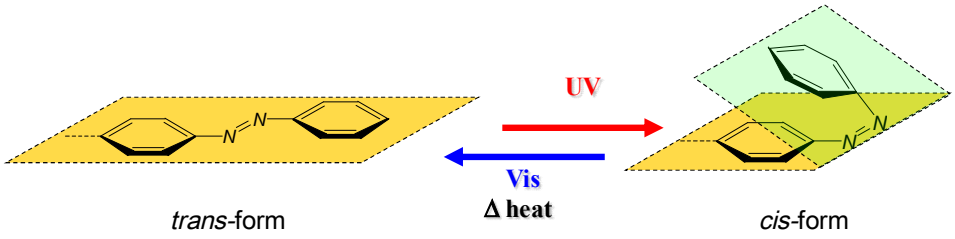

Figure 3-1. Isomerization of azobenzene.

In addition to photoisomerization, *cis*-azobenzene isomerizes to *trans*-form without photo irradiation (thermal isomerization). Like as photoisomerization, thermal isomerization is also influenced by chemical modification.[2] If the azobenzene derivatives isomerization first thermally, it causes unintended change of regulation. Therefore, to understand the thermal isomerization of azobenzene derivatives is important for efficient photoregulation of DNA function. Although several researchers has been proposed the mechanism of thermal isomerization the azobenzene and its

derivatives, the details have not cleared.[2]

In this chapter, photoisomerization and thermal isomerization was cleared among **2′,6′-Me-Azo** which showed excellent photoregulation ability of DNA hybridization. In addition, the effect of *ortho*-methylation for thermal isomerization was also investigated.

3-3 Result and Discussions

3-3-1 Photoisomerization of azobenzene derivatives

HPLC analysis of the rate of *trans*- or *cis*-form: Analyzing the DNA samples involving azobenzene moiety after visible light and UV light irradiation with HPLC around 340 nm (λ_{max} of azobenzene derivatives used in this study), the rate of *trans*- or *cis*-form of azobenzene after visible and UV light irradiation can be obtained together with the ratio between extinction coefficient of *trans*- and *cis*-form of azobenzene at analyzed wave length ($\varepsilon_t/\varepsilon_c$).[3] In this analysis, the HPLC retention area was used for the calculation, the concentration and volume of two samples (visible light irradiation and UV light irradiation) must be same. The calculation methods were as follows.

By analyzing the DNA involving azobenzene samples irradiated with visible or UV

light, HPLC charts like show in Figure 3-2 could be obtained.

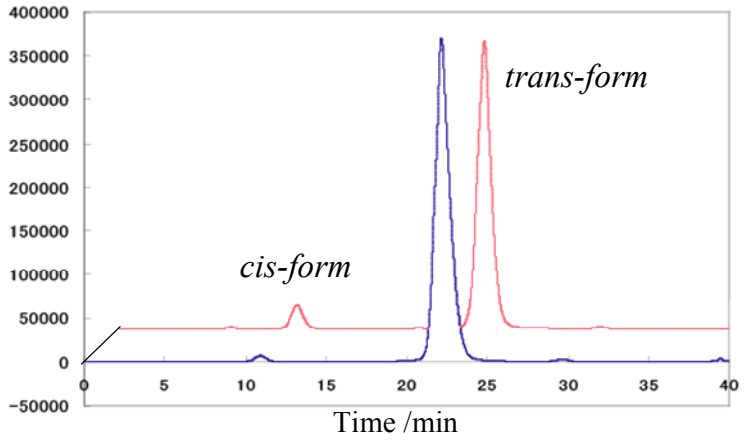

Figure 3-2. HPLC patterns of 2,6-Me-Azo tethered into DNA sequence CXG after visible light irradiation (front / blue line) and after UV irradiation (back / red line). W.l. = 334 nm.

Here, the extinction coefficient of *trans*- and *cis*-form of azobenzene at analyzed wavelength called ε_t and ε_c, and the rate of *trans*-form after visible light irradiation and UV light irradiation called X and Y, respectively. As a result, the retention area (S) could be shown in expressions as follows.

$$S_{cis-Vis} = k \times (1 - X) \times \varepsilon_c \qquad (1)$$

$$S_{trans-Vis} = k \times X \times \varepsilon_t \qquad (2)$$

$$S_{cis-UV} = k \times (1 - Y) \times \varepsilon_c \qquad (3)$$

$$S_{trans-UV} = k \times Y \times \varepsilon_t \qquad (4)$$

From these expressions, X, Y, and $\varepsilon_t/\varepsilon_c$ (the ratio of extinction coefficient of *trans*- and *cis*-form) could be obtained.

The rates of *trans*-azobenzenes tethered into **CXG** after visible or UV light irradiation and the $\varepsilon_t/\varepsilon_c$ of **Azo**, **2-Azo**, **2′-Me-Azo**, **2′-Et-Azo**, **2,2′-Me-Azo**, **2,6-Me-Azo** and **2′,6′-Me-Azo** were analyzed by this method. The rates of *trans*-**3′-Me-Azo**, **4′-Me-Azo** and **3′,5′-Me-Azo** were analyzed by the area of HPLC charts based on the 260 nm absorbance. In addition the $\varepsilon_t/\varepsilon_c$ of **3′-Me-Azo**, **4′-Me-Azo** and **3′,5′-Me-Azo** were presupposed 20.

UV-vis absorbance spectra analysis of the rate of *trans*- or *cis*-form: The rate of *trans*- or *cis*-form azobenzene could be also obtained from the absorbance around 340 nm (λ_{max} of azobenzene derivatives used in this study) with calculation as follows.

Here, X represent the rate of *trans*-form, A_X represent the absorbance of sample including X of *trans*-form azobenzene and A_{trans} represent the absorbance of *trans*-form (all azobenzene took *trans*-form).

$$A_X = A_{trans} \times X + A_{trans} \times \varepsilon_c / \varepsilon_t (1 - X) \qquad (5)$$

So, $A_{trans} = \dfrac{A_X}{X \times (1 - \varepsilon_c / \varepsilon_t) + \varepsilon_c / \varepsilon_t}$ (6) was obtained.

From HPLC analysis, right side was known, so A_{trans} could be calculated. In addition, after A_{trans} obtained, the rate of *trans*-form (X') could be obtained from the absorbance A' as follows.

$$X' = \frac{A' - A_{trans} \times \varepsilon_c / \varepsilon_t}{A_{trans} \times (1 - \varepsilon_c / \varepsilon_t)} \qquad (7)$$

3-3-1-1 Photoisomerization of azobenzene derivatives in single-stranded DNA

As shown in Table 3-1, after visible light irradiation, over 80 % of azobenzenes isomerized to *trans*-form in the case of all azobenzene derivatives used in this study: clear effect of chemical modification did not appear. On the other hand, for the *trans*- to *cis*-isomerization were clearly restricted by the modification of two *ortho*-position of one benzene ring clearly; the rate of *cis*-form of **2,6-Me-Azo** or **2′,6′-Me-Azo** after UV light irradiation was only 57 % whereas that of others was over 70 %. ISOp, the *trans*- to *cis*-form isomerization rate, was also lowered modification of two *ortho*-position of one benzene ring; ISOp of **2,6-Me-Azo** or **2′,6′-Me-Azo** was about 10 % lower than that of others. According Diau, *trans*-to *cis*-photoisomerization occurred via concerted inversion mechanism in which the CNNC angle of azobenzene is changed, not cleaving of N=N double bound.[1-c] Therefore, modifications of two *ortho*-position of one benzene ring might caused steric hindrance with nitrogen atom and restrict the *trans*-to

cis- isomerization.

Table 3-1. Rates of *cis*-form azobenzene derivatives tethered into **CXG** after irradiation of visible and UV light at 60 °C.

Azobenzene	Rate of *cis*-form		ISOp[c]	$\varepsilon_t/\varepsilon_c$
	Visible light[a]	UV light[b]		
Azo[d]	0.20	0.80	0.75	26.9
2-Me-Azo[e]	0.21	0.74	0.67	22.4
2′-Me-Azo[d]	0.18	0.75	0.70	22.6
2′-Et-Azo[e] [f]	0.10	0.72	0.69	14.3
3′-Me-Azo[d]	0.17	0.71	0.65	-[h]
4′-Me-Azo[d]	0.19	0.79	0.74	-[h]
2,2′-Me-Azo[g]	0.13	0.71	0.67	12.7
2,6-Me-Azo[g]	0.23	0.57	0.44	18.5
2′,6′-Me-Azo[g]	0.14	0.57	0.52	14.9
3′,5′-Me-Azo[d]	0.15	0.66	0.60	-[h]

[a] Visible light was irradiated for 1 minute at 60 °C. [b] UV light was irradiated for 5 minutes at 60 °C. [c] ISOp represents the *trans*- to *cis*-form isomerization rate. [d] Analyzed at 340 nm. [e] Analyzed at 338 nm. [f] **2′-Et-Azo** was tethered into DNA sequence 5′-CGA-X-GTC-3′ (X represent **2′-Et-Azo**). [g] Analyzed at 334 nm. [h] As described in body, $\varepsilon_t/\varepsilon_c$ presupposed 20.

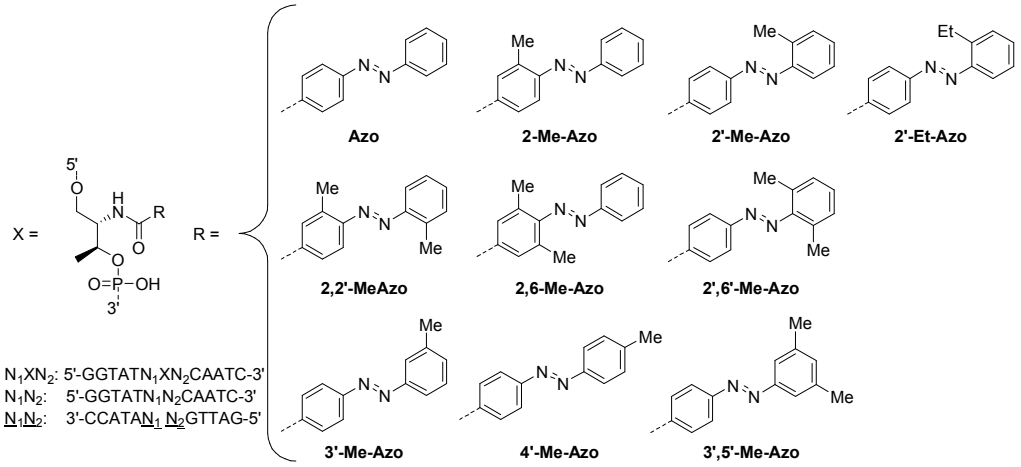

Figure 3-3. Structures and DNA sequence used for measurement of photoisomerization and thermal isomerization.

3-3-1-2 Photoisomerization of 2′,6′-Me-Azo in several conditions

To photoregulated DNA function, the photoisomerization of azobenzene derivatives in DNA duplex is important. Therefore, the detail of photoisomerization of **2′,6′-Me-Azo** which showed most efficient photoregulation ability was investigated in single-stranded DNA and duplex. In this section, the rate of *cis*-form was calculated from the absorbance spectra and the absorbance of *trans*-form was obtained by keep the samples at high temperature (using thermal isomerization). In DNA duplex, $\varepsilon_t/\varepsilon_c$ (the ratio of extinction coefficient of *trans*- and *cis*-form) obtained in HPLC analysis in single- stranded DNA was also used.[4]

In Single-stranded DNA: Figure 3-4 showed the change of absorbance spectra of **2′,6′-Me-Azo** tethered into single-stranded **CXG** in buffer solution. Irradiated with UV light, the absorbance around 340 nm decreased: *trans*-**2′,6′-Me-Azo** isomerized to *cis*-form. As shown in Figure 3-4, 3 or more minutes UV light irradiation, the spectra did not change. In other world, in single-stranded DNA, **2′,6′-Me-Azo** reached photostationary states about 4 minutes UV light irradiation.

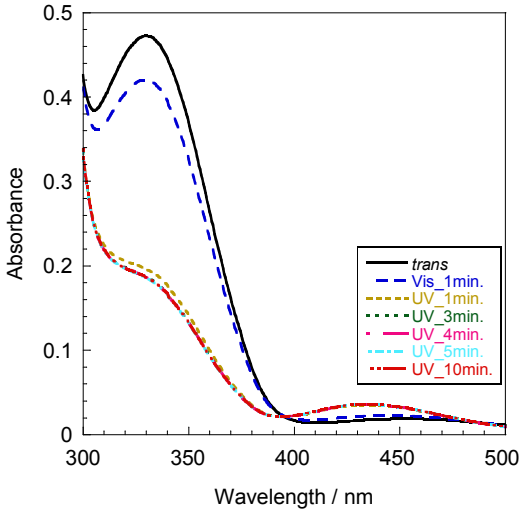

Figure 3-4. Absorbance spectra of **2′,6′-Me-Azo** tethered into single-strand **CXG** irradiated with visible or UV light at 60 °C Solution conditions: [DNA] = 20 μM, [NaCl] = 100 mM, pH 7.0 (phosphate 10 mM buffer).

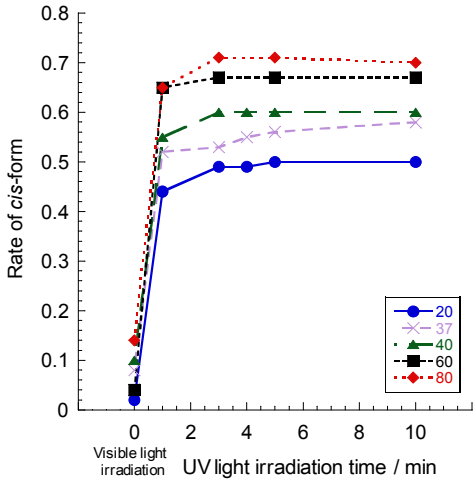

Figure 3-5. Rate of *cis*-**2′,6′-Me-Azo** tethered into single-stranded **CXG** irradiated with visible or UV light. The dependency on irradiation time of the sample irradiated at 20 °C, 37 °C, 40 °C 60 °C, and 80 °C were shown. Solution conditions: [DNA] = 20 μM, [NaCl] = 100 mM, pH 7.0 (phosphate 10 mM buffer).

Figure 3-5 showed the rate of *cis*-form of **2′,6′-Me-Azo** tethered into single-stranded **CXG** in buffer solution after visible and UV light irradiation at several

temperatures. In the case of UV light irradiation, in low temperature, the rate of *cis*-form became lower than high temperature.[5] In low temperature, hydrophobic *trans*-azobenzene might be interacting with DNA nucleotides and that interaction interfere the isomerization. In the case of visible light irradiation, 90 % or more of **2′,6′-Me-Azo** became *trans*-form. Clear dependency on temperature was not appeared.

In DNA duplex: In the case **2′,6′-Me-Azo** tethered into DNA duplex, the rate of *cis*-form was clearly depended on temperature (T_ms) of duplex. Figure 3-7 showed the rate of *cis*-form after visible or UV light at several temperatures. In this analysis, 44mer DNA including two **2′,6′-Me-Azo** moieties (**D_{44}**) was used. To focused on irradiation time, as same as tethered into single-stranded DNA, after 3 or more minutes UV light irradiation, **2′,6′-Me-Azo** tethered into DNA duplex reached photo stationary states at any temperatures (Figure 3-6A). On the other hand, the rate of *cis*-form both after visible light irradiation and UV light irradiation clearly depended on the temperature (Figure 3-6B and C). Both visible and UV light irradiation, the rate of *cis*-isomer became low when the irradiation temperature became low. In the photoregulation system, *trans*-azobenzene moiety stabilized DNA duplex by stacking effect. However, in other word, it also means that *trans*-azobenzene moiety is stabilized by DNA duplex. Therefore, in the condition of DNA duplex formed, *trans*- to *cis*-photoisomerization

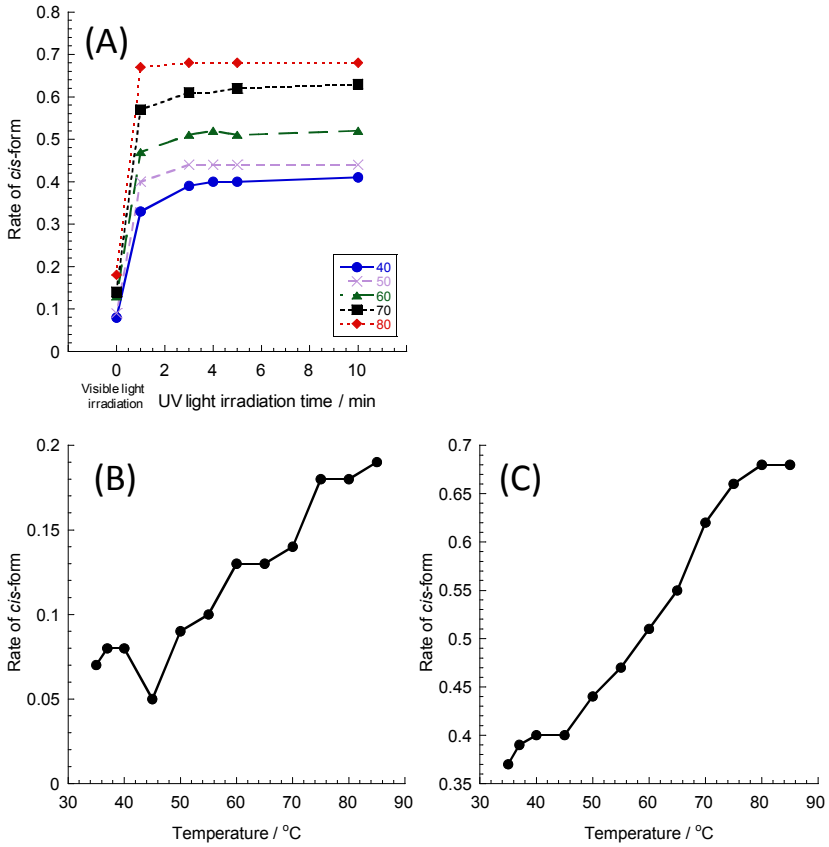

Figure 3-6. Rate of *cis*-**2′,6′-Me-Azo** tethered into $\mathbf{D_{44}}$ duplex irradiated with visible or UV light. (A) The dependency on irradiation time of the sample irradiated at 40 °C, 50 °C, 60 °C 70 °C, and 80 °C were shown. (B) The dependency on irradiation temperatures of the sample with visible light irradiation for 1 minute. (C) The dependency on irradiation temperatures of the sample with UV light irradiation for 5 minute. Solution conditions: [DNA] = 10 μM, [NaCl] = 100 mM, pH 7.0 (phosphate 10 mM buffer).

would have been interfered and *cis*-to *trans*-photoisomerization would have been accreted. The results that the rate of *cis*-form with UV light irradiation became lower under 70 °C also support these discussions because the T_m of the duplex used in this analysis was about 70 °C.

3-3-2 Thermal isomerization of azobenzene derivatives

For using azobenzene derivatives as a photo switch, *cis*-to *trans*-thermal isomerization also affect the regulation efficiency and applicational usability. In addition, chemical modification of azobenzene affect the thermal isomerization.[2] In this section, first, the thermal isomerization of modified azobenzene tethered into DNA was investigated. Then, in order to investigate the effect of *ortho*-methylation on thermal isomerization of azobenzene, various *ortho*-methylated azobenzene derivatives were measured.

3-3-2-1 Thermal isomerization in DNA

Calculation of Thermal isomerization rate (half life of azobenzene):[6] By measuring the absorbance of samples containing *cis*-azobenzene derivatives at fixed temperature under dark, the spectra like shown in Figure 3-7 can be obtained. From the absorbance around 340 nm and the expression (7), the rate of *cis*-isomer (r) can be calculated. On the other hand, thermal isomerization rate was obtained from the slope of time vs. logarithm of the ration of the rate of *cis*-isomer at that time to that of initial states (r_0/r_t). From the expression (7), r_0/r_t can be described as follow expression (8).

$$r_o / r_t = (1 - X_0)/(1 - X_t) = \frac{A_{trans} - A_0}{A_{trans} - A_t} \qquad (8)$$

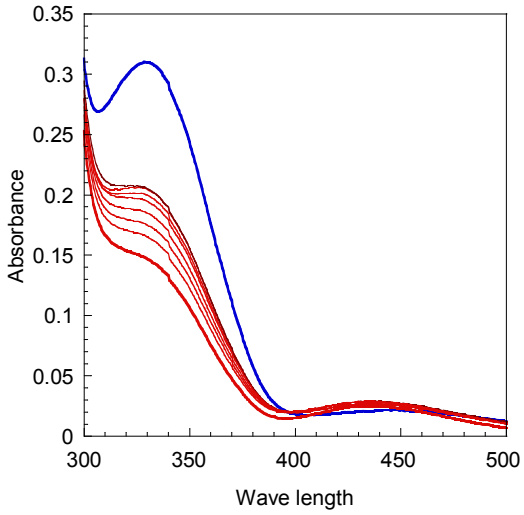

Figure 3-7. Change of UV-vis spectra of *cis*-**2′,6′-Me-Azo** tethered onto DNA with time at 60 °C. The measurements were performed every 2 hours red lines). The increase of the absorbance around 340 nm indicated that the azobenzene isomerized *cis* to *tans*-form. The blue line showed the absorbance spectra after 1 minute Visible light irradiation.

In single-stranded DNA: Generally, *cis*- to *trans*- thermal isomerization was accelerated by chemical modification.[2] In particular, donor–acceptor (‘‘push–pull’’) modification at the *para*- (or *ortho*-position) of azobenzene usually lowers the thermal stability of *cis*-azobenzene. In the cases of azobenzene moiety introducing into DNA, the amide bound vicinity of the threoninol pull and alkyl groups push the electron, so thermal isomerization should be accelerated. In fact, the mono-alkylation of azobenzene (2′-, 3′-, 4′-) accelerated the thermal isomerization; in a single-stranded **CXG**, the half-life ($\tau_{1/2}$) of *cis*-**4′-Me-Azo** was one-third of that of unmodified *cis*-**Azo** at 60 °C (Figure 3-8). In the case of di-methylation, thermal isomerization was also accelerated

for almost azobenzene derivatives. However, Unexpectedly, **2′,6′-Me-Azo**, in which both two *ortho*-potions of distal benzene ring was methylated and which displays the largest photoregulation efficiency, showed very slow thermal isomerization. Its $\tau_{1/2}$ was as long as 25 h at 60 °C, which was 8-times as long as that of unmodified *cis*-**Azo**.

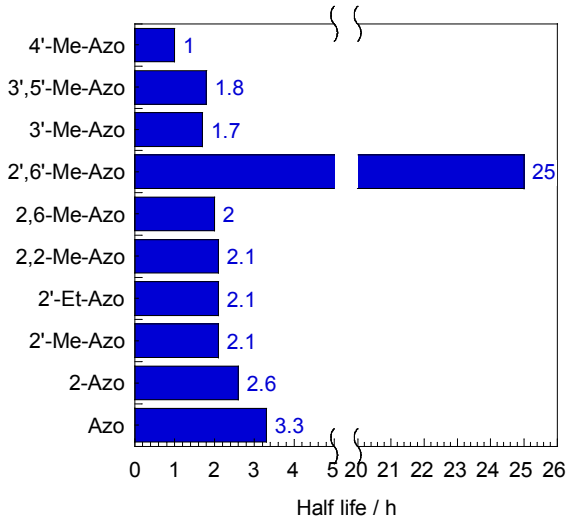

Figure 3-8. Half lives of *cis*- to *trans*- thermal isomerization of azobenzene derivatives tethered into single-stranded DNA **CXG** at 60 °C. Solution conditions: [DNA] = 20 μM, [NaCl] = 100 mM, pH 7.0 (phosphate 10 mM buffer).

Interestingly, **2,6-Me-Azo** or **2,2′-Me-Azo**, which was methylated on the other two *ortho*-positions, did not show such enhanced stability of *cis*-form in DNA. This remarkable effect was observed only when the two *ortho*-positions of the distal benzene were methylated.

In DNA duplex: As described in photoisomerization section, *trans*-form of azobenzene was stabilized in DNA duplex. Therefore, the thermal isomerization may be

Table 3-2. Half life ($\tau_{1/2}$) and rate constant of ***cis*-2′,6′-Me-Azo** both in single-stranded DNA and DNA duplex at several temperatures.

	In single-stranded DNA[a]		In duplex[b]	
Temperature / ^{o}C	$\tau_{1/2}$ / h	k_{iso} /h^{-1}	$\tau_{1/2}$ / h	k_{iso} /h^{-1}
50	-	-	37	0.0187
60	31	0.0223	14	0.0496
65	-	-	14	0.0497
70	12	0.0565	9.4	0.0738
75	-	-	8.6	0.0807
80	4.9	0.142	6.1	0.114
85	-	-	3.6	0.194
90	2.2	0.312	1.9	0.361

[a] DNA strand **D_{44}**. [b] DNA duplex **D_{44}/C_{44}**. Solution conditions: [DNA] = 10 μM, [NaCl] = 100 mM, pH 7.0 (phosphate 10 mM buffer). The sequence of **D_{44}** was as follow: 5′-CCCGCGAAATTAATACGAXCTCACTXATAGGGGAATTGTGAGCG -3′ (X indicated **2′,6′-Me-Azo**). The sequence of **C_{44}** was as follows: 3′-GGGCGCTTTAATTATGCTGAG TGATATCCCCTTAACACTCGA-5′.

accelerated in DNA duplex. In order to investigate the effect of DNA duplex, thermal isomerization of *cis*-**2′,6′-Me-Azo** both in DNA single-stranded **D_{44}** and duplex **D_{44}/C_{44}** (T_m = ~70 ^{o}C) was measured. Table 3-2 showed the $\tau_{1/2}$ of *cis*-**2′,6′-Me-Azo** at several temperatures. At high temperature (90 or 80 ^{o}C), the $\tau_{1/2}$ of *cis*-**2′,6′-Me-Azo** both in single-stranded and duplex were almost corresponded each others. On the other hand, at low temperature, the $\tau_{1/2}$ of *cis*-**2′,6′-Me-Azo** in duplex became clearly shorter than that of in single-stranded DNA: at 60 ^{o}C, $\tau_{1/2}$ in duplex was14 h, whereas that of in single strand was 31 h. (Note that the $\tau_{1/2}$ of **D_{44}** was different with that of **CXG**. It was only measurement error or the effect of neighboring bases.)

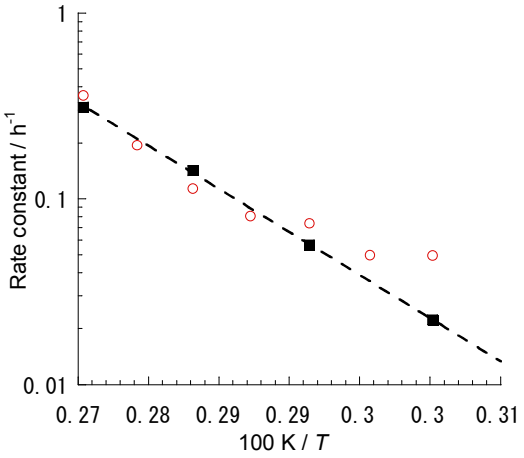

Figure 3-9. Arrhenius plots of the rate constants of thermal *cis- to trans* isomerization of **2′,6′-Me-Azo** tethered into both single-stranded DNA $\mathbf{D_{44}}$ (black square symbol) and $\mathbf{D_{44}/C_{44}}$ DNA duplex (circle symbol). Solution conditions: [DNA] = 10 μM, [NaCl] = 100 mM, pH 7.0 (phosphate 10 mM buffer).

Figure 3-9 showed the Arrhenius plots of the rate constants of thermal isomerization of *cis*-**2′,6′-Me-Azo** both in duplex and single-stranded DNA. In the case of in single-stranded DNA, the Arrhenius equation consisted; square symbol in Figure 3-9 lined up on the line. On the other hand, in the case of in duplex, the Arrhenius equation did not consist at the temperature under the T_m of $\mathbf{D_{44}/C_{44}}$ (about 70 ^oC); the circle symbol in Figure 3-9 came from off the line. These results indicated that thermal isomerization of *cis*-**2′,6′-Me-Azo** was influenced by DNA duplex; the stacking effect of neighboring base-pairs destabilized *cis*-**2′,6′-Me-Azo**, so the thermal isomerization was accelerated. However, even in DNA duplex, the $\tau_{1/2}$ of *cis*-**2′,6′-Me-Azo** was still long, so, it was cleared that **2′,6′-Me-Azo** was the excellent photo switch molecule for

the efficient photoregulation of DNA hybridization.

3-3-2-2 Mechanism of the effect of *ortho*-modification for thermal isomerization

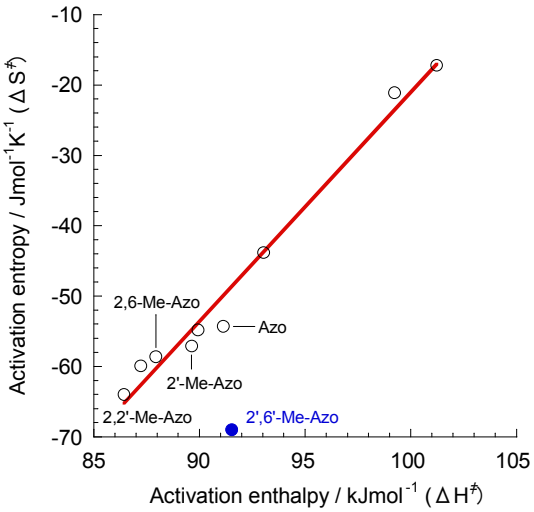

Figure 3-10. Plot of activation entropy ($\Delta S^{\ddagger}$) as a function of activation enthalpy ($\Delta H^{\ddagger}$) at T = 333 K for the thermal *cis*-to-*trans* isomerization of azobenzenes tethered to single-stranded **CXG** on D-threoninol in buffer solution. The detail value of $\Delta S^{\ddagger}$ *and* $\Delta H^{\ddagger}$ of each azobenzenes were shown in Appendix Table 3-3.

Figure 3-10 showed the plot of activation entropy ($\Delta S^{\ddagger}$) as a function of activation enthalpy ($\Delta H^{\ddagger}$) at T = 333 K for the thermal *cis*-to-*trans* isomerization of azobenzenes tethered into single-stranded **CXG** on D-threoninol in buffer solution. Generally, push-pull modification of azobenzene accelerates thermal isomerization.[2] Since the amide bound (or carboxyl group, *vide infra*) pulled and the alkyl group weakly pushed the electron, the *ortho*-modification slightly decreased the $\tau_{1/2}$ compared with **Azo** in buffer solution. Furthermore, compensation of $\Delta H^{\ddagger}$ and $\Delta S^{\ddagger}$ indicated that the decreased

$\tau_{1/2}$ by *ortho*-methylation was caused by a similar electronic effect.[7] However, *cis*-**2′,6′-Me-Azo** exclusively showed different thermal isomerization behavior, as evidenced from the definite deviation in results.

Thermal isomerization of azobenzene derivatives in carboxylic acid form: In order to investigate the unusual restrict of thermal isomerization by methylation at two *ortho*-positions of specific benzene ring, the thermal isomerization of several *ortho*-methylated azobenzene moieties in several solvents were measured without DNA.

Table 3-3. Half-lives ($\tau_{1/2}$) of thermal *cis*-to-*trans* isomerization of azobenzenes in carboxylic acid form various solvents at 60 °C

	$\tau_{1/2}$ / h[b]		
Azobenzene[a]	Toluene	DMF	Buffer[b]
Azo	0.28	1.3	3.4
2-Me-Azo	0.34	0.79	3.7
2′-Me-Azo	0.47	1.1	3.5
2,2′-Me-Azo	0.29	0.95	3.3
2,6-Me-Azo	0.14	0.73	10
2′,6′-Me-Azo	3.9	9.2	36

[a] Azobenzene in the carboxylic acid form before introduction into DNA was used for the $\tau_{1/2}$ measurement. [b] Solution conditions: [NaCl] =100 mM, pH 7.0 (10 mM phosphate buffer).

First, in order to confirm that the enhancement of thermal stability of *cis*-**2′,6′-Me-Azo** related the effects of DNA, the thermal isomerization of carboxylic acid form (without DNA) of azobenzene derivatives were measured. The carboxylic

acid form (without DNA) also showed similar results in buffer solution except for **2,6-Me-Azo** (not **2′,6′-Me-Azo**). The $\tau_{1/2}$ of **2,6-Me-Azo** in the carboxylic form was 10 h, which was 5-fold longer than that tethered into DNA (2.0 h), but still shorter than **2′,6′-Me-Azo** (36 h, *vide infra*). Other azobenzenes had the same or slightly longer $\tau_{1/2}$ compared with those in DNA, indicating that improved thermal stability of **2′,6′-Me-Azo** was intrinsic, not due to the effect of DNA.

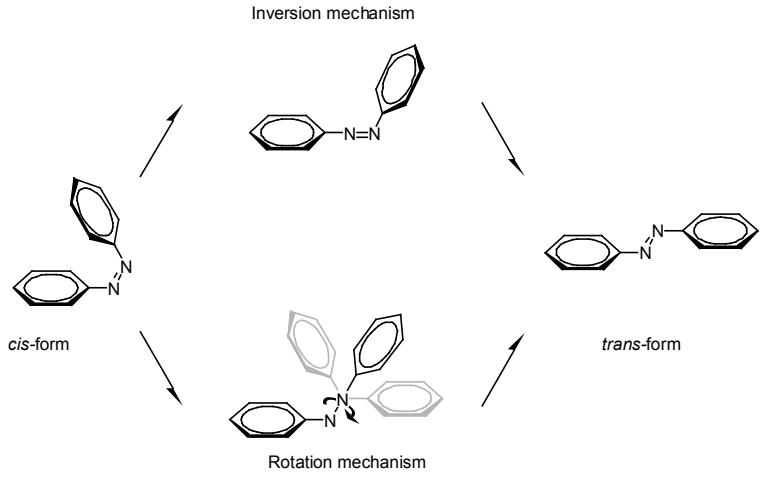

Figure 3-11. Two possible pathways of *cis*-to-*trans* thermal isomerization. Upper pathway: inversion route through a transition state in which one of the nitrogen atoms is sp-hybridized. Lower pathway: rotation route through the rupturing of a nitrogen-nitrogen π-bond and rotation around the remaining σ-bond.

Asano *et al.* reported two different routes of thermal *cis*-to-*trans* isomerization,[8] inversion and rotation. The inversion route proceeds through a transition state in which one of the N atoms is sp hybridized, whereas the rotation route involves the disruption of a N-N π-bond and rotation around the remaining σ-bond, as shown in Figure 3-11.

These two routes could be discriminated from the $\tau_{1/2}$ dependence on the polarity of the solvent. Since the transition state of the inversion route, sp hybridized N is stabilized in the apolar solvent due to its hydrophobicity, the $\tau_{1/2}$ decreases as the polarity of the solvent decreases. In contrast, the transition state of the rotation route has a single -N-N- (not double -N=N-) bond that is stabilized in a polar environment, resulting in a smaller $\tau_{1/2}$ with a polar solvent.[2] As shown in Table 3-3, as the polarity of the solvent decreased (water (buffer) $\rightarrow$ DMF $\rightarrow$ toluene), the $\tau_{1/2}$ of the *cis*-form was decreased. For example, the $\tau_{1/2}$ of **2′-Me-Azo** was as long as 3.5 h in buffer solution, but only 0.79 h in DMF and 0.47 h in toluene. **2′,6′-Me-Azo** also showed the same solvent effect on the $\tau_{1/2}$. Irrespective of the solvent, however, **2′,6′-Me-Azo** had about a 10-fold longer $\tau_{1/2}$ than other azobenzenes. These results indicated that azobenzene derivatives with carboxyl group thermal isomerize via inversion mechanism.

Nishimura *et al*. reported on the effect of substituent on the inversion center. They proposed that an electron accepting substituent enhances the s-character of the C-N bond so that an N atom near the electron-accepting substituent becomes the inversion center.[9] In contrast, an electron-donating substituent allows a distant N atom as the

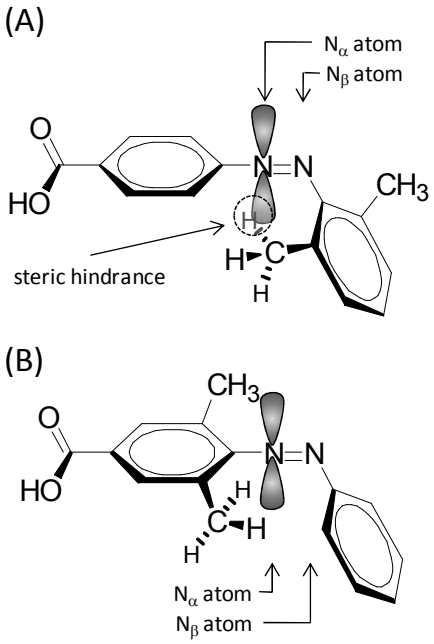

Figure 3-12. Possible *trans*ition states of (A) **2′,6′-Me-Azo** and (B) **2,6-Me-Azo**, both of which have an inversion center at the N_α atom. (Sphere-images of *trans*ition states of both **2′,6′-Me-Azo** and **2,6-Me-Azo** constructed from InsightII/Discover are shown in appendix section).

inversion center. According to this hypothesis, an electron-accepting carboxylate group on the distal ring enhances the s-character of C-N_α (Figure 3-12),[2-c] which facilitates inversion on the N_α atom rather than on N_β. This hypothesis explains the transition states of **2′,6′-Me-Azo** and **2,6-Me-Azo** as depicted in Figure 3-8 due to the electron-accepting property of the carboxylic group, thereby leading to the enhanced thermal stability of **2′,6′-Me-Azo**. At the transition state, lone pair electrons of the π orbital of the N_α atom cause steric hindrance with the methyl groups on the twisted distal benzene ring (Figure 3-12A and Appendix Figure 3-3A), which could markedly

retard the inversion to the *trans*-form. However, the two methyl groups on **2,6-Me-Azo** did not induce such steric hindrance with the inversion center of the N_α atom (Figure 3-12B and Appendix Figure 3-3B). Consequently, *cis*-to-*trans* isomerization of **2,6-Me-Azo** occurred smoothly via an inversion mechanism. In the case of both mono-substituted **2′-Me-Azo** and di-substituted **2′,2′-Me-Azo**, this hindrance could be avoided through the smaller hydrogen on other *ortho*-position of the distal benzene ring.

As described above, in buffer solution, the $\tau_{1/2}$ of **2,6-Me-Azo** in the carboxylic acid form was 5-fold longer than that tethered into DNA (2.0 h), whereas other modified azobenzenes did not elongate the $\tau_{1/2}$ in the carboxylate form. At pH 7, carboxylic acid is mostly deprotonated to form a carboxylate anion thus reducing the electron-accepting property. In addition, methyl groups on the proximal ring in **2,6-Me-Azo** act as a weak electron donor, which prefers the N_β to N_α atom as an inversion center. Presumably, both the weakened electron-accepting property of the carboxylate anion and the electron-donating methyl groups on the same benzene ring allowed N_β as well as N_α to be inversion centers, and so the thermal isomerization of *cis*-**2,6-Me-Azo** became slower in pH 7 buffer solution**.** Consistently, the $\tau_{1/2}$ decreased from 10 to 4.8 h when the pH of the solution was lowered from 7 to 5 (Appendix Table3-2).[9] On the other hand, the $\tau_{1/2}$ of **2′,6′-Me-Azo** in the carboxylate form did not depend on the pH; the $\tau_{1/2}$

was as long as 32 h at pH 5.0, which was even longer than that of **2′,6′-Me-Azo** tethered to DNA. Although deprotonation of the carboxyl group similarly reduced its electron-donating property, the electron-donating effect of the methyl groups on the distal benzene ring fixed the inversion center at the N_α atom even under neutral-basic conditions. In other organic solvents or by conjugation with DNA, however, only the N_α atom functioned as an inversion center due to the absence of deprotonation.

3-3-2-3 Thermal isomerization of several azobenzene derivatives

In order to check the validity of hypothesis, new azobenzene derivatives which have a nitro group or methylthio group at the *para*-position were synthesized (Figure 3-13) and the *cis*- to *trans*- thermal isomerization was investigated in various solutions. In the case of nitro azobenzene derivatives, methylation at two *ortho*-positions of opposite side benzene ring (**2′,6′-Me Nitro Azo**) would be expected to enhance the $\tau_{1/2}$ of *cis*-form because nitro groups act as electro accepter. On the other hand, in the case of methylthio azobenzene derivatives, methylation at two *ortho*-positions of same benzene ring (**2,6-Me Thio Azo)** would be expected to enhance the $\tau_{1/2}$ of *cis*-form because methylthio groups act as electro donor.

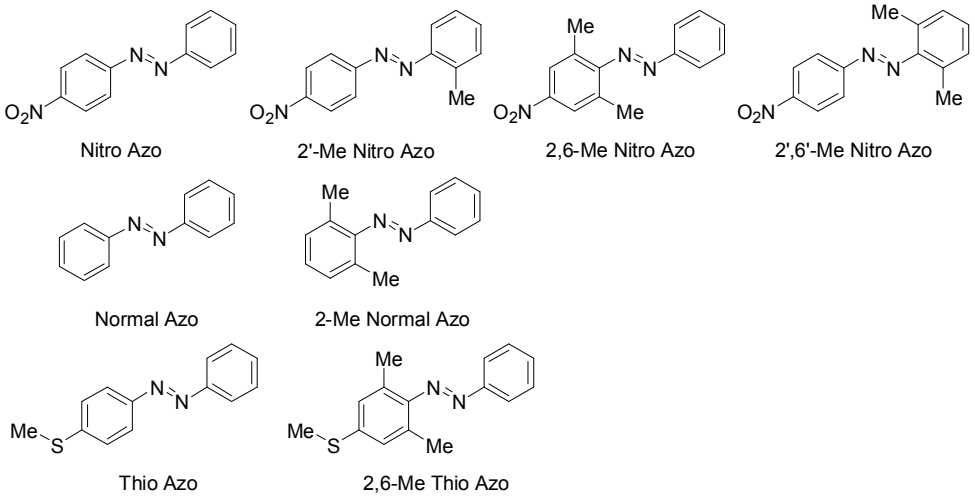

Figure 3-13. Structures of nitro azobenzene derivatives and normal azobenzenes.

Table 3-4. Half-lives ($\tau_{1/2}$) of thermal *cis*-to-*trans* isomerization of azobenzene derivatives various solvents at 45 °C

	$\tau_{1/2}$ / h[a]		
Azobenzene	Toluene	Ethanol	DMF
Normal Azo	10.7	10.0	13.6
2,6-Me Normal Azo	43.9	105	118[b]
Nitro Azo	0.42	0.25	0.086
2′-Me Nitro Azo	0.50	0.36	0.27
2,6-Me Nitro Azo	0.11	0.030	0.033[b]
2′,6′-Me Nitro Azo[c]	5.53	3.76	0.32
Thio Azo	1.25	1.99[d]	1.78
2,6-Me Thio Azo	12.8	20.8	17.8

[a] All the azobenzene was dissolved in ethanol as a stock solution. For measurement, the stock solution was diluted to 1000 times. The final concentrations except for **2′,6′-Me Nitro Azo** were 50 μM. [b] Calculated by Arrhenius plots. [c] The final concentration of **2′,6′-Me Nitro Azo** was 100 μM. [d] Diluted to 2000 times for final concentration was 25 μM.

Normal azobenzene derivatives: As shown in Table 3-4, as the polarity of the solvent decreased (DMF → Ethanol→ toluene), the $\tau_{1/2}$ of both **Normal Azo** and

2,6-Me Normal Azo decreased. Therefore, these two azobenzene derivatives isomerize via inversion mechanism. Because they did not have electro donating or accepting group, both N atoms could act as inversion center. If so, methylation at two *ortho*-positions of one benzene ring was expected to not restrict the thermal isomerization. However, as shown in Table 3-4, the $\tau_{1/2}$ of **2,6-Me Normal Azo** was cleary longer than that of **Noromal Azo** in any solvents. Methyl group itself acts as weak electron donor, so, N atom far from the methylated benzene ring could become the inversion center, preferentially. Therefore, the thermal stability of *cis*-**2,6-Me Normal Azo** would have been enhanced.

Nitro azobenzene derivatives: As the polarity of the solvent decreased (DMF → Ethanol→ toluene), the $\tau_{1/2}$ of all the *cis*-nitro azobenzene derivatives increased. This result indicated that nitro azobenzene derivatives isomerize via rotation mechanism in high polarity solvents (DMF). However, in Toluene, in which nitro azobenzene derivatives would have isomerized via inversion mechanism, almost expected results were obtained. By methylation at two *ortho*-positions of opposite side benzene ring (**2′,6′-Me Nitro Azo**), the $\tau_{1/2}$ became 5.5 hours, which was 10 times as long as that of **Nitro Azo** (0.42 hours). In contrast, by methylation at two *ortho*-positions of same benzene ring (**2,6-Me Nitro Azo**), the $\tau_{1/2}$ in toluene was 0.11 hours, which was 4 times

as short as that of **Nitro Azo**. In DMF, in which nitro azobenzene isomerize partially via rotation mechanism, the $\tau_{1/2}$ of **2′,6′-Me Nitro Azo** was also longer than that of **Nitro Azo**, however, the differences was only 4-times. In addition, focused on the $\tau_{1/2}$ of **2′-Me Nitro Azo** in DMF, it was also about 4 times as long as that of **Nitro Azo**. According to the hypothesis discussed here, thermal isomerization via inversion mechanism does not restrict by only one methylation: in fact, $\tau_{1/2}$ of **2′-Me Nitro Azo** in Toluene was almost the same as that of **Nitro Azo**. The enhancement of $\tau_{1/2}$ of **2′-Me Nitro Azo** and **2′,6′-Me Nitro Azo** in DMF may be based on other hypothesis like restriction in rotation mechanism. (The plot of activation entropy ($\Delta S^{\ddagger}$) as a function of activation enthalpy ($\Delta H^{\ddagger}$) of nitro azobenzene derivatives in Toluene and DMF were shown in appendix Figure 3-4).

In Ethanol, although the dielectric constant is high, all the nitro azobenzene derivatives would have isomerized mainly via inversion mechanism. Nitro azobenzene derivatives used in this study have only one strong electro donating group. The changes of mechanism of thermal isomerization on the polarity of solvents of such azobenzene derivatives are unknown.

Methylthio azobenzene derivatives: In the case of methylthio modified

azobenzene derivatives (**Thio Azo** and **2,6-Me Thio Azo**), as the polarity of the solvent decreased (DMF $\rightarrow$ toluene), the $\tau_{1/2}$ decreased. So, these azobenzene derivatives isomerized via inversion mechanism. Methylthio group acts as electro donor, so, the N atom distant from methylthio group the inversion center. As shown in Table 3-4, by methylation at two ortho positions of benzene ring which has electro donating methylthio group, the thermal stability was enhanced: the $\tau_{1/2}$ of **2,6-Me Thio Azo** were about 10-times as long as those of **Thio Azo** in all the solvents. The results of methylthio azobenzene derivatives also supported the hypothesis of the improvement of thermal stability of *cis*-azobenzene by methylation at specific position of azobenzene. In Ethanol, the dependence of $\tau_{1/2}$ on solvent polarity was unique compared with other azobenzene derivatives: the half lives were longer than in DMF although the polarity of Ethanol was smaller than DMF. Ethanol acts as protic polar solvent whereas DMF acts as aprotic polar solvent. The proton in Ethanol might protect interfere the thermal isomerization via inversion mechanism.

3-4 Conclusions

(1) The rates of *cis*-form azobenzene derivatives tethered into single-stranded DNA both with visible and UV light irradiations were investigated by HPLC analysis and

UV-Vis absorbance spectra. Methylation at two *ortho*-positions of benzene ring decreased *trans*- to *cis*-photoisomerization. The rates of *cis*-form decreased about 20 % by methylation at two *ortho*-positions compared with other those of other azobenzene derivatives.

(2) After UV light irradiation in DNA duplex under the T_m of that duplex, the rate of *cis*-**2′,6′-Me-Azo**, which showed most effective photoregulation efficiency, was also deceased compared with that of in single-stranded DNA. In addition, the rate of *trans*-**2′,6′-Me-Azo** after visible light irradiation increased.

(3) The thermal stability of *cis*-form of modified azobenzene using for the DNA hybridization were investigated. In single-stranded DNA, *cis*-**2′,6′-Me-Azo**, which showed most efficient photoregulation efficiency, showed extremely long half life ($\tau_{1/2}$) compared with other azobenzene including non-modified azobenzene. In DNA duplex under the T_m of that duplex, the $\tau_{1/2}$ of *cis*-**2′,6′-Me-Azo** became shorter due to DNA duplex destabilize the *cis*-isomer.

(4) In the case of *cis*-azobenzene derivatives thermo isomerize via inversion mechanism, the $\tau_{1/2}$ was enhanced by methylation of two *ortho*-position of benzene ring far from the inversion centered N atom because at the transition state, lone pair

electrons of the π orbital of the inversion centered N atom cause steric hindrance with the methyl groups on the twisted distal benzene ring. The validity of this hypothesis was verified by investigating of several di-methylated azobenzene derivatives in organic solvents.

3-5 Experimental section

3-5-1 Synthesis of DNAs involving alkylated azobenzene derivatives

The modified DNAs containing modified azobenzenes expect for $\mathbf{D_{44}}$ were synthesized on an automated DNA synthesizer (ABI-3400, Applied Biosystems) using conventional and azobenzene-carrying phosphoramidite monomers as described in Chapter 2. The DNA $\mathbf{D_{44}}$ including **2′,6′-Me-Azo** and its complementary strand $\mathbf{C_{44}}$ were supplied by Mr. Fujioka in Asanuma lab.[10] The DNAs containing only native bases were supplied by Integrated DNA Technologies, Inc. (Coralville, IA. U.S.A.).

3-5-2 Synthesis of methylated azobenzene derivatives used for thermal isomerization measurement

Aluminum chloride and azobenzene were purchased from Kishida Chemical Co., Ltd. (Osaka, Japan). 2,6-dimethyl aniline, dimethyl disulfide and 4-Phenylazo benzoic acid (carboxylic acid of **Azo**) were purchased from Tokyo Chemical Industry (Tokyo, Japan). Other carboxylic acid form of azobenzene derivatives were synthesized as described in Chapter 2. Other azobenzene derivatives were synthesized as follows.

Materials: Nitrosobenzene, 2-methyl aniline, 2,6-dimethyl aniline, 4-methylthio aniline and tosyl chloride were purchased from Tokyo Chemical Industry (Tokyo, Japan). Concentrated nitlic acid, anhydrous pyridine were purchased from Kishida Chemical Co., Ltd. (Osaka, Japan).

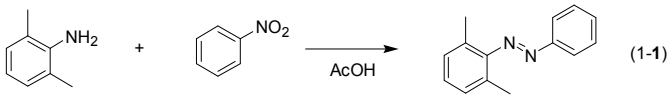

Scheme 1. Synthesis of **2,6-dimethyl azobenzene**.

Synthesis of 2,6-dimethyl azobenzene: 2,6-dimethyl azobenzene (compound 1-**1**)[11] was synthesized as follows: 0.49 g (3.98 mmol) of nitrosobenzene and0.58 g (4.79 mmol) of 2,6-dimethyl aniline was dissolved in 30 ml of acetic acid and steered at room temperature over night under dark. The mixture was poured into water followed by the extraction with ethyl acetate. The organic layer was washed with distilled water (once), saturated solution of NaCl, and dried over $MgSO_4$. After the removal the solvent, the crude mixture was subjected to silica gel column chromatography. (Hexane : AcOEt = 20 : 1) to afford 0.45 g (2.14 mmol) of **2,6-dimethyl azobenzene** (yield: 53.8%). ^{1}H NMR (500 MHz, [D_6]DMSO): δ = 7.87 – 7.60 (m, 8H, aromatic protons of azobenzene), 2.29 (s, 6H, -NC_6H_3-(CH_3)$_2$).

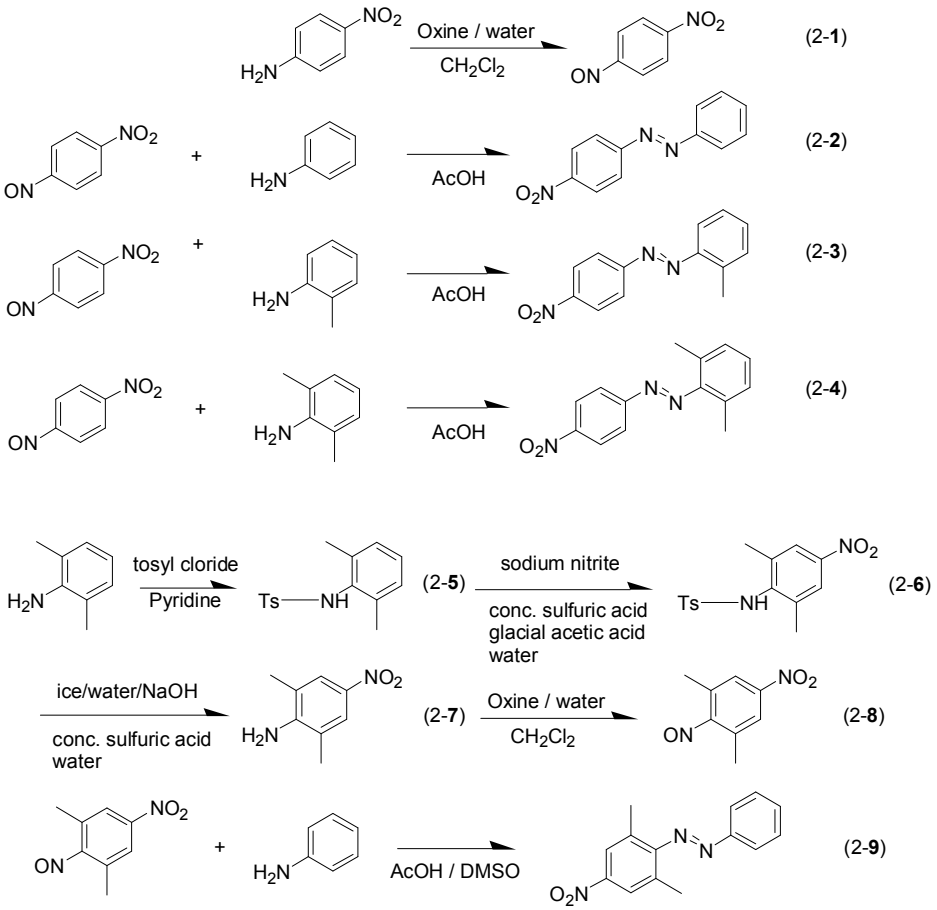

Scheme 2. Synthesis of **4-Nitoro azobenzene derivatives.**

Synthesis of 4-Nitoro azobenzene derivatives: 4-nitroso nitrobenzene (compound 2-**1**)[12] was synthesized as follows: 1.5 g (10.9 mmol) of 4-nitoro aniline was dissolved in 60 ml of CH_2Cl_2 (not anhydrous) under nitrogen atmosphere. 100 ml water solution of 6.7 g (10.9 mmol) of oxone was added and stirred for 4 hours. The organic phase of reaction mixture was corrected, then the removal water phase was washed with CH_2Cl_2 three times. All the organic phase was washed with 1 N HCl twice, saturated solution of $NaHCO_3$ three times and saturated solution of NaCl three times. After removal the solvent, 1.31 g (8.61 mmol) of 4-nitroso nitrobenzene was obtained (yield: 79.0 %).

4-phenilazo nitrobenzene (compound 2-**2**)[11] was synthesized as follows: 0.16 g (1.05

mmol) of 4-nitroso nitrobenzene was dissolved in 30 ml of acetic acid and 0.10 g (1.07 mmol) of aniline was added. The mixture was stirred over nigh under dark. Then the solution was poured into water and extracted with ethyl acetate. The organic layer was washed with distilled water, saturated solutions of $NaHCO_3$ and saturated solutions of NaCl, and dried over $MgSO_4$. After removal the solvent, the crude mixture was subjected to silica gel column chromatography (hexane : AcOEt = 15 : 1) to afford 0.18 g (0.79 mmol) of 4-phenilazo nitrobenzene (yield: 75.2 %). ^{1}H NMR (500 MHz, $CDCl_3$): δ = 8.41- 7.58 (m, 9H, aromatic protons).

4-(2-methyl phenilazo) nitrobenzene (compound 2-**3**)[11] was synthesized as follows: 0.20 g (1.31 mmol) of 4-nitroso nitrobenzene and 0.17 g (1.59 mmol) of 2-methyl aniline were dissolved in 25 ml of acetic acid. The mixture was stirred over nigh under dark. Then the solution was poured into water and extracted with ethyl acetate. The organic layer was washed with distilled water, saturated solutions of $NaHCO_3$ and saturated solutions of NaCl, and dried over $MgSO_4$. After removal the solvent, the crude mixture was subjected to silica gel column chromatography (hexane : AcOEt = 20 : 1) to afford 0.15 g (0.62 mmol) of 4-phenilazo nitrobenzene (yield: 47.3 %). ^{1}H NMR (500 MHz, $CDCl_3$): δ = 8.41- 7.32 (m, 8H, aromatic protons) , 2.77 (s,3H, Ph-CH_3).

4-(2,6-dimethyl phenylazo) nitrobenzene (compound 2-**4**)[11] was synthesized as follows: 0.30 g (1.97 mmol) of 4-nitroso nitrobenzene was dissolved in 50 ml of acetic acid and 0.29 g (2.36 mmol) of 2,6-dimethyl aniline was added. The mixture was stirred over nigh under dark. Then the solution was poured into water and extracted with ethyl acetate. The organic layer was washed with distilled water, saturated solutions of $NaHCO_3$ and saturated solutions of NaCl, and dried over $MgSO_4$. After removal the

solvent, the crude mixture was subjected to silica gel column chromatography (hexane : AcOEt = 9 : 1) to afford 0.05 g (0.20 mmol) of 4-(2,6-dimethyl phenylazo) nitrobenzene (yield: 10.2 %). ^{1}H NMR (500 MHz, $CDCl_3$): δ = 8.40- 7.17 (m, 7H, aromatic protons), 2.45 (s, 6H, Ph-C*H*$_3$).

N-tosyl 2,6-dimethyl aniline (compound 2-(compound 2-**5**)[13] was synthesized as follows: 7.00 g (0.058 mol) of 2,6-dimethyl aniline and 13.27 (0.070 mol) of tosyl chloride were dissolved in 15 ml of pyridine and refluxed for 4 hours. The reaction mixture was poured into 60 ml of 2N HCl,and extracted with ethyl acetate. After removal the solvent, the crude was recrystallized from ethanol and 16.8 g of *N*-tosyl 2,6-dimethyl aniline (yield: quant.). ^{1}H NMR (500 MHz, $CDCl_3$): δ = 7.60, 7.25 (m, 4H, aromatic protons of Ts), 7.10, 7.02 (m, 2H, aromatic protons of aniline), 6.09 (s, 1H, Ph-N*H*-Ts), 2.42 (s, 3H, C*H*$_3$ of Ts), 2.04 (s, 6H, C*H*$_3$ of aniline).

N-tosyl 2,6-dimethyl 4-nitro aniline (compound 2-**6**)[13] was synthesized as follows: 7.05 g (0.026 mol) of *N*-tosyl 2,6-dimethyl aniline was suspended in 145 ml of glacial acid, 30 ml of con. nitric acid and 145 ml of water. To this was added 3.53 (0.051 mmol) of sodium nitrite and the reaction was heated at 140 ^{o}C for 4 hours. The reaction mixture was cooled to room temperature and then cooled in refrigerator. The resulting colorless crystals were filtered of and washed repeatedly with water until the washings were neutral. As a result, 3.09 g (9.65 mmol) of *N*-tosyl 2,6-dimethyl 4-nitro aniline was obtained (yield: 37.1 %). ^{1}H NMR (500 MHz, $CDCl_3$): δ = 7.90 (s, 2H, aromatic protons of aniline), 7.61, 7.30 (d, ^3J = 8.5 Hz, 4H, aromatic protons of Ts), 6.06 (s, 1H, Ph-N*H*-Ts), 2.45 (s, 3H, C*H*$_3$ of Ts), 2.16 (s, 6H C*H*$_3$ of aniline).

2,6-dimethyl 4-nitor aniline (compound 2-**7**)[13] was synthesized as follows: 3.02 g

(9.43 mmol) of *N*-tosyl 2,6-dimethyl 4-nitro aniline was dissolved in15 ml of conc. nitric and 1 ml of water and warmed 40 ^{o}C for 16 hours with stirring. The reaction mixture was poured slowly into ice/water/NaOH mixture. The mixture was extracted with ethyl acetate. After removal the solvent, the crude mixture was subjected to silica gel column chromatography (toluene only) to afford 0.83 g (4.99 mmol) of 2,6-dimethyl 4-nitor aniline (yield: 52.9 %). ^{1}H NMR (500 MHz, $CDCl_3$): δ =7.90, (s, 2H, aromatic protons), 4.28, (s, 2H, NH_2), 2.23 (s, 6H, Ph-CH_3).

3,5-dimethyl 4-nitroso nitrobenzene (compound 2-**8**)[12] was synthesized as follows: 0.67 g (4.03 mmol) of 2,6-dimethyl 4-nitoro aniline was dissolved in 20 ml of CH_2Cl_2 (not anhydrous) under nitrogen atmosphere. 40 ml water solution of 4.95 g (8.06 mmol) of oxone was added and stirred for 4 hours. The organic phase of reaction mixture was corrected, then the removal water phase was washed with CH_2Cl_2 three times. All the organic phase was washed with 1 N HCl twice, saturated solution of $NaHCO_3$ three times and saturated solution of NaCl three times. After removal the solvent, 0.65 g (3.61 mmol) of 2,6-dimethyl 4-nitro nitorsobenzene was obtained (yield: 89.6 %). ^{1}H NMR (500 MHz, $CDCl_3$): δ = 8.10 (s, 2H, aromatic protons), 2.57 (s 6H, Ph-CH_3).

3,5-dimethyl 4-phenilazo nitrobenzene (compound 2-**9**)[11] was synthesized as follows: 0.20 g (1.11 mmol) of 3,5-dimethyl 4-nitroso nitrobenzene was dissolved in 30 ml of acetic acid and 4 ml of DMSO and then 0.12 g (1.33 mmol) of aniline was added. The mixture was stirred 6 days under dark. Then the solution was poured into water and extracted with ethyl acetate. The organic layer was washed with distilled water, saturated solutions of $NaHCO_3$ and saturated solutions of NaCl, and dried over $MgSO_4$. After removal the solvent, the crude mixture was subjected to silica gel column

chromatography (hexane : AcOEt = 10 : 1) to afford 28.0 mg (0.11 mmol) of 4-phenilazo nitrobenzene (yield: 9.91 %). ^{1}H NMR (500 MHz, $CDCl_3$): δ = 8.02, 7.94, 7.58 (m, 1H, 2H, 3H, aromatic protons), 2.34, (s, 6H, Ph-CH_3).

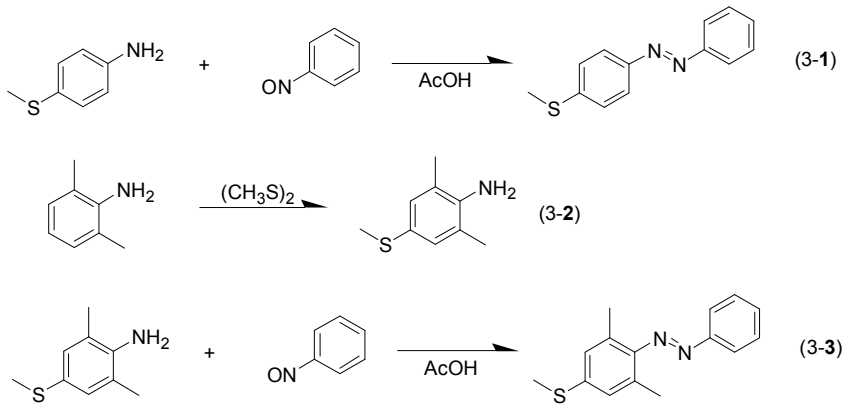

Scheme 3. Synthesis of **4-Methylthio azobenzene derivatives**.

Synthesis of 4-Methylthio azobenzene derivatives: 4-pehylazo methylthio benzene (compound 3-**1**)[11] was synthesized as follows: 0.23 g (2.15 mmol) of 1nitrosobenzene was dissolved in 30 ml of acetic acid and 0.34 g (2.24 mmol) of 4-methylthio aniline was added. The mixture was stirred over nigh under dark. Then the solution was poured into water and extracted with ethyl acetate. The organic layer was washed with distilled water, saturated solutions of $NaHCO_3$ and saturated solutions of NaCl, and dried over $MgSO_4$. After removal the solvent, the crude mixture was subjected to silica gel column chromatography (hexane : AcOEt = 40 : 1) to afford 0.17 g (0.74 mmol) of 4-phenilazo nitrobenzene (yield: 34.4 %). ^{1}H NMR (500 MHz, $CDCl_3$): δ = 7.91- 7.34 (m, 9H, aromatic protons), 2.56 (s, 3H, -S-CH_3).

2,6-dimethyl 4-methylthio aniline[14] (compound 3-**2**) was synthesized as follows: 0.72 g (5.40 mmol) of aluminum chloride and 9.84 g (81.2 mmol) of 2,6-dimethyl aniline was putted in two-necked flask and heated at 150 ^{o}C for 30 minutes. The

solution cooled down for 100 ^{o}C, then 7.63 g (81.0 mmol) of dimethyldisulfide was added in the mixture, and refluxed for 14 hours. After cooled down the mixture for room temperature, 24.3 ml of 1N solution of NaOH was added and extracted with ethyl acetate. The organic phase was separated, the aqueous phase was extracted twice. All the organic phase was combined and washed with solution of saturated NaCl and dried over MgSO4. After removed the solvent, the crude mixture was subjected to silica gel column chromatography (hexane : AcOEt = 20 : 1) to afford 6.74 g (40.3 mmol) of ethyl ester of 2,6-dimethy 4-Methylthiol aniline (yield: 49.4 %). 1H NMR (500 MHz, $CDCl_3$): δ = 7.00 (s,2H, aromatic protons), 2.41 (s,3H, S-CH_3), 2.16 (s, 6H, C_6H_3-(CH_3)$_2$).

4-(2,6 dimethyl 4-thiomethyl phenylazo) benzene (Compound 3-**3**)[12] was synthesized as follows: 0.23 g (2.15 mmol) of nitrosobenzoic and 0.30 g (1.79 mmol) of 2,6-dimethyl 4-thiomethyl aniline was dissolved in 10 ml of acetic acid and stirred overnight at room temperature. Then, the solution was poured into water and extracted with ethyl acetate. The organic layer was washed with distilled water, saturated solutions of $NaHCO_3$ and saturated solutions of NaCl, and dried over $MgSO_4$. After removal the solvent, the crude mixture was subjected to silica gel column chromatography (hexane : AcOEt = 40 : 1) to afford 0.22 g (0.86 mmol) of 4-(2,6 dimethyl 4-thiomethyl phenylazo) benzene (yield: 48.0%). 1H NMR (500 MHz, $CDCl_3$): δ = 7.88 - 7.00 (m, 7H, aromatic protons), 2.51 (s, 3H, -S-CH_3), 2.41 (s, 6H, C_6H_3-(CH_3)$_2$).

3-5-3 Measurements of the rate of *cis*-form

The absorbance spectra were measured with a JASCO V-530 UV-Vis

spectrophotometer equipped with a temperature controller. Conditions for the single-stranded DNA: [DNA] = 20 μM, [NaCl] = 100mM, pH 7.0 (phosphate 10 mM buffer). For the DNA duplex (**D_{44}/C_{44}**), the conditions were same as that of single-stranded DNA expect for the concentration of DNA was 10 μM.

For the HPLC analysis, the modified DNAs dissolved in water and then dived them into two tubes. One of them, the visible light was irradiated for 1minute at60 ^{o}C , and another was irradiated with UV light for 5minutes at 60 ^{o}C. The each samples was analyzed with HPLC in the eluting solution composed of contain water, acetonitrile and ammonium formate.

3-5-4 Half-life ($\tau_{1/2}$) measurement of thermal isomerization of *cis*-azobenzene to the *trans*-form

UV light (λ = 300-400 nm: 5.3 mW•cm-2) was used to irradiate a solution of single-stranded DNA involving azobenzene at 60 °C for 5 min to isomerize *trans*-azobenzene to the *cis*-form. Then the solution was measured with a JASCO V-530 UV-Vis spectrophotometer equipped with a temperature controller, and spectra were monitored at fixed temperature at predetermined intervals. $\tau_{1/2}$ was obtained from the change of absorption maximum of *trans*-azobenzene (320 - 350 nm).

Conditions for measurement of azobenzenes tethered into DNA and carboxylic acid forms: [NaCl] = 100 mM, pH 7.0 (10 mM phosphate buffer), [DNAs] = 20 μM. Half-life measurements of modified azobenzenes in the carboxylic acid form (without tethering to DNA) were also carried out in the same manner as that with DNA, except for the concentration of azobenzenes was 60 μM.

Other azobenzene derivatives except for 4-(2,6-dimethyl phenylazo) nitrobenzene were dissolved in ethanol as a stock solution to be 0.05 M. For measurement, the solution was diluted to 1000 times for the final concentration became 50 μM. In the case of 4-(2,6-dimethyl phenylazo) nitrobenzene, the concentration of stock solution was 0.1 M and the final concentration was 100 μM.

Calculation of the activation entropy and enthalpy: $\Delta S^{\ddagger}$ and $\Delta H^{\ddagger}$ were calculated based on the following equation:

$$\Delta H^{\ddagger} = Ea - RT,\ \Delta S^{\ddagger} = R[\ln A - \ln(kT/h) - 1.00],$$

where *Ea* is the activation energy of thermal isomerization, *A* is the frequency factor of thermal isomerization, *R* is the gas constant, *k* is the Boltzmann constant, and *h* is the Planck constant.[16]

3-6 Note and References

[1] a) S. Yamamoto, N. Nishimura, S. Hasegawa, *Bull. Chem. Soc. Jpn*., **1971**, **44**, 2018-2025. b) C. L. Forber, E. C. Kelusky, N. J. Bunce, M. C. Zerner, *J. Am. Chem. Soc*., **1985**, *107*. 5884-5890. c) E. Diau, W.-G. J. Phys. Chem. A ***2004****, 108, 950-956.* d) I. Coni, M. Garavelli, G. Orlandi, *J. Am. Chem. Soc.*, **2008**, *130*, 5216-5230.

[2] a) P. Haberfield, P. M. Block, M. S. Lux, *J. Am. Chem. Soc.* **1975**, *97*, 5804-5806; b) K. Baba, H. Ono, E. Itoh, S. Itoh, K. Noda, T. Usui, K. Ishihara, M. Inamo, H. D. Takagi, T. Asano, *Chem. Eur. J.* **2006**. *12*, 5328-5333. c) N. Nishimura, T. Sueyoshi, H. Yamanaka, E. Imai, S. Yamamoto, S. Hasegawa, *Bull. Chem. Soc. Jpn.* **1976**, *49*, 1381-1387.

[3] 劉明哲 2006 年度博士(工学)学位論文 東京大学工学系研究科化学生命工学専攻「アゾベンゼン導入 DNA を用いた酵素反応の光制御」.

[4] Note that if the $\varepsilon_t/\varepsilon_c$ is enough high (>10), the rate of *trans*-form calculated form expression (7) is not almost same.

[5] Note that the solution conditions were different to the analysis with HPLC.

[6] P. W Atkins, (千原秀昭, 中村亘男 訳), 「アトキンス物理化学」第 4 版下巻 **1993**, 第 26 省 5 節, 1188-1191.

[7] R. C. Petersen, *J. Org. Chem.* **1964**, *29*, 3133-3135.

[8] T. Asano, T. Okada, *J. Org. Chem.* **1986**, *51*, 4454-4458.

[9] Note that pKa of benzoic acid is 4.20, indicating that 14-15% of **2,6-Me-Azo** is protonated at pH 5. Therefore, $\tau_{1/2}$ did not elongate to 2 h corresponding to that of **2,6-Me-Azo** tethered to DNA. $\tau_{1/2}$ at pH lower than 4, pKa of benzoic acid was also tried to measure. But both **2′,6′-Me-Azo** and **2,6-Me-Azo** did not solve at all under acidic conditions.

[10] 藤岡健太, 2009 年度修士(工学)学位論文 名古屋大学大学院工学研究科物質制御工学専攻 「アゾベンゼン導入遺伝子の構築およびそのタンパク質発現の光スイッチング」.

[11] H. Kagechika, T. Himi, K. Namikawa, E. Kawachi, Y. Hashimoto, K. Shudo, *J. Med. Chem.* **1989**, *32*, 1098-1108.

[12] B-C. Yu, Y. Shirai, J. M. Tour, *Tetrahedron*, **2006**, *62*, 10303-10310.

[13] S. L. Cockroft, J. Perkins, C. Zonta, H. Adams, S. E. Spey, C. M. R. Low, J. G.

Vinter, K. R. Lawson. C. J. Urch, C. A. Hunter, *Org. Biomol. Chem.*, **2007**, *5*, 062–1080.

[14] P. F. Ranken, B. G. Mckinnie, *J. Org. Chem.* , **1989**, *54*, 2985-2988.

[15] Z. F. Liu, K. Morigaki, T .Enomoto, K Hashimoto, A. Fujishima, *J. Phys. Chem.* **1992**, *96*, 1875-1880.

3-7 Appendixes

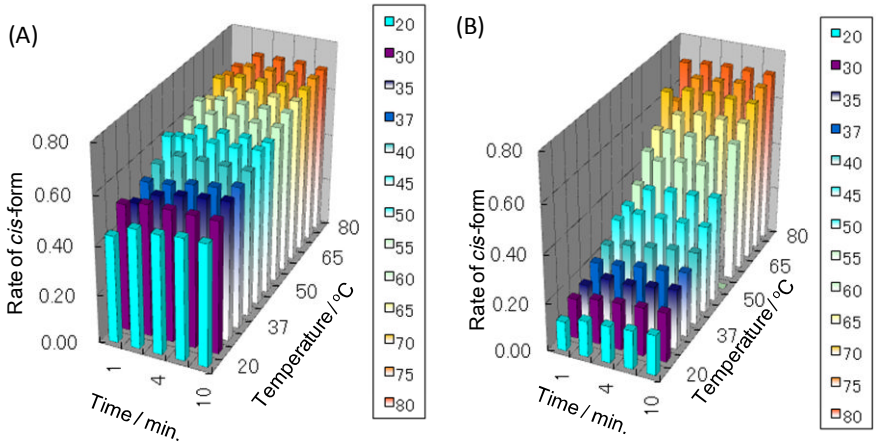

Appendix Figure 3-1. Rate of *cis*- **2′,6′-Me-Azo** tethered into single-stranded **CXG** (A) and **AXC (B)** irradiated with visible or UV light. Solution conditions: [DNA] = 20 μM, [NaCl] = 100 mM, pH 7.0 (phosphate 10 mM buffer). Note that **AXC** can form 8 base-pairs self dimer.

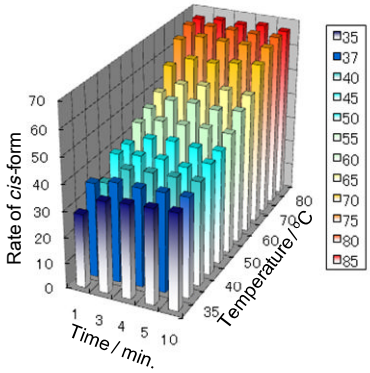

Appendix Figure 3-2. Rate of *cis*- **2′,6′-Me-Azo** tethered into $\mathbf{D_{44}}$ duplex irradiated with visible or UV light. Solution conditions: [DNA] = 20 μM, [NaCl] = 100 mM, pH 7.0 (phosphate 10 mM buffer). The Tm of this duplex was about 70 °C.

Appendix Table 3-1. Half lives ($\tau_{1/2}$) of alkylated azobenzenes tethered into CXG on D-threoninol in buffer solution at several temperatures.

Azobenzene	half life ($\tau_{1/2}$)[a] / h		
	37 °C	45 °C	60 °C
Azo	40.5 (0.017)	17.0 (0.041)	3.3 (0.21)
2-Me-Az	29.1 (0.024)	12.8 (0.054)	2.5 (0.28)
2′-Me-Azo	35.4 (0.020)	14.7 (0.047)	3.0 (0.23)
2′-Et-Azo	28.1 (0.025)	10.9 (0.064)	2.1 (0.32)
3′-Me-Azo	26.2 (0.027)	11.0 (0.063)	1.7 (0.42)
4′-Me-Azo	15.6 (0.045)	6.5 (0.11)	1.0 (0.66)
2,2′-Me-Azo	22.8 (0.029)	8.8 (0.079)	2.1 (0.33)
2,6-Me-Azo	22.5 (0.031)	8.8 (0.079)	2.0 (0.35)
2′,6′-Me-Azo[c]	25.0 (0.028) at 60 °C	5.9 (0.12) at 75 °C	1.4 (0.49) at 90 °C
3′,5′-Me-Azo	20.0 (0.035)	8.3 (0.083)	1.8 (0.39)

[a] Solution conditions: [DNA] = 20 μM, [NaCl] = 100 mM, pH 7.0 (10 mM phosphate buffer). [b] Parenthetic showed the rate constant of thermal isomerization (h^{-1}). [c] Because the half life of *cis*-2′,6′-Me-Azo was very long, the half life of 75 °C and 90 °C were measured instead of 37 °C and 45 °C.

Appendix Table 3-2. Half-lives ($\tau_{1/2}$) of thermal *cis-to-trans* isomerization of azobenzenes in water at various pH.

Azobenzene [a]	$\tau_{1/2}$ / h	
	pH 5.0 [b]	pH 7.0 [c]
2,6-Me-Azo	4.8	10
2′,6′-Me-Azo	32	36

[a]: Azobenzene in carboxylic acid form before the introduction into DNA was used for the $\tau_{1/2}$ measurement. [b]: [NaCl] = 100 mM, pH 5.0 (10 mM phosphate), 60 °C, [azobenzene] = 15 μM. [c]: [NaCl] = 100 mM, pH 7.0 (10 mM phosphate buffer), 60 °C, [azobenzene] = 60 μM.

Appendix Table 3-3. Activation entropy ($\Delta S^{\ddagger}$) and activation enthalpy ($\Delta H^{\ddagger}$) at T = 333 K for the thermal *cis*-to-*trans* isomerization of azobenzenes tethered into single-stranded **CXG** on D-threoninol in buffer solution.

Azobenzene	Activation entropy ($\Delta S^{\ddagger}$) / $Jmol^{-1}K^{-1}$ [a]	Activation enthalpy ($\Delta H^{\ddagger}$) /kJ^{-1} [a]
Azo	-54.3	91.1
2-Me-Az	-57.8	89.9
2′-Me-Azo	-57.1	89.6
2′-Et-Azo	-43.8	93.0
3′-Me-Azo	-17.2	101.2
4′-Me-Azo	-21.1	99.2
2,2′-Me-Azo	-64.0	86.4
2,6-Me-Azo	-58.6	87.9
2′,6′-Me-Azo[c]	-69.0	91.5
3′,5′-Me-Azo	-59.9	87.2

[a] Solution conditions: [DNA] = 20 μM, [NaCl] = 100 mM, pH 7.0 (10 mM phosphate buffer).

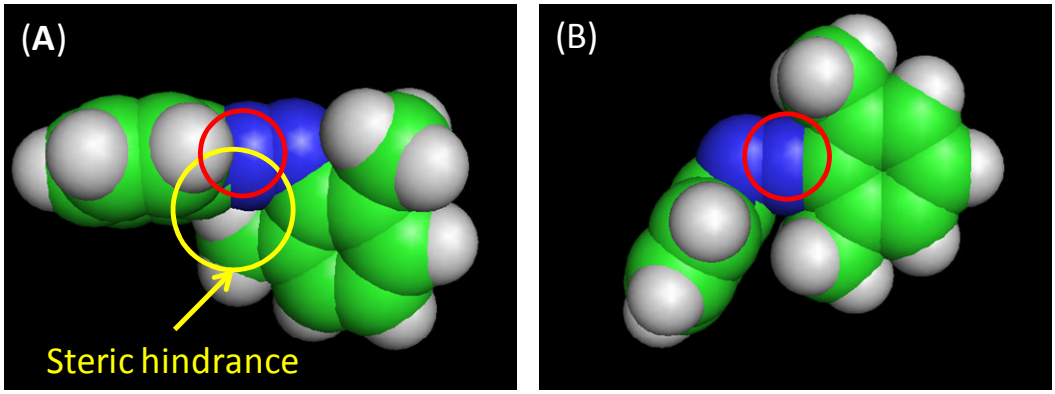

Appendix Figure 3-3. Nolecule modeling of the transition states of thermal isomerization via inversion mechanism either (A) *ortho*-positions of benzene ring far from inversion center nitrogen atom (red cycle) were methylated or (B) *ortho*-positions of benzene ring near inversion center nitrogen atom (red cycle) were methylated.

Appendix Table 3-4. Rate constant of modified azobenzene derivatives in organic solvents. I) **Normal Azo** and **2,6-Me Normal Azo**.

Azobenzene	Solvent (dielectric constant)	Rate constant of thermal isomerization / h^{-1} ($\tau_{1/2}$ / h) [a]						
		20 °C	37 °C	45 °C	50 °C	60 °C	70 °C	80 °C
Normal Azo	Toluene (2.4)	0.006 (116)	0.0382 (18.1)	0.0646 (10.7)		0.410 (1.69)		
	Ethanol (24)		0.023 (30.1)	0.0694 (9.99)	0.116 (5.97)	0.440 (1.58)		
	DMF (38)		0.0194 (35.7)	0.051 (13.6)	0.0917 (7.56)	0.270 (2.56)		
2,6-Me Normal Azo	Toluene (2.4)			0.0158 (43.9)	0.0235 (29.5)	0.0741 (9.35)	0.258 (2.68)	
	Ethanol (24)			0.0066 (105)	0.0111 (62.4)	0.0763 (9.08)	0.126 (5.47)	
	DMF (38)				0.0118 (58.7)	0.0346 (20.0)	0.112 (6.19)	0.361 (1.92)

[a] Solution conditions: All the azobenzene was dissolved in ethanol as a stock solution. For measurement, the stock solution was diluted to 1000 times. The final concentrations were 50 μM.

Appendix Table 3-5. Rate constant of modified azobenzene derivatives in organic solvents. II) **Nitro azobenzene**.

Azobenzene	Solvent (dielectric constant)	Rate constant of thermal isomerization / h^{-1} ($\tau_{1/2}$ / h) [a]					
		5 °C	15 °C	20 °C	37 °C	45 °C	60 °C
Nitro Azo	Toluene (2.4)		0.0414 (16.7)	0.0871 (7.96)	0.705 (0.984)	1.63 (0.424)	6.92 (0.100)
	Ethanol (24)		0.075 (9.24)	0.146 (4.75)	0.974 (0.712)	2.79 (0.249)	
	DMF (38)		0.444 (1.56)	0.723 (0.959)	3.24 (0.214)	8.08 (0.0858)	
2′-Me Nitro Azo	Toluene (2.4)		0.0273 (25.4)	0.052 (13.3)	0.538 (1.29)	1.340 (0.495	
	Ethanol (24)		0.0581 (11.9)	0.103 (6.72)	0.785 (0.883)	1.93 (0.360)	
	DMF (38)		0.174 (3.99)	0.308 (2.25)	1.51 (0.460)	2.58 (0.269)	
2,6-Me Nitro Azo	Toluene (2.4)		0.340 (2.04)	0.555 (1.25)	2.78 (0.250)	6.15 (0113)	
	Ethanol (24)		0.550 (1.26)	0.939 (0.738)	6.14 (0.112)	22.9 (0.0302)	
	DMF (38)[b]	0.178 (3.90)	0.65 (1.07)	1.41 (0.491)	8.617 (0.0804)		
2′,6′-Me Nitro Azo[c]	Toluene (2.4)			0.0048 (144)	0.045 (15.4)	0.125 (5.53)	0.679 (1.02)
	Ethanol (24)			0.0106 (65.4)	0.0747 (9.28)	0.184 (3.76)	1.08 (0.639)
	DMF (38)		0.249 (2.78)	0.334 (2.07)	1.26 (0.550)	2.176 (0.318)	

[a] All the azobenzene was dissolved in ethanol as a stock solution. For measurement, the stock solution was diluted to 1000 times. The final concentrations except for **2′,6′-Me Nitro Azo** were 50 μM. [b] Diluted to 2000 times for final concentration was 25 μM. [c] The final concentration of **2′,6′-Me Nitro Azo** was 100 μM.

Appendix Table 3-6. Rate constant of modified azobenzene derivatives in organic solvents. III)**Methylthio azobenzene**.

Azobenzene	Solvent (dielectric constant)	Rate constant of thermal isomerization / h^{-1} ($\tau_{1/2}$ / h) [a]				
		20 °C	37 °C	45 °C	50 °C	60 °C
Thio Azo	Toluene (2.4)		0.195 (3.55)	0.555 (1.25)	0.874 (0.793)	3.21 (0.216)
	Ethanol (24)	0.0137 (50.6)	0.137 (5.06)	0.345 (1.99)		1.82 (0.380)
	DMF (38)		0.168 (4.13)	0.39 (1.78)	0.661 (1.05)	2.37 (0.293)
2,6-Me Thio Azo	Toluene (2.4)		0.0448 (15.5)	0.0543 (12.8)	0.111 (6.26)	0.369 (1.88)
	Ethanol (24)		0.0033 (83.5)	0.0334 (20.8)	0.0749 (9.25)	0.219 (3.16)
	DMF (38)		0.0146 (47.5)	0.0389 (17.8)	0.0884 (7.84)	0.263 (2.67)

[a] Solution conditions: All the azobenzene was dissolved in ethanol as a stock solution. For measurement, the stock solution was diluted to 1000 times. The final concentrations were 50 μM.

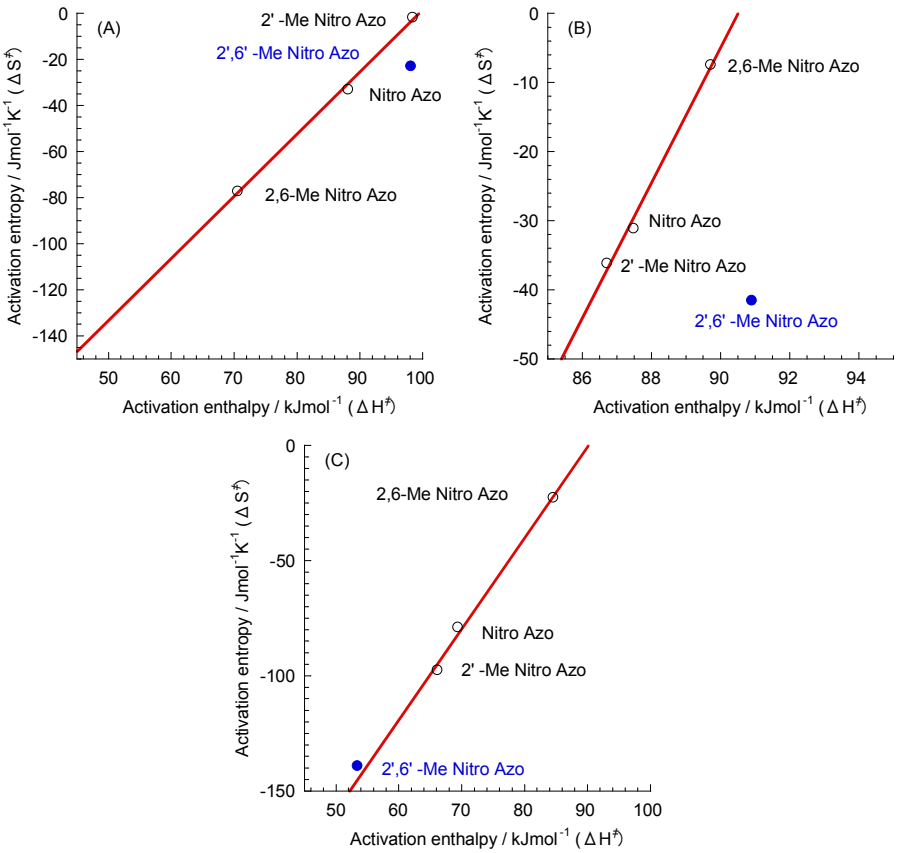

Appendix Figure 3-4. Plot of activation entropy ($\Delta S^{\ddagger}$) as a function of activation enthalpy ($\Delta H^{\ddagger}$) at T = 318 K for the thermal *cis*-to-*trans* isomerization of Nitro azobenzenes in (A) Toluene, (B) Ethanol and (C) DMF.

Appendix Table 3-7. λ_{max} of the absorbance spectra of modified azobenzene in organic solvents.

	λ_{max} of the absorbance / nm		
Azobenzene	Toluene	Ethanol	DMF
Normal Azo	321.0	317.0	321.0
2,6-Me Normal Azo	319.5	314.5	315.0[a]
Nitro Azo	332.5	329.5	335.0
2′-Me Nitro Azo	345.0	340.5	343.5
2,6-Me Nitro Azo	319.5	316.5	320[b]
2′,6′-Me Nitro Azo	340.0	335.5	339.5
Thio Azo	365.0	362.0	367.0
2,6-Me Thio Azo	363.0	359.0	358.5

[a] Measured at 50 ^{o}C. [b] Measured at 37 ^{o}C.

Chapter 4. Photoregulation of DNA hybridization with Visible Light

4-1 Abstract

New azobenzene derivatives **Thio-DMAzo**, in which methylthio group was introduced at the *para*-position and two methyl group were introduced at *ortho*-positions of distal benzene ring, was synthesized introduced into DNA for the efficient photoregulation of DNA hybridization with visible light (without UV light). **Thio-DMAzo** reversibly photoisomerized *trans*- ↔ *cis*-form by visible light irradiation due to introduced methylthio group and showed large ΔT_m due to introduced methyl groups. Although electro donating methylthio group was introduced, the half life of *cis*-**Thio-DMAzo** was almost same as that of non-modified azobenzene due to methylation at two *ortho*-positions of distal benzene ring.

4-2 Introduction

As described in Chapter 2, photoregulation efficiency of DNA hybridization was improved by modified the *ortho*-position of azobenzene. Especially for **2′,6′-Me-Azo**, in which tow *ortho*-positions of distal benzene ring were methylated, the photoregulation efficiency based on ΔT_m became 3-times as large as that of

non-modified azobenzene (**Azo**). However, these modified azobenzene derivatives need UV light irradiation for *trans*- to *cis*-photoisomerization. Especially for biological use like photoregulation of enzymatic reactions, UV light irradiation is harmful because it causes damages to biological molecule like enzyme and sometimes regulation efficiency decreased after several time photoregulation.[1] Therefore, new azobenzene derivative which can isomerize with irradiation of visible region light and also have efficient photoregulation efficiency has been required. If photoregulation of DNA hybridization will be attained by irradiation of visible region light, advanced photon-driven DNA nanodevices will also expected to be created by using new azobenzene derivative together with previous azobenzene derivatives which isomerize with UV light.

Generally, azobenzene and its derivatives have absorbance at UV light region (λ_{max} = 340 ~ 360 nm) based on π-π* transition and visible light region (λ_{max} = 450 nm) based on n-π* transition. By excitation of UV right region, azobenzene derivatives isomerize to *cis*-form. It is known that in order to shift the π-π* absorbance to visible light region, introducing functional group which has electric effect to the azobenzene to enhance the electric conjugate system.[2] For the photoregulation of DNA hybridization, azobenzene derivatives were attached to D-threoninol via electric accepting amide bond at *para*-position with respect to –N=N- bound. Therefore, in order to enhance the electric

conjugate system, electric donating functional group should be introduced at *para*-position. In fact, in previous study, by introducing methylthio group at *para*-position of azobenzene, the absorbance based on π-π* transition was shifted and reversibly photoisomerized *trans*- ↔*cis*- form by visible light irradiation.[1, 3, 4] However, as shown in chapter 2, modification at *para*-position of distal benzene ring decreased the photo regulation efficiency and thermal stability of *cis*-azobenzene. On the other hand, modification at two *ortho*-positions of distal benzene ring, both the photoregulation efficiency and the thermal stability of *cis*-form were dramatically improved. Therefore, by synthesizing new azobenzene derivative (**Thio-DM-Azo**, Figure 4-1) which has methylthio group at *para*-position and methyl group at two *ortho*-positions of distal benzene ring, the photoregulation efficiency and both photo and thermal isomerization were investigated.

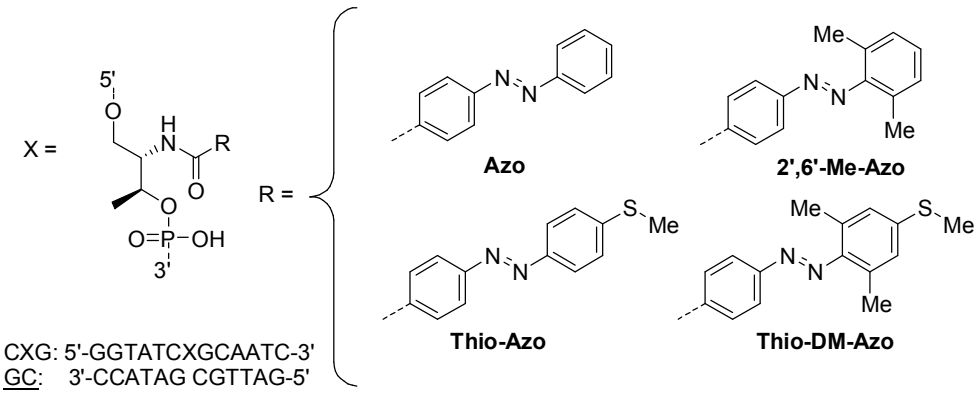

Figure 4-1. Modified azobenzene derivativesused in this study.

4-3 Results and Discussions

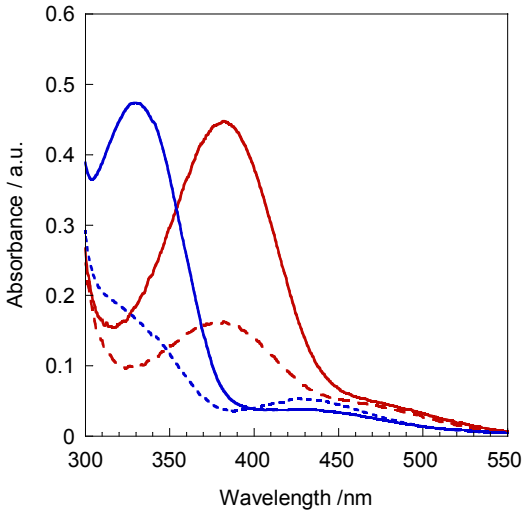

Figure 4-2. Absorbance spectra of **Thio-DMAzo** tethered into **CXG** (red line) and that of **Azo** (blue line) either *trans*-form (solid line) or *cis*-form (dot line) at 60 °C. Solution conditions: [**CXG**] = 20 μM, [NaCl] = 100 mM, pH 7.0 (10 mM phosphate buffer).

Figure 4-2 showed the absorbance spectra of newly synthesized azobenzene derivative **Thio-DMAzo** tethered into DNA strands **CXG** together with **Azo**. In the case of *trans*-form, the maximum absorbance based on π-π* transition shifted from 330 nm to 390 nm at 60 °C (red sold line in Figure 4-2). Irradiated with 400 nm light to that sample, the spectra changed to red dot line in Figure 4-2. This result indicated that *trans*-**Thio-DMAzo** isomerized to *cis*-form by irradiated with visible region light. In addition, by irradiated with 450 nm visible light or kept at high temperature, the absorbance increased; isomerized to *trans*-form. In theses ways, **Thio-DMAzo** reversibly photoisomerized irradiated with visible region light. The detail of

photoisomerization and thermal isomerization was discussed in section **4-3-2** and **4-3-3.**

4-3-1 Photoregulation efficiency of Thio-DMAzo

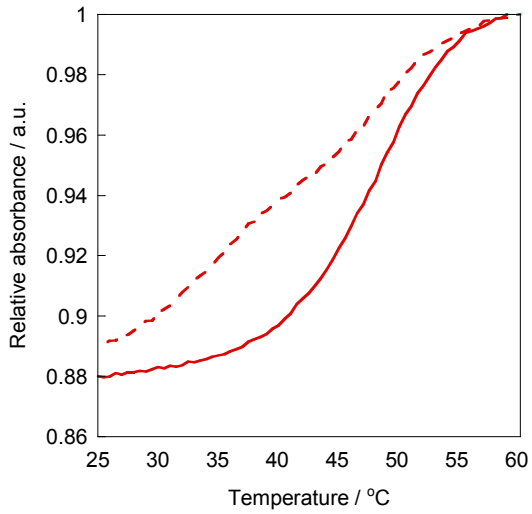

Figure 4-3. Melting curves of **CXG/GC** duplex involving **Thio-DMAzo** either in the *trans*-form (solid line) or the *cis*-form (dot line). Solution conditions: [DNA] = 5 μM, [NaCl] = 100 mM, pH 7.0 (10 mM phosphate buffer).

Figure 4-3 showed the melting curves of DNA duplex involving either *trans*- or *cis*-**Thio-DMAzo** and the T_m was shown in Table 4-1. The T_m of *trans*-**Thio-DMAzo** (48.3 °C) was almost same as that of **Azo** (48.9 °C). As discussed in chapter 2, *trans*-**2′,6′-Me-Azo** stabilized the DNA duplex than *trans*-**Azo** due to the methyl groups introduced at *ortho*-positions of azobenzene. In the case of **Thio-DMAzo**, the stabilization effect of methyl groups introduced at *ortho*-positions and destabilization effect of methylthio group introduced at *para*-position would be canceled each other, so, the T_m of *trans*-**Thio-DMAzo** was almost same as that of **Azo**. In fact, in the case of

Thio-Azo, in which only methylthio group was introduced at *para*-position, the T_m of *trans*-form was 46.1 ^oC which was lower than the T_m of non-modified DNA (without azobenzene, 47.7 ^oC).

Table 4-1. Effect of chemical modification of azobenzene on the T_m of **CXG/GC** in *trans*- and *cis*-forms.

	T_m / ^oC[a]		
Azobenzene	*trans*	*cis*	ΔT_m[b]
Azo	48.9	43.2	5.7
2′,6′-Me-Azo	50.9	36.3	14.6
Thio-Azo[c]	46.1	45.2	0.9
Thio-DMAzo	48.3	34.9	13.4

[a] Solution conditions: [DNA] = 5 μM, [NaCl] = 100 mM, pH 7.0 (10 mM phosphate buffer). [b] Change in T_m induced by *cis- trans* isomerization. [c] The data came from the master thesis of Department of Molecular Design and Engineering, Graduate school of engineering, Nagoya university written by K. Fujioka. [1]

On the other hand, the T_m of *cis*-**Thio-DMAzo** (34.9 ^oC) was lower than that of *cis*-**Azo** (43.2 ^oC), almost same as that of *cis*-**2′,6′-Me-Azo** (36.9 ^oC). In the case of *cis*-**Thio-DMAzo**, the methyl groups introduced at *ortho*-positions would have caused steric hindrance with neighbor base-pairs like as *cis*-**2′,6′-Me-Azo**. As a result, **Thio-DMAzo** showed efficient photoregulation efficiency: ΔT_m of **Thio-DMAzo** (13.4 ^oC) was larger than that of **Azo** (5.7 ^oC), and almost same as that of **2′,6′-Me-Azo** (14.6 ^oC).

As same as other *ortho* di-methylated azobenzenes like **2,6-Me-Azo** or

2′,6′-Me-Azo, *trans*- to *cis*-photoisomerization was decreased by modification at both *ortho*-positions of one benzene ring. As a result, even after irradiation of 400 nm light, *trans*-**Thio-DMAzo** remained. Therefore, in the T_m curve of *cis*-**Thio-DMAzo**, there was two sigmoid could be found: the upper one corresponded remained *trans*-**Thio-DMAzo** and lower one corresponded *cis*-**Thio-DMAzo**.

4-3-2 Photoisomerization of Thio-DMAzo

As described above, newly synthesized azobenzene derivative **Thio-DMAzo** isomerized *trans*- ↔ *cis*- form by irradiation of visible region light. In this section, photoisomerization of **Thio-DMAzo** with several wavelengths light was investigated.

4-3-2-1 Dependence of absorbance spectra on temperatures

Figure 4-4 showed the absorbance spectra of *trans*-**Thio-DMAzo** in single-stranded DNA and DNA duplex at several temperatures. As the temperature decreased, the maximum absorbance wavelength (λ_{max}) clearly shifted to long wavelength both in single-stranded DNA and DNA duplex. In particular, in DNA duplex at low temperatures (under 50 ^{o}C), the shits became large (the λ_{max} was listed in appendix Table 4-1). In addition, the absorbance also clearly changed as the change of temperature; the absorbance increased as the temperature decreased both in

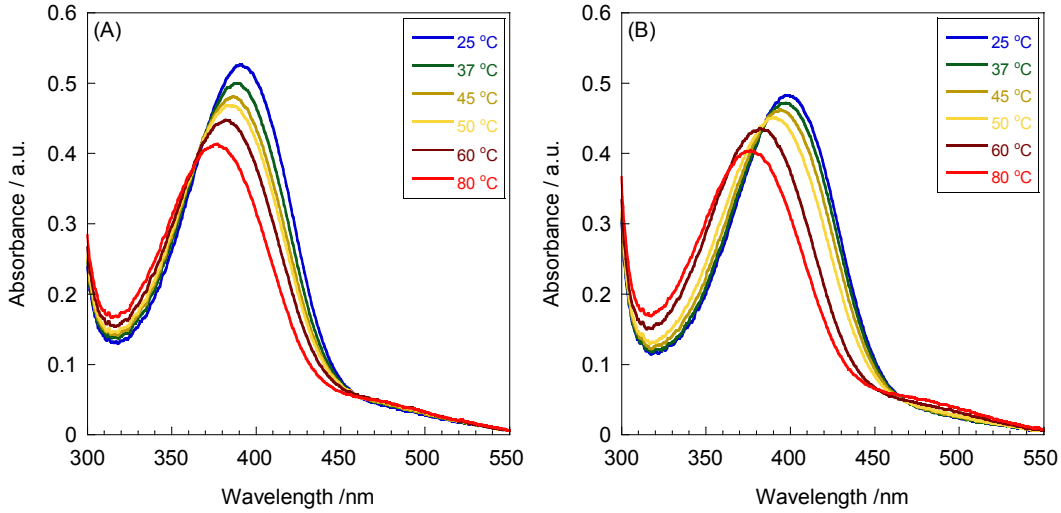

Figure 4-4. Absorbance spectra of *trans*-**Thio-DMAzo** tethered into (A) single-stranded **CXG** and DNA duplex **CXG/GG** at 25, 37, 45, 50, 60 and 80 °C. Solution conditions: [DNA] = 20 μM, [NaCl] = 100 mM, pH 7.0 (10 mM phosphate buffer). The *trans*-form was obtained by keep the sample at 90 °C long hour.

single-stranded DNA and duplex. Such clearly changes of both the λ_{max} and absorbance intensity were observed for **2′,6′-Me-Azo**. Theses clear changes of absorbance spectra would have based on the effect of neighboring bases (or base-pairs). At high temperature, the interaction between *trans*-**Thio-DMAzo** and the neighboring bases (or base-pairs) was weak, so the *trans*-**Thio-DMAzo** was twisted because of the steric hindrance of methyl groups at *ortho*-positions of azobenzene and azo bound (the computer modeling of *trans*-**Thio-DMAzo** and **Azo** were shown in Appendix Figure 4-1). As the temperature decreased, the interaction between the neighboring bases (or base-pairs) and *trans*-**Thio-DMAzo** increased and so the planarity of *trans*-**Thio-DMAzo** was increased. Therefore, electro conjugate system expanded as the

temperature decreased. As a result, the λ_{max} of absorbance and absorbance intensity of *trans*-**Thio-DMAzo** changed as the temperature changed. The interaction of duplex (neighboring base-pairs) was larger than that of single-stranded DNA (neighboring bases) so, the shift of λ_{max} in duplex at low temperatures would have became larger than that of in single-stranded DNA. The absorbance of *trans*-azobenzene in duplex was generally decreased by the interaction with base-pairs, so, the increasing rate of absorbance of *trans*-**Thio-DMAzo** in duplex at low temperature was smaller than that of in single-stranded DNA. In the case of *ortho*-unmodified azobenzene, such a clear dependency of absorbance spectra on temperature was not observed because the planarity of *trans*-form itself was high. In addition, in the case of **Thio-DMAzo** without DNA, such a clear dependency of absorbance spectra on temperature was not also observed (Appendix Figure 4-2).

4-3-2-2 Rate of *cis*-Thio-DMAzo after light irradiation

The rate of *cis*-form was calculated the absorbance spectra as described in Chapter 3. For **Thio-DMAzo**, the $\varepsilon_t/\varepsilon_c$ (the ratio of extinction coefficient of *trans*- and *cis*-form) at 366 nm was 16 obtained by HPLC analysis. (The method of HPLC analysis was different with Chapter 3. See experimental section in this chapter.) In all case, after 10

minutes light irradiation, **Thio-DMAzo** reached photostationary states (Appendix Figure 4-3).

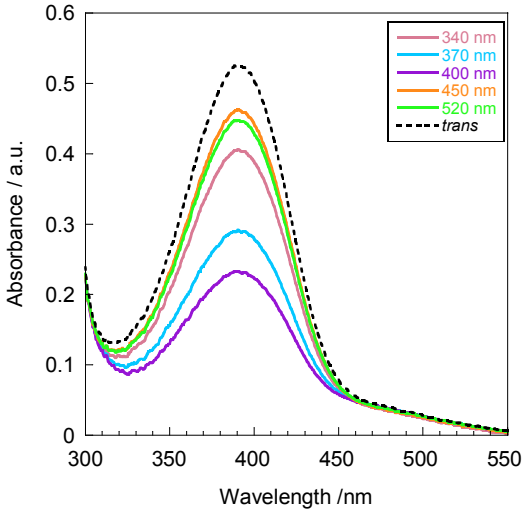

Figure 4-5. Change of absorbance spectra of **Thio-DMAzo** tethered into single-stranded **CXG** irradiated with 340 nm, 370 nm, 400 nm, 450 nm and 520 nm wavelength light at 25 °C. Solution conditions: [DNA] = 20 μM, [NaCl] = 100 mM, pH 7.0 (10 mM phosphate buffer). The each light was irradiated for 10 minutes.

Table 4-2. Rate of *cis*-**Thio-DMAzo** tethered into single-stranded **CXG** irradiated with several wavelengths light at several temperatures.

	The rate of *cis*-form[a]				
Temperatures	340 nm	370 nm	400 nm	450 nm	520 nm
25 °C	0.22	0.45	0.56	0.12	0.15
37 °C	0.26	0.51	0.61	0.14	0.22
60 °C	0.42	0.66	0.66	0.17	0.25
80 °C	0.45	0.70	0.65	0.19	0.27

[a] Solution conditions: [DNA] = 20 μM, [NaCl] = 100 mM, pH 7.0 (10 mM phosphate buffer). Each light was irradiated for 10 minutes.

In single-stranded DNA: Figure 4-5 showed the absorbance spectra after light irradiation in DNA strand at 25 °C. The rates of *cis*-**Thio-DMAzo** were listed in Table

4-2. The **Thio-DMAzo** isomerized to *cis*-form by irradiated with 400 nm wavelength at any temperature. As like as **2′,6′-Me-Azo**, the rate of *cis*-form decreased as the temperature decreased. It would have been also the effect of neighboring bases. Interestingly, at high temperature (80 ^{o}C), the rates of *cis*-form irradiated 370 nm were higher than that of irradiated with 400 nm. At high temperature, as discussed above, the λ_{max} of absorbance spectra shifted to short wavelength. Therefore, at high temperature, **Thio-DMAzo** isomerized to *cis*-form irradiated with 370 nm light than that of irradiated with 400 nm. On the other hand, irradiated with 450 nm wavelength light, **Thio-DMAzo** isomerized to *trans*-form at any temperatures.

In DNA duplex: As like as **2′,6′-Me-Azo** or other azobenzene derivatives, the rates of *cis*-**Thio-DMAzo** after light irradiation showed dependency on temperature. As shown in Table 4-3, at high temperature, the rates of *cis*-**Thio-DMAzo** were almost the same as those of in single-stranded DNA. At low temperatures, the rate of *cis*-form decreased compared with those of in single-stranded DNA irradiated with any wavelength light. In DNA duplex, *trans*-azobenzene moiety was stabilized by DNA duplex. Therefore, in the condition of DNA duplex formed, the rates of *cis*-isomer would have decreased.

Interestingly, in DNA duplex at the temperature lower than T_m, **Thio-DMAzo** isomerized to *trans*-form after irradiation of 340 nm wavelength light whereas azobenzene without methylthio group isomerized to *cis*-form by that light. By using this property, advanced type of DNA nonomachine could be created (Chapter 6).

Table 4-2. Rate of *cis*-**Thio-DMAzo** tethered into DNA duplex **CXG**/**GC** irradiated with several wavelengths light at several temperatures.

	The rate of *cis*-form[a]				
Temperatures	340 nn	370 nm	400 nm	450 nm	520 nm
25 °C	0.09	0.25	0.40	0.07	0.06
37 °C	0.11	0.29	0.41	0.04	0.05
60 °C	0.40	0.64	0.63	0.14	0.22
80 °C	0.47	0.66	0.65	0.17	0.25

[a] Solution conditions: [DNA] = 20 μM, [NaCl] = 100 mM, pH 7.0 (10 mM phosphate buffer). Each light was irradiated for 10 minutes.

4-3-3 Thermal isomerization of Thio-DMAzo

In single-stranded DNA: Generally, by chemical modification of azobenzene the thermal stability of *cis*-isomer was decreased.[5] The methylthio group acts as electro

Table 4-3. Half lives ($\tau_{1/2}$) of azobenzene derivatives modified with methylthio group tethered into single-stranded **CXG** at 60 °C.

Azobenzene	Half life ($\tau_{1/2}$) /h[a]
Azo	3.3
Thio-Azo[b]	0.42
Thio-DMAzo	6.4

[a] Solution conditions: [DNA] = 20 μM, [NaCl] = 100 mM, pH 7.0 (10 mM phosphate buffer). [b] The data came from the master thesis of Department of Molecular Design and Engineering, Graduate school of engineering, Nagoya university written by K. Fujioka.[1]

donor and carboxyl group (amide bound) acts as electro accepter, so the decrease of the thermal stability would be large. In fact, as shown in Table 4-3, the half life ($\tau_{1/2}$) of **Thio-Azo**, in which methylthio group was introduced at *para*-position, tethered into single-stranded **CXG** at 60 ^{o}C was only 0.42 h which was shorter than that of **4′-Me-Azo**, in which methyl group was introduced at *para*-position (1.0 h). As discussed in Chapter 3, by methylation at two *ortho*-positions of specific benzene ring, thermal isomerization was restricted: same benzene ring in the case of azobenzene has electro donating group at *para*-position or the opposite side benzene ring in the case of azobenzene has electro accepting group. Therefore, the thermal isomerization of *cis*-**Thio-DMAzo** expected to be restricted. As shown in Table 4-3, at 60 ^{o}C the $\tau_{1/2}$ was 6.4 h, which was 15 times as long as that of **Thio-Azo** and even longer than that of **Azo**.

Table 4-4. Half lives ($\tau_{1/2}$) of carboxylic acid form of **Thio-DMAzo** in various solvents at 60 ^{o}C.

Half life ($\tau_{1/2}$)[a]		
Toluene	Ethanol	DMF
0.66	1.7	1.83

[a] Carboxylic acid from of **Thio-DMAzo** was dissolved in ethanol as a stock solution. For measurement, the stock solution was diluted to 1000 times. The final concentrations: were about 10 μM.

As shown in Table 4-4, as the polarity of the solvent decreased (DMF → Ethanol → Toluene), the $\tau_{1/2}$ of carboxylic acid form of **Thio-DMAzo** was decreased. This result indicated that thermal isomerization of **Thio-DMAzo** was through the inversion

mechanism. Therefore, the increase of thermal stability of *cis*-**Thio-DMAzo** would have been also due to the steric hindrance between methyl groups introduced at *ortho*-positions of benzene ring and nitrogen atom in transition states. The detail of thermal isomerization was discussed in Chapter 3.

In DNA duplex: The thermal isomerization in DNA duplex **CXG/GC** was also investigated. The $\tau_{1/2}$ of *cis*-**Thio-DMAzo** in DNA duplex at several temperatures was shown in Figure 4-6 together with that of in single-stranded DNA. At 60 or 45 °C, the $\tau_{1/2}$ of in duplex was almost as same as those of in single-stranded DNA. On theater hand, at 37 or 25 °C at which DNA duplex formed, the $\tau_{1/2}$ became shorter than those of in single-stranded DNA. The neighboring base-pairs would have destabilized the

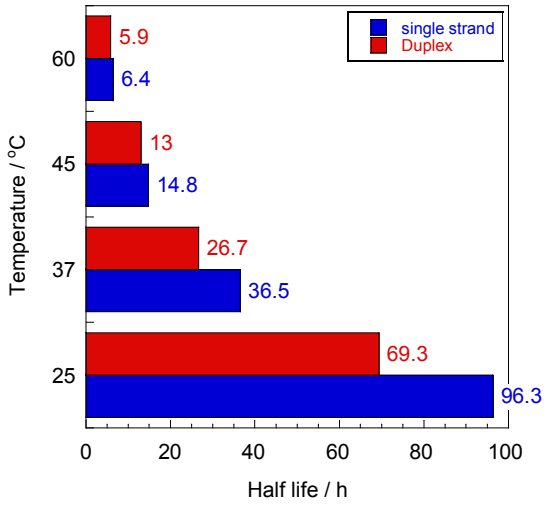

Figure 4-6. Half lives ($\tau_{1/2}$) of *cis*-**Thio-DMAzo** either in single-stranded **CXG** (blue bar) or DNA duplex **CXG/GC** (red bar). Solution conditions: [DNA] = 20 μM, [NaCl] = 100 mM, pH 7.0 (10 mM phosphate buffer).

cis-**Thio-DMAzo** and stabilized *trans*-**Thio-DMAzo** so, the thermal stability decreased in DNA duplex under the T_m. These results were corresponded in **2′,6′-Me-Azo**, as shown in Chapter 3.

4-4 Conclusions

(1) Efficient photoregulation of DNA hybridization was attained by newly synthesized azobenzene derivative **Thio-DMAzo** which had methylthio group at *para*-position and two methyl groups at *ortho*-positions of distal benzene ring. The photoregulation efficiency based on T_m was 3 times as large as that of non-modified azobenzene (**Azo**).

(2) **Thio-DMAzo** isomerized to *cis*-form irradiated with 400 nm wavelength light and isomerized to *trans*-form irradiated with 450 nm wavelength light by the effect of introduced methylthio group.

(3) By the effect of methyl groups introduced at *ortho*-positions, the thermal stability of *cis*-**Thio-DMAzo** was improved compared with **Thio-Azo** in which methylthio group was introduced at *para*-position.

4-5 Experimental section

4-5-1 Synthesis of modified DNA involving methylthiolated azobenzene

The modified DNA containing modified azobenzene **Thio-DMAzo** were synthesized on automated DNA synthesizer (ABI-3400, Applied Biosystems) using conventional and azobenzene-carrying phosphoramidite monomers. The DNAs containing only native bases were supplied by Integrated DNA Technologies, Inc. (Coralville, IA. U.S.A.).

4-5-2 Synthesis of methylthiolated azobenzene

Materials: Aluminum chloride, hydrochloric acid and sodium hydrate were purchased from Kishida Chemical Co., Ltd. (Osaka, Japan). 2,6-dimethyl aniline, dimethyl disulfide and 4-nitrobenzoic acid ethyl ester were purchased from Tokyo Chemical Industry (Tokyo, Japan). D-threoninol and 1-hydroxy 1H-benzotriazol (HOBt) were purchased from Sigma-Aldrich (St. Louis, MO, U.S.A.). N, N′-dicyclohexylcarbodiimde (DCC) was purchased from WATANABE CHEM. IN., LTD. (Hiroshima, Japan). 2-Cyanoethyl *N,N,N′,N′*-tetraisopropylphosphordiamidite was purchased from ChemGenes (Wilmington, MA, U.S.A.).

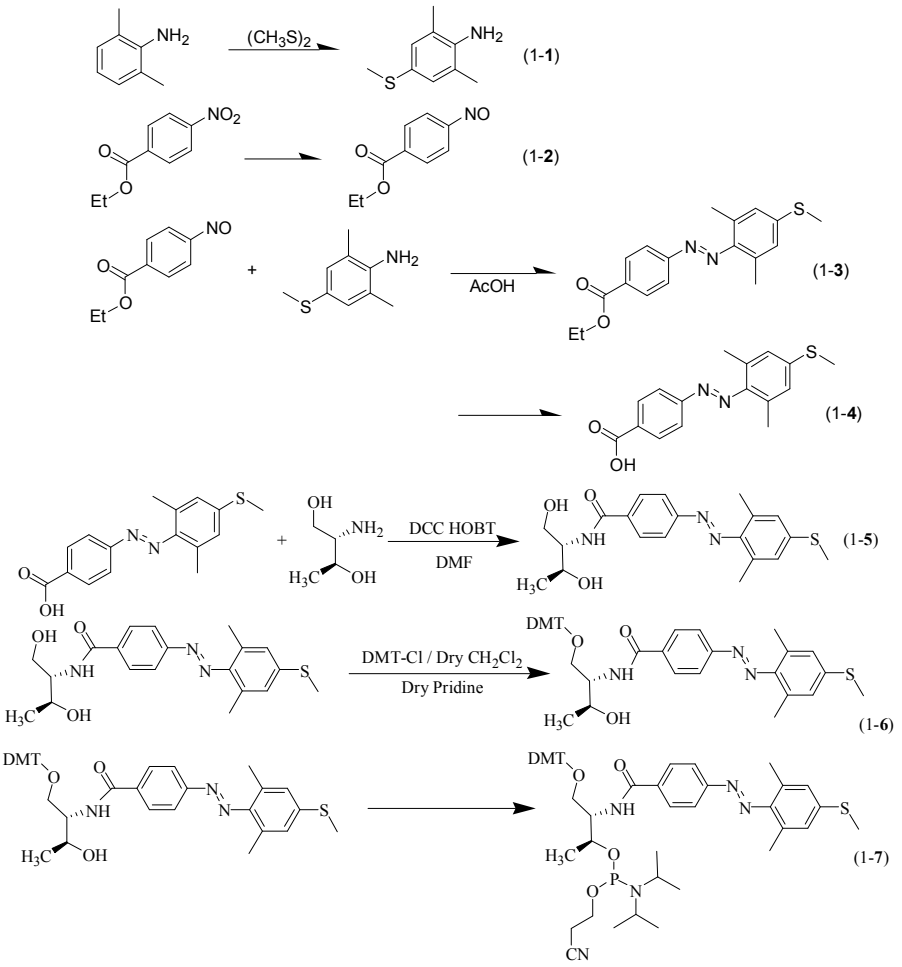

Scheme 1. Synthesis of phosphoramidite monomer of **Thio-DMAzo**.

Synthesis of phosphoramidite monomer of Thio-DMAzo: 2,6-dimethyl 4-methylthio aniline (compound 1-**1**) and Ethyl *p*-nitrosobenzoate (compound 1-**2**) were synthesized as shown in Chapter 2 and 3, respectively.

4-(2,6 dimethyl 4-methylthio phenylazo) benzoic acid ethyl ester (Ethyl ester of **Thio-DMAzo**)[6] (Compound **1-3**) was synthesized as follows: 1.08 g (6.03 mmol) of 4-nitrosobenzoic acid ethyl ester and 0.87 g (5.20 mmol) of 2,6-dimethyl 4-methylthio aniline was dissolved in 30 ml of acetic acid in flask and stirred overnight at room temperature. Then, the solution was poured into water and extracted with ethyl acetate. The organic layer was washed with distilled water, saturated solutions of $NaHCO_3$ and

saturated solutions of NaCl, and dried over $MgSO_4$. After removal the solvent, the crude mixture was subjected to silica gel column chromatography (hexane : AcOEt = 20 : 1) to afford 1.14 g (3.47 mmol) of 4-(2,6 dimethyl 4-methylthio phenylazo) benzoic acid ethyl ester (yield: 66.7 %). 1H NMR (500 MHz, $CDCl_3$): δ = 8.19, 7.89, 7.00 (m, 6H, aromatic protons), 4.43 (q, ^3J(H,H) = 7.0 Hz, 2H, -O-CH_2-CH_3), 2.52 (s, 3H, -S-CH_3), 2.47 (s, 6H, C_6H_3-(CH_3)$_2$), 1.44 (t, ^3J(H,H) = 7.0 Hz, 3H, -O-CH_2-CH_3).

4-(2,6-dimethyl 4-methylthio phenylazo) benzoic acid (Carboxyl acid of Thio-DMAzo)[6] (Compound 1-**4**) was synthesized as follows: 1.14 g (3.47 mmol) of ethyl ester of **Thio-DMAzo** was dissolved in 80 ml of ethanol. Then 0.26 g (4.45 mmol) of 10 ml of NaOH solution was added and the mixture was stirred overnight under dark. After the hydrolysis was completed, HCl solution (1N) was added to the mixture until the solution became acidify and extracted with ethyl acetate. The organic layer was washed with distilled water and saturated solution of NaCl and dried over $MgSO_4$. After removal the solvent, the crude product was used in the next step without further purification (1.04 g (3.47 mmol), yield: quant.). 1H NMR (500 MHz, $CDCl_3$): δ = 8.26, 7.92, 7.01 (m, 6H, aromatic protons), 2.53 (s,3H, -S-CH_3), 2.49 (s, 6H, C_6H_3-(CH_2)$_2$).

Compound 1-**5** was synthesized as follows: 0.42 g (3.99 mmol) of D-threoninol was coupled with 1.47 g (3.47 mmol) of carboxyl acid of **Thio-DMAzo** in the presence of 0.89 g (4.31 mmol) of dicyclohexylcarbodiimide and 0.58 g (4.29 mmol) of 1-hydroxybenzotriazole in 30 ml of DMF. After the reaction mixture was stirred at room temperature for 24 h under dark, the solvent was removed and the remained oil was subjected to silica gel column chromatography (chloroform : MeOH = 20 : 1) to afford 1.34 g (3.47 mmol) of compound 1-**5** (yield: quant). 1H NMR (500 MHz, $CDCl_3$): δ =

7.99, 7.92, 7.27, 7.00 (m, 7H. aromatic protons and –N*H*CO-), 4.35 (m, 1H, $CH_3C\mathit{H}(OH)$-), 4.13 (m, 1H, $-CH_2(OH)C\mathit{H}(NH)CO$-)-), 3.99 (m, 2H, $HOC\mathit{H}_2CH(NH)CO$-), 2.53 (s, 3H, -S-$C\mathit{H}_3$), 2.47 (s, 6H, C_6H_3-$(C\mathit{H}_2)_2$), 1.31 (m, $CH(OH)C\mathit{H}_3$).

Compound 1-**6** was synthesized as follow: Dry pyridine solution (20 ml) containing 1.34g (3.47 mmol) of compound 1-**5** was cooled on ice under nitrogen, and 1.46 g (4.31 mmol) of 4,4-dimethoxytrityl chloride in 10 ml of dry dichloromethane was added to the above mixture. After 6 h of stirring, the solvent was removed, followed by silica gel column chromatography (Hexane : AcOEt : Et_3N = 50 : 50 : 3) to afford 1.41 g (2.04 mmol) of compound 1-**6** (yield: 58.8 %). ^{1}H NMR (500 MHz, $CDCl_3$): δ = 7.96 – 6.77 (m, 20H, aromatic protons of azobenzene and DMT and –N*H*CO-), 4.25, (m, 1H, -C*H*(OH)CH_3), 4.15 (m, 1H, $-CH_2(OH)C\mathit{H}(NHCO$-)-), 3.77 and 3.76 (s, 6H, -C_6H_5-$OC\mathit{H}_3$), 3.63 and 3.40 (dd, ^2J(H,H) = 10 Hz, ^3J(H,H) = 4.0 Hz, 2H; $C\mathit{H}_2$-ODMT),2.53 (s, 3H, -S-$C\mathit{H}_3$), 2.48 (s, 6H, C_6H_3-$(C\mathit{H}_3)_2$).

Compound 1-7 was synthesized as follows: In dry acetonitrile (4 ml) under nitrogen, 0.42 g (0.61 mmol) of compound 1-**6** and 0.22 g (0.73 mmol) of 2-cyanoethyl *N,N,N',N'*-tetraisopropylphosphordiamidite were reacted with 0.051 g (0.73 mmol) of 1*H*-tetrazole with ice bath. Prior to the reaction, compound 1-**6** and 1*H*-tetrazole were dried by coevaporation with dry acetonitrile (twice). After 0.5 h, the ice bath was removed, the mixture reacted more 0.5 h. The 1*H*-tetrazole was quenched with methanol, then the solvent was removed by evaporation then the crude mixture was dissolved in ethyl acetate. The solvent was washed with distilled water and saturated solution of $NaHCO_3$ and saturated solution of NaCl and dried over $MgSO_4$. After

removal the solvent, followed by silica gel column chromatography (Hexane : AcOEt : Et_3N = 50 : 50 : 3) to afford 0.45 g (0.056 mmol) of compound **2-3**. (yield: 83.2 %).

MALDI-TOFMS for **CXG** with **Thio-DM Azo**: obsd. 4094 (calculated for protonated form: 4094).

4-5-3 Calculation of the concentration of DNA involving Thio-DMAzo moieties

Generally, the concentration of DNA was calculated from the absorbance at 260 nm because the extinction coefficient at260 nm can be obtained from the DNA sequence in theory.[7] However, the azobenzene derivatives also have large absorbance at 260 nm. In the case of DNA involving **Thio-DMAzo**, the absorbance at 260 nm of **Thio-DMAzo** was calculated by the maximum absorbance around 400 nm. In the case carboxylic acid form of **Thio-DMAzo** dissolved in water including 5 % of ethanol, the ratio of absorbance at 260 nm and 393 nm (maximum absorbance wavelength of **Thio-DMAzo** in DNA strand **CXG**) A_{260}/A_{393} was 1.12. Note that in chapter 6, the ration of absorbance at 260 nm and 360 nm (maximum absorbance of carboxylic acid form of **Thio-DMAzo**) A_{260}/A_{393} (0.832) was applied for the maximum absorbance in that DNA.

4-5-4 HPLC analysis

In order to obtain the $\varepsilon_t/\varepsilon_c$ (the ratio of extinction coefficient of *trans*- and *cis*-form) at 366 nm, HPLC analysis was performed as follows.

The sample including modified DNA including **Thio-DMAzo** was irradiated with 400 nm wavelength light. Then, the sample was dived two parts, and one part was

analyzed with HPLC at 290 nm (isosbestic point wavelength) to get the rate of *trans*- and *cis*-form of **Thio-DMAzo**. Another part of sample was analyzed with another HPLC at 366 nm. Here, next expression (1) consisted.

$$\frac{S_{trans-290}}{S_{cis-290}} = \frac{S_{trans-366}}{S_{cis-366}} \div \varepsilon_t/\varepsilon_c \qquad (1)$$

Here, $S_{trans\text{-}X}$ represents the area of HPLC chart of *trans*-form at X nm and $S_{cis\text{-}X}$ represents that of *cis*-form. From this expression, the $\varepsilon_t/\varepsilon_c$ (the ratio of extinction coefficient of *trans*- and *cis*-form) at 366 nm can be calculated.

4-5-5 T_m measurements

See chapter 2.

4-5-6 Photoisomerization of Thio-DMAzo

A xenon light source (MAX-301, Asahi Spectra Co.,Ltd. Tokyo, Japan) equipped with an interference filter was used for photoisomerization. The properties of interference filters were follows: 340 nm: (half bandwidth 9 nm) centered at 340.5 nm, 370 nm: (half bandwidth 12 nm) entered at 369.0 nm, 400 nm: (half bandwidth 11 nm) entered at 398.5 nm, 450 nm: (half bandwidth 9 nm) centered at 449.5 nm, 520 nm: (half band width 11.0 nm) centered at 520.5 nm.

4-5-7 Measurements of the rate of *cis*-form

In order not to remain the single-stranded **CXG**, complementary strand **GC** was added for 1.2 eq in the case of duplex analysis. The absorbance at 366 nm was used for calculation. See chapter 3.

4-5-8 Half-life ($\tau_{1/2}$) measurement of thermal isomerization of *cis*-azobenzene to the *trans*-form

In order not to remain the single-stranded **CXG**, complementary strand **GC** was added for 1.2 eq in the case of duplex analysis. The absorbance at 380 nm was used for calculation. See Chapter 3.

4-6 Notes and References

[1] 藤岡健太, 2009 年度修士(工学)学位論文 名古屋大学大学院工学研究科物質制御工学専攻 「アゾベンゼン導入遺伝子の構築およびそのタンパク質発現の光スイッチング」.

[2] P. C. Chen, Y. C. Chieh, J. C. Wu, *Journal of Molecular Structure*, **2005**, *715*, 183-189.

[3] T. Fujii, H. Kashida, H. Asanuma, *Chem, Eur, J*., **2009** *15*, 10092-10102.

[4] Modification at ortho-position of distal benzene ring also expected to be enhance the electro conjugate system and the absorbance based on π-π* shifted to visible light region. However, in the case modified the azobenzene at *ortho*-position of distal benzene with methylthio group, ring the absorbance was not shifted to visible light region. See the appendix section for detail information of that azobenzene.

[5] a) P. Haberfield, P. M. Block, M. S. Lux, *J. Am. Chem. Soc.* **1975**, *97*, 5804-5806; b) K. Baba, H. Ono, E. Itoh, S. Itoh, K. Noda, T. Usui, K. Ishihara, M. Inamo, H. D. Takagi, T. Asano, *Chem. Eur. J.* **2006**. *12*, 5328-5333.

[6] H. Kagechika, T. Himi, K. Namikawa, E. Kawachi, Y. Hashimoto, K. Shudo, *J. Med.*

Chem. **1989**, *32*, 1098-1108.

[7] C. R. Cantor, *Bioplymers*, **1970**, *9*, 1059-1077.

4-7 Appendixes

AppendixTable 4-1. λ_{max} of absorbance spectra of **Thio-DMAzo** either in single-stranded **CXG** or in DNA duplex **CXG**/**GC** at several temperatures.

	λ_{max} of absorbance / nm [a]	
Temperature / °C	In **CXG**	In **CXG**/**GC**
25	391.1	397.0
37	388.5	397.5
45	386.5	394.5
50	382.0	390.0
60	382.0	382.0
80	377.0	376.0

[a] Solution conditions: [DNA] = 20 μM, [NaCl] = 100 mM, pH 7.0 (10 mM phosphate buffer).

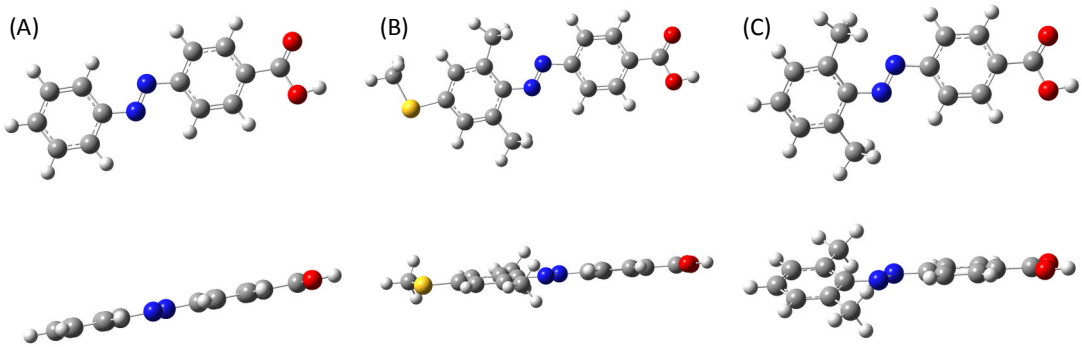

Appendix Figure 4-1. The computer modeling of (A) *trans*-**Thio-DMAzo** (B) *trans*-**Azo** and (C) *trans*-**2′,6′-Me-Azo** of top view (above) and side view (bottom). The gaushian was used for molecular modeling.

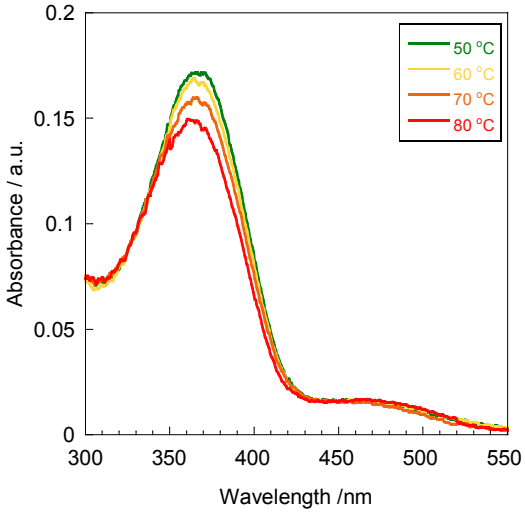

Appendix Figure 4-2. Dependence of absorbance spectra on temperatures of carboxylic acid form of **Thio-DMAzo** in ethanol. Solution conditions: [carboxylic acid form of **Thio-DMAzo**] = about 10 μM.

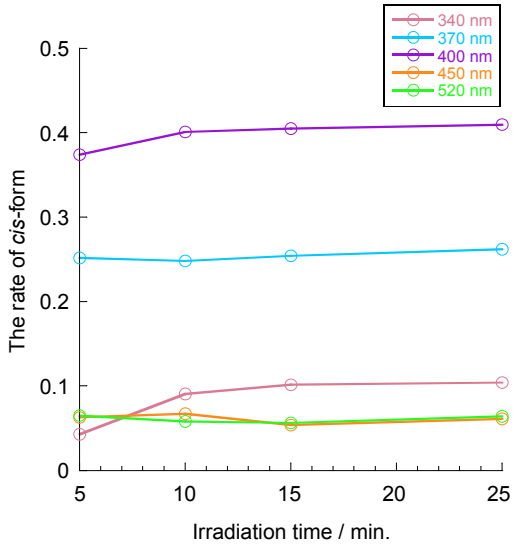

Appendix Figure 4-3. Change of the rates of *cis*-**Thio-DMAzo** tethered into DNA duplex **CXG**/**GC** after light irradiation at 25 °C. In the initial states, almost **Thio-DMAzo** took *trans*-form. Then, light was irradiated in following order::340 nm→ 520 nm → 370 nm → 450 nm →400 nm. Solution conditions: [DNA] = 20 μM, [NaCl] = 100 mM, pH 7.0 (10 mM phosphate buffer).

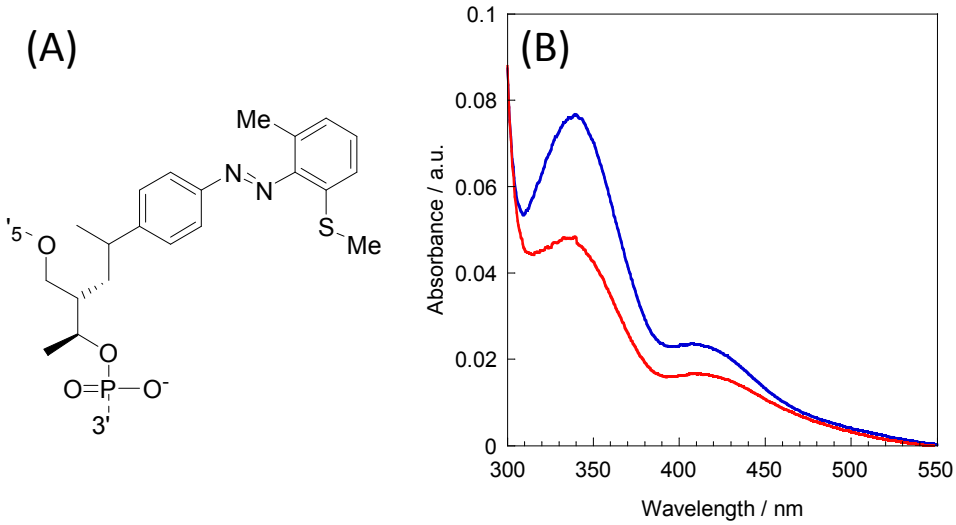

Appendix Figure 4-4. (A) Structure of 2′-methyl 6′-methylthio azobenzene and (B) its absorbance spectra tethered into DNA duplex **CXG/<u>GC</u>** either *trans*- (blue solid line) or *cis*-form (red dot line) at 60 °C. Solution condition: [DNA] = 5 μM, [NaCl] = 100 mM, pH 7.0 (10 mM phosphate buffer). Note that the T_ms of this DNA strand were 50.6 °C (*trans*-form) and 34.2 °C (*cis*-form).

Chapter 5. Direct observation of efficient photoregulation of DNA hybridization by introducing multiple azobenzene moieties

5-1 Abstract

Photoregulation of DNA hybridization involving multiple (five or nine) non-modified azobenzene (**Azo**), *ortho*-methylated azobenzene (**2′-Me-Azo**) or *ortho*-dimethylated azobenzene (**2′,6′-Me-Azo**) moieties were observed by the change of fluorescence intensity at fixed temperature. The fluorescence dye FAM and its quencher dye Dabcyl were attached to the DNA strand and its complementary strand, respectively for the direct observation of DNA hybridization. Calculated from the intensity of FAM, efficient photoregulation was attained at wide range of temperature by introducing nine modified azobenzene moieties.

5-2 Introduction

As described previous chapters, efficient photoregulation of DNA hybridization was attained with *ortho*-methylated azobenzene derivatives. However, the photoregulation efficiency of only one azobenzene moiety was not enough high for the clear-cut photoregulation of DNA function. In addition, the photoregulation efficiency

of azobenzene derivatives was estimated only by the differences of the stability of DNA duplex induced by photoisomerization of azobenzene moieties (ΔT_m). In this chapter, clear-cut photoregulation was attained by introducing multiple azobenzene moieties and the photoregulation of DNA hybridization at a fixed certain temperature was directly monitored from change of fluorescence intensity.

For the direct observation of DNA hybridization, at the 5′ end of the DNA sequence composed of twenty native bases, FAM was attached as a fluorophore and at the 3′ end of its complementary strand involving azobenzene moieties. Dabcyl was attached as a quencher (Figure 5-1).[1] By this designing, in the case of DNA duplex dissociated, the fluorescence of FAM was observed strongly. On the other hand, in the case of DNA duplex formed, the fluorescence of FAM decreased (Figure 5-3).[2] In addition, the rate of dissociated (or formed) DNA duplex can be calculated from the fluorescence intensity.

In this chapter, $\mathbf{D_{Azo}}$, $\mathbf{D_{MAzo}}$ or $\mathbf{D_{DMAzo}}$ represent the DNA involving non-modified azobenzene (**Azo**) moieties, *ortho*-methylated azobenzene (**2′-Me-Azo**) moieties or *ortho*-dimethylated azobenzene (**2′,6′-Me-Azo**) moieties, respectively. The number shown with the sequence represents the number of introduced azobenzene moieties.

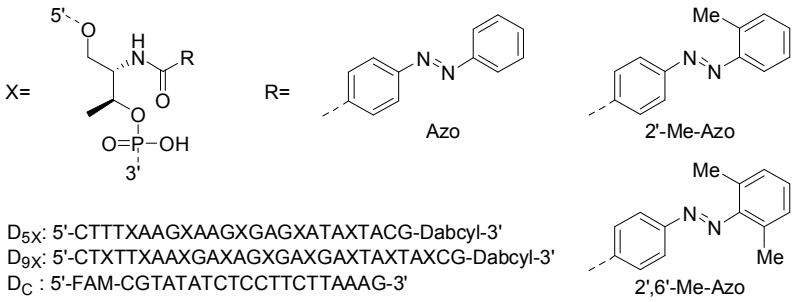

Figure 5-1. Structures of azobenzene moieties and the sequences of DNA used in this study.

5-3 Results and Discussions

5-3-1 Melting temperatures (T_ms) analysis

The melting temperatures (T_ms) of DNA duplexes both irradiated with visible light (450 nm) and UV light (360 nm) were measured to estimate the photoregulation efficiencies from the change of stability of DNA duplex induced by photoisomerization of azobenzene moieties.

Introducing five azobenzene moieties: As shown in Table 5-1, the T_m of $\mathbf{D_{MAzo5}/D_C}$ involving five **2′-Me-Azo** moieties with visible light irradiation was higher than that of duplex involving five **Azo** moieties ($\mathbf{D_{Azo5}/D_C}$). In contrast, The T_m with UV light was lower than that of duplex involving five **Azo** moieties. As a result, ΔT_m (the change of T_m between irradiation of visible light and UV light) of $\mathbf{D_{MAzo5}/D_C}$ became 26.5 ^oC, which was almost as twice as that of $\mathbf{D_{5Azo}/D_C}$ (13.3 ^oC).

Table 5-1. Melting temperature (T_m) of DNA duplex involving multiple azobenzene moieties.

Azobenzenes	sequences	T_m / °C[a]		
		Visible light[b]	UV light[c]	ΔT_m [d]
Azo	D_{5Azo}/D_C	57.6	44.3	13.3
	D_{9Azo}/D_C	52.5	19.1	33.4
2′-Me-Azo	D_{5MAzo}/D_C	60.8	34.3	26.5
	D_{9MAzo}/D_C	59.8	20.0	39.8
2′,6′-Me-Azo	D_{5DMAzo}/D_C	64.3	38.9	25.4
	D_{9DMAzo}/D_C	64.2	23.2	41.0

[a] Solution conditions: [DNA] = 0.1 μM, [NaCl] = 100 mM, pH 8.0 (10 mM phosphate buffer). [b] Irradiation of Visible light (450 nm) for 1minute at 80 °C. [c] Irradiation of UV light (360 nm) for 5 minutes at 75 °C. [d] Change of T_m induced by the Vis – UV light irradiation.

On the other hand, by introducing five **2′,6′-Me-Azo** moieties (**D_{5DMAzo}/D_C**), the ΔT_m of **D_{5DMAzo}/D_C** (25.4 °C) was almost the same as that of **D_{MAzo5}/D_C** (26.5 °C) although the photoregulatory efficiency of one **2′,6′-Me-Azo** was larger than that of **2′-Me-Azo**. As shown in Table 5-1, the T_m of **D_{5DMAzo}/D_C** with visible light (64.3 °C) was 3.7 °C higher than that of **D_{MAzo5}/D_C** corresponded with the result of only one azobenzene moiety took *trans*-form by visible light irradiation. In contrast, the T_m of **D_{5DMAzo}/D_C** with UV light was higher than that of **D_{MAzo5}/D_C** although one *cis*-form of **2′,6′-Me-Azo** (irradiated with UV light) moiety father destabilized the DNA duplex than that of **2′-Me-Azo**. As described in Chapter 3, *trans*-to *cis*- photoisomerization is inhibited because of steric hindrance caused by methylation of both two *ortho*-positions

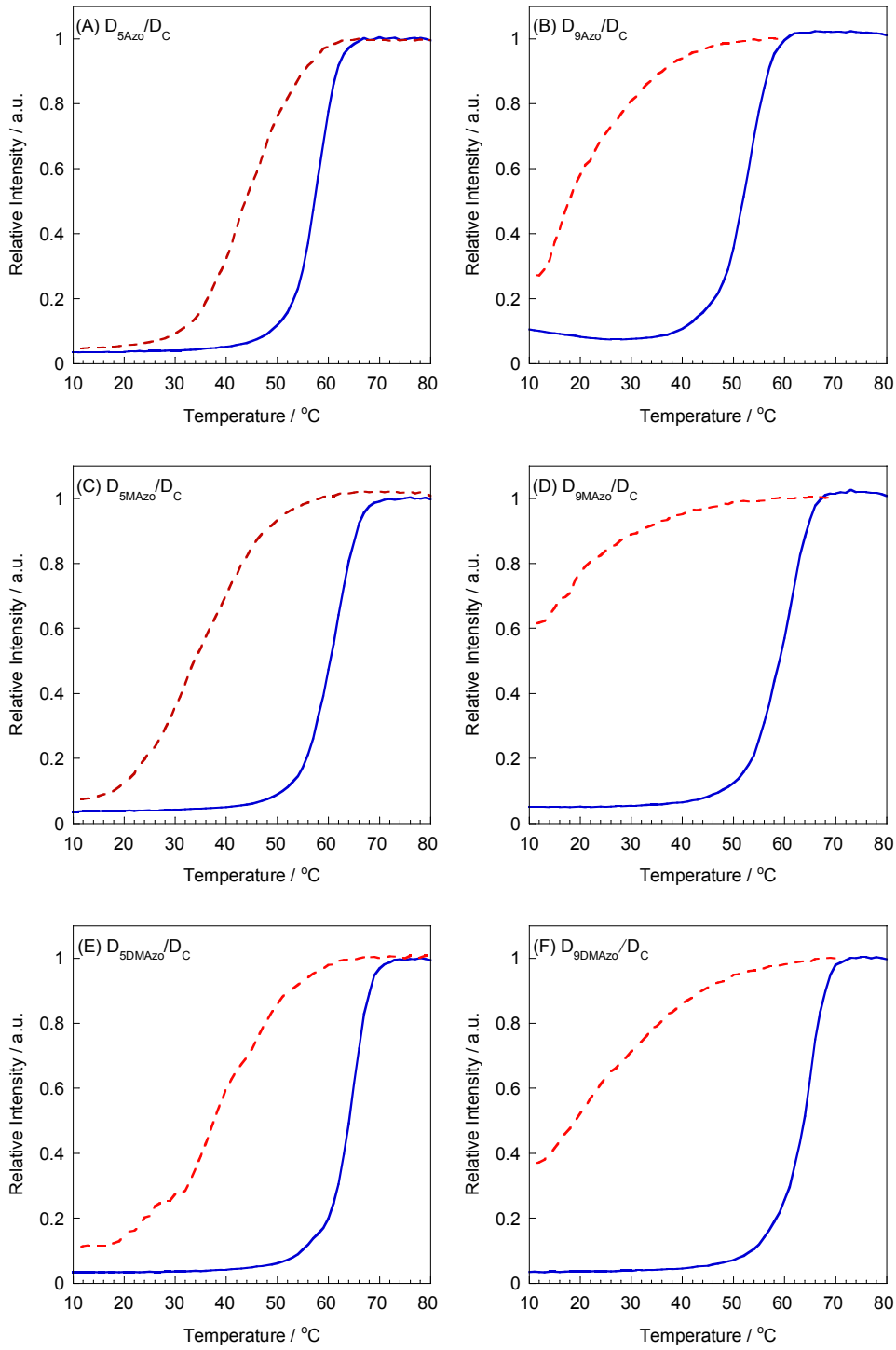

Figure 5-2. Melting curves of the DNA duplex (A) $\mathbf{D_{5Azo}/D_C}$, (B) $\mathbf{D_{9Azo}/D_C}$, (C) $\mathbf{D_{5MAzo}/D_C}$, (D) $\mathbf{D_{9MAzo}/D_C}$, (E) $\mathbf{D_{5DMAzo}/D_C}$ and (F) $\mathbf{D_{9DMAzo}/D_C}$ either in the visible light irradiation (blue solid line) or UV light irradiation (red dot line). Solution conditions: [DNA] = 0.1 μM, [NaCl] = 100 mM, pH 8.0 (10 mM phosphate buffer).

of benzene ring; for example, after 5 minutes UV light irradiation, almost 65 % of **2′,6′-Me-Azo** takes *cis*-form whereas almost 80 % of **2′-Me-Azo** or **Azo** takes *cis*-form. Therefore, even after UV light irradiation, a lot of **2′,6′-Me-Azo** moieties remained as *trans*-form and would have stabilized DNA duplex.

Introducing nine azobenzene moieties: In the case of involving nine azobenzene moieties, further interesting results were obtained. Although *trans*-**Azo** stabilize the DNA duplex, the T_m of $\mathbf{D_{9Azo}/D_C}$ irradiated with visible light (52.5 ^oC) was almost 5 ^oC lower than that of $\mathbf{D_{5Azo}/D_C}$ involving five **Azo** moieties (57.6 ^oC, involving five **Azo** moieties). In addition, the T_ms of both $\mathbf{D_{9MAzo}/D_C}$ and $\mathbf{D_{9DMAzo}/D_C}$ which involving nine of **2′-Me-Azo** and **2′,6′-Me-Azo** with visible light irradiation were not higher than those of $\mathbf{D_{5MAzo}/D_C}$ and $\mathbf{D_{5DMAzo}/D_C}$ involving five azobenzene moieties. In this study, multiple azobenzene moieties were introduced into only one strand of DNA duplex additionally, as shown in Figure 5-1. Therefore, by introducing too many azobenzene moieties, the length of one side DNA strand became longer than another strand. The large difference of DNA strand of one DNA duplex caused strain in the DNA duplex and decreased the symmetry of DNA duplex. As a result, although *trans*-**Azo** can stabilize the DNA duplex,[3] the stability of DNA duplex involving nine **Azo** moieties might decreased compared with that of involving five **Azo** moieties. However,

trans-**2′-Me-Azo** or **2′,6′-Me-Azo** stabilize DNA duplex than *trans*-**Azo**, so the T_m of $\mathbf{D_{9MAzo}/D_C}$ or $\mathbf{D_{9DMAzo}/D_C}$ irradiated with visible light was not decreased compeered with involving five azobenzene moieties ($\mathbf{D_{5MAzo}/D_C}$ or $\mathbf{D_{5DMAzo}/D_C}$). After UV light irradiation, The T_ms were obtained for all the duplex used in this study. However, as shown in Figure 5-2, the change of fluorescence intensity of D_{9MAzo}/D_C or D_{9DMAzo}/D_C (especially for $\mathbf{D_{9MAzo}/D_C}$) was little. These results indicated that after UV light irradiation, $\mathbf{D_{9MAzo}/D_C}$ and $\mathbf{D_{9DMAzo}/D_C}$, especially for $\mathbf{D_{9MAzo}/D_C}$ did not form duplexes even at 10 ^oC, although the T_m was calculated as almost 20 ^oC. As described above, after irradiated with UV light a lot of **2′,6′-Me-Azo** remained as *trans*-form. Therefore, although *cis*-**2′,6′-Me-Azo** destabilized DNA duplex than *cis*-**2′-Me-Azo** (described in Chapter 2), $\mathbf{D_{9MAzo}/D_C}$ could form duplex than $\mathbf{D_{9DMAzo}/D_C}$ after UV light irradiation. Anyway, by introducing nine azobenzene moieties, the stability of DNA duplex was decreased irradiation with UV light than by introducing five azobenzene moieties. The photoregulation efficiency based on T_m was increased as the number of introduced azobenzene moieties.

5-3-2 Direct observation of photo regulation of DNA duplex at fixed temperatures

In previous section, photoregulation efficiency was discussed based on the stability of DNA duplex. In addition, the light was irradiated in the conditions that azobenzene moieties were isomerized well. In this section, the formation and dissociation of DNA duplex induced by light irradiation at fixed temperature was observed. Figure 5-3 showed the change of fluorescence intensity induced by visible or UV light irradiation. From the intensity of fluorescence, the rate of dissociated duplex and regulation efficiency was estimated.

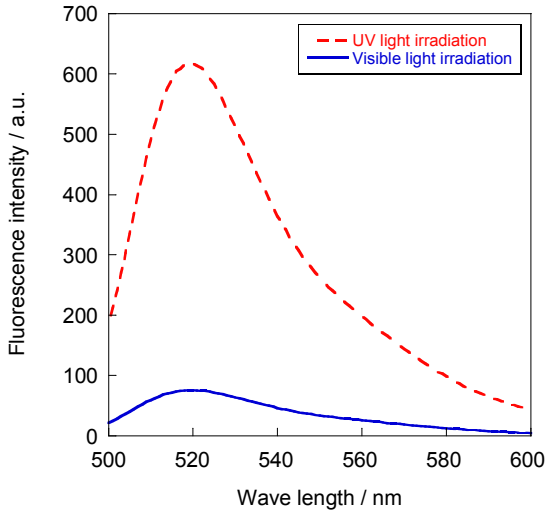

Figure 5-3. Change of fluorescence intensity induced by irradiation of visible light (blue solid line) or UV (red dot line) light to the $\mathbf{D_{9DMAzo}/D_C}$ DNA duplex at 45 °C. Solution conditions: [DNA] = 0.1 μM, [NaCl] = 100 mM, pH 8.0 (10 mM phosphate buffer).

In the case of introducing **Azo** moieties, most efficient photoregulation was attained

introducing five azobenzene moieties, not nine moieties (see bar graph in Figure 5-3); the regulation efficiency of $\mathbf{D_{Azo9}/D_C}$ (involving nine **Azo** moieties) was only 57.5 % at 40 °C, although that of $\mathbf{D_{Azo5}/D_C}$ (involving five **Azo** moieties) was as high as 75.4 % at 50 °C. Note that this result did not correspond with that of ΔT_m: ΔT_m of $\mathbf{D_{Azo9}/D_C}$ was

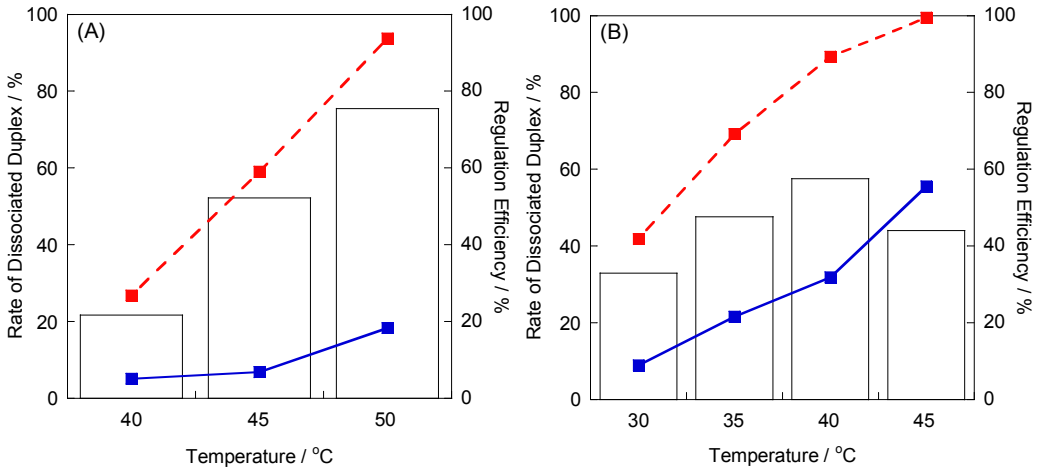

Figure 5-4. Change of the rate of dissociated DNA duplex involving **Azo** moieties: (A) $\mathbf{D_{5Azo}/D_C}$ and (B) $\mathbf{D_{9Azo}/D_C}$ induced by visible light (blue square) or UV light (red square) irradiation and photoregulation efficiency (bar graph) at fixed temperatures. Solution conditions: [DNA] = 0.1 μM, [NaCl] = 100 mM, pH 8.0 (10 mM phosphate buffer).

larger than that of $\mathbf{D_{Azo5}/D_C}$. As shown in Figure 5-4, in the case of involving nine **Azo** moieties, the DNA duplex still open after visible light irradiation: only 70 % of DNA duplex formed even at 35 °C which was 15 °C as low as the T_m of $\mathbf{D_{9Azo}/D_C}$ irradiated with visible light. As described above, by introducing too many azobenzene moieties, the DNA duplex destabilized because the length of DNA strands are different. In addition, the difference of DNA back born might cause winding in DNA duplex.[1]

Therefore, to form the duplex, the slow change of condition would be required. In the case of light irradiation, because the change of condition (photoisomerization of azobenzene) was drastic (the irradiation time was only 1 minute), the duplex did not form well. In contrast, in the case of temperature changed slowly (1 °C / min), the duplex formed well because the change of condition (temperature) was slow and the

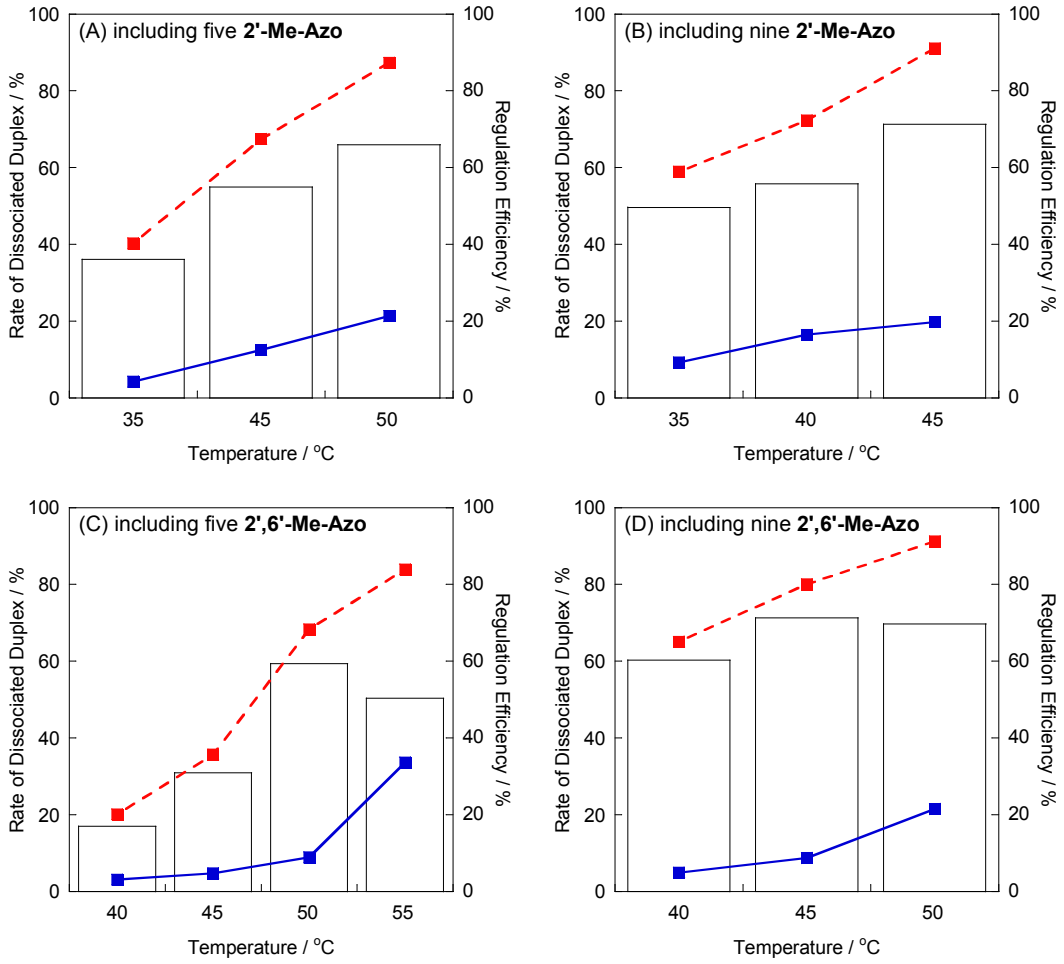

Figure 5-5. Change of the rate of dissociated DNA duplex involving **2′-Me-Azo** moieties or **2′,6′-Me-Azo** moieties: (A) $\mathbf{D_{5Azo}/D_C}$, (B) $\mathbf{D_{9Azo}/D_C}$ (involving **2′-Me-Azo**) (C) $\mathbf{D_{5Azo}/D_C}$ and (D) $\mathbf{D_{9Azo}/D_C}$ (involving **2′,6′-Me-Azo**) induced by visible light (blue square) or UV light (red square) irradiation and photoregulation efficiency (bar graph) at fixed temperatures. Solution conditions: [DNA] = 0.1 μM, [NaCl] = 100 mM, pH 8.0 (10 mM phosphate buffer).

duplex could form well. In contrast, dissociation of DNA duplex did not required the slow change of conditions. Therefore, the rate of dissociated duplex after 5 minutes UV light irradiation was almost corresponded with the result of melting temperature.

On the other hand, in the case of introducing **2′-Me-Azo** or **2′,6′-Me-Azo** moieties, efficient photoregulation at fixed temperature was attained with nine azobenzene moieties (**D_{9MAz_o}/D_C** or **D_{9DMAz_o}/D_C**). Most efficient photoregulation efficiency (75.4 %) was attained with **D_{5Az_o}/D_C** at 50 ^oC, not **D_{9DMAz_o}/D_C**. However, in the case of **D_{9DMAz_o}/D_C**, efficient photoregulation was attained at wide range of temperatures. Interestingly, in the case UV light was irradiated at high temperature, the photoregulation efficiency of **D_{9MAz_o}/D_C** involving **2′-Me-Azo** estimated by T_m curve was efficient than that of **D_{9DMAz_o}/D_C** involving **2′,6′-Me-Azo** (for example at 30 ^oC, the relative fluorescence intensity of **D_{9MAz_o}/D_C** was stronger than that of **D_{9DMAz_o}/D_C**), efficient photoregulation was attained at wide range of temperature with **D_{9DMAz_o}/D_C** (involving **2′,6′-Me-Azo**), not **D_{9MAz_o}/D_C** (involving **2′-Me-Azo**). In the case of **D_{9MAz_o}/D_C** or **D_{9DMAz_o}/D_C**, if the UV light was irradiated at high temperature (over T_m of duplex), the rate of *cis*-**2′,6′-Me-Azo** was lower than that of *cis*-**2′-Me-Azo**, so the rate of dissociated **D_{9MAz_o}/D_C** was larger than that of **D_{9DMAz_o}/D_C**. (It was also applied for introducing five azobenzene moieties.) However, in the case of irradiated under T_m, the

change of condition (photoisomerization of azobenzene) was drastic and the stability of the DNA duplex involving nine azobenzene moieties would have decrease because of its symmetry was low. Therefore, even the rate of *cis*-**2′,6′-Me-Azo** was small, the rate of dissociated duplex would increase because the destabilization effect of *cis*-**2′,6′-Me-Azo** was larger than *cis*-**2′-Me-Azo**. In the case of visible light irradiation under the T_m, the duplex $\mathbf{D_{9MAzo}/D_C}$ or $\mathbf{D_{9DMAzo}/D_C}$ involving nine **2′-Me-Azo** or **2′,6′-Me-Azo** formed well compared with $\mathbf{D_{9Azo}/D_C}$ involving nine **Azo** moieties. As discussed in Chapter 2, *trans*-form of **2′-Me-Azo** or **2′,6′-Me-Azo** can stabilize the DNA duplex more efficiently than that of **Azo**, and the stability effect of *trans*-form of **2′-Me-Azo** or **2′,6′-Me-Azo** almost overcome the destabilization effect caused by introducing nine azobenzene moieties. As a result, $\mathbf{D_{9MAzo}/D_C}$ and $\mathbf{D_{9DMAzo}/D_C}$ formed duplexes as high as 80 % by visible light irradiation and so, efficient photoregulation was attained at wide range of temperature in the case of $\mathbf{D_{9MAzo}/D_C}$ or $\mathbf{D_{9DMAzo}/D_C}$. In contrast, in the case of introducing five **2′-Me-Azo** or **2′,6′-Me-Azo**, the duplex was not dissociated well by UV light irradiation: for example, by introducing **2′,6′-Me-Azo** ($\mathbf{D_{9DMAzo}/D_C}$), only 20 % of duplex dissociated irradiate UV light at 40 ^oC whereas almost 60 % of duplex dissociated at 40 ^oC in the case of UV light irradiated at high temperature. The difference of the rate of dissociated duplex between the irradiation temperatures would

have based on the difference of photoisomerization of azobenzene. In addition, the number of introduced azobenzene moieties was small, so asymmetric diversity of the duplex involving five azobenzene moieties would have been lower than that of involving nine azobenzene moieties. As a result, in the case of $\mathbf{D_{9MAzo}/D_C}$ or $\mathbf{D_{9DMAzo}/D_C}$, the duplex was not dissociated well by UV light irradiation.

In the case of introducing same number of azobenzene moieties into both strand of DNA duplex in order to keep the symmetry, the stability of DNA duplex was increased with visible light irradiation. In addition, by UV light irradiation, the duplex absolutely dissociated.[4]

5-4 Conclusions

(1) Photoregulation of DNA hybridization was directly observed from the change of fluorescence intensity by introducing fluorophore and its quencher at the end of DNA duplex.

(2) By introducing multiple **Azo 2′-Me-Azo** or **2′,6′-Me-Azo** moieties, efficient photoregulation at fixed temperatures was attained. Especially for introducing nine **2′-Me-Azo** or **2′,6′-Me-Azo** moieties, efficient photoregulation was attained at wide range of temperatures.

(3) By introducing nine **Azo** moieties, the stability of duplex irradiated with visible light decreased compared with that of involving five moieties. In addition, in the case of introducing nine **2′-Me-Azo** or **2′,6′-Me-Azo** moieties, the stabilities of duplexes irradiated with visible light was not increased compared with those of involving five moieties although *trans*-azobenzene derivatives stabilize DNA duplex. In the case of azobenzene moieties introduced into only one side of duplex additionally, the symmetry of DNA duplex decreased and the stability of DNA duplex also decreased.

5-5 Experimental sections

5-5-1 Preparation of DNA samples

The DNAs containing azobenzene moieties and Dabcyl (named $\mathbf{D_{5Azo}}$. $\mathbf{D_{9Azo}}$, $\mathbf{D_{5MAzo}}$, $\mathbf{D_{9MAzo}}$, $\mathbf{D_{5DMAzo}}$ and $\mathbf{D_{9DMAzo}}$) were supplied by Tsukuba Oligo services CO., LTD. (Tsukuba, Japan) and purified by RP HPLC. The DNA containing FAM (named D_C) was supplied by Integrated DNA Technologies, Inc. (Coralville, IA. U.S.A.) and purified by RP HPLC.

5-5-2 Fluorescence measurement

The fluorescence of FAM was measured by JASCO FP-6500 fluorescence spectrometer (JASCO, Tokyo, JAPAN) exited 494 nm (3 nm bandwidth). For obtaining T_ms and the rate of dissociated Duplex, the fluorescence intensity at 520 nm was used.

5-5-3 T_m measurement

In order to obtain T_m, the fluorescence intensity of DNA duplex solution at 520 nm was measured as a function of temperature. Because the intensity of FAM itself depends on the temperature, the fluorescence intensity of DNA strand D_C (containing FAM) at 520 nm was also measured as a function of temperature. Dividing the melting curves of DNA duplex by that of single-stranded D_C, relative melting curves of Duplex was obtained. The T_m values were determined from the maximum in the first derivative of the relative melting curve. The temperature ramp was 1.0 ˚C /min. The T_ms shown in Table 5-1 were obtained hearting curves. Solution conditions of the samples: [DNAs] = 0.1 μM, [NaCl] = 100 mM, pH 8.0 (10 mM phosphate buffer).

5-5-4 Photo irradiation

The irradiation was carried out 100 W xenon light source (MAX-301, Asahi Spectra Co., Ltd. Tokyo, Japan) equipped with an influence filter (half-band width 9 nm) centered at 449.5 nm (half bandwidth 9 nm) as visible light irradiation and 150 W xenon light source equipped with a UV-D36C filter (Asahi Tech. Co., Ltd. Tokyo, Japan) was used for UV light (λ = 300-400 nm: 5.3 mW•cm^{-2}) irradiation. For visible light irradiation, 150 W xenon light source and filter was not used because he FAM becomes retrograded by strong visible light. The irradiation time was one minute for visible light irradiation and five minutes for UV light irradiation, respectively. For T_m measurements, the visible light irradiation was carried out at 80 ^{o}C and UV light irradiation was carried out at 75 ^{o}C.

5-5-5 Calculation of the rate of dissociated DNA duplex

The rate of dissociated duplex was calculated from the fluorescence intensity at 520 nm compared with that of formed duplex and closed duplex. The standards fluorescence intensities of formed and dissociated duplex were shown in Appendix Table 5-1. Before calculation, all the fluorescence intensities were divided by those of FAM itself (DNA strand D_C only) at same temperatures to remove the temperature dependency of FAM.

5-6 Notes and References

[1] H. Asanuma, D. Matsunaga, M. Komiyama, *Nucleic Acids Symp Ser.*, **2005**, *49*, 35-36.

[2] S. A. E. Marras, F. R. Kramer, S. Tyagi, *Nucleic Acids Research*, **2002**, *30*, e122.

[3] H. Asanuma, T. Takarada, T. Yoshida, D. Tamaru, X. G. Liang, M. Komiyama, *Angew. Chem., Int. Ed.* **2001**, *40*, 2671-2673.

[4] In the case of introducing of **Azo** or **2′,6′-Me-Azo** into the both DNA strands to place the azobenzene moieties every one base-pairs, clear-cut photoregulation was attained. See X. G. Liang, T. Mochizuki, H. Nishioka, H. Asanuma, *Nucleic Acids Symposium Series*, **2009**, *53*, 189-190. or X. G. Liang, H. Nishioka, T. Mochizuki, H. Asanuma, *J. Mater. Chem.*, **2010**, *20*, 575-581.

5-7 Appendixes

Appendix Table 5-1. Standard of formed and dissociated duplex.

Azobenzene	Duplex	Visible light irradiation		UV light irradiation	
		Formed	Dissociated	Formed	Dissociated
Azo	D_{5Azo}/D_C	Visible light irradiation 20 °C	Visible light 80 °C	Average of UV light and Visible light irradiation 20 °C	UV light 70 °C
	D_{9Azo}/D_C	Visible light 20 °C	Visible light 80 °C	Visible light 20 °C	UV light 70 °C
2′-Me-Azo	D_{5MAzo}/D_C	Visible light irradiation 20 °C	Visible light 80 °C	Average of UV light and Visible light irradiation 20 °C	UV light 70 °C
	D_{9MAzo}/D_C	Visible light 20 °C	Visible light 80 °C	Visible light 20 °C	UV light 70 °C
2′,6′-Me-Azo	D_{5DMAzo}/D_C	Visible light irradiation 20 °C	Visible light 80 °C	Average of UV light and Visible light irradiation 20 °C	UV light 70 °C
	D_{9DMAzo}/D_C	Visible light 20 °C	Visible light 80 °C	Visible light 20 °C	UV light 70 °C

Chapter 6. The DNA nanodevices composed with photo responsive DNA

6-1 Abstract

Nanoscale DNA tweezers operated by photo-irradiation were constructed by using azobenzene-modified DNA as materials. The photoresponsive DNA including non-modified azobenzene moieties (**Azo**) were used as the engines to open and close the tweezers. The tweezers were opened after UV light irradiation, and closed after visible light irradiation. As compared with the DNA-fueled DNA machines, the nanomachines constructed here were "environment-friendly" because no DNA duplex waste was produced. Furthermore, the operation can be repeated many times simply by switching the photo-irradiation without any decrease of the cycling efficiency. In addition, DNA seesaw by using both non-modified azobenzene (**Azo**) and methylthiolated azobenzene (**Thio-DMAzo**) derivatives was also created. Irradiation of 340 nm and 370 nm wavelength light, the part including **Azo** opened (Azo isomerized to *cis*-form) whereas the part including **Azo** closed with 400 nm and 450 nm wavelength light irradiation (**Azo** isomerized *trans*-form). On the other hand, irradiated with 370 nm and 400 nm wavelength light, the part including **Thio-DMAzo** opened (**Thio-DMAzo** isomerizes to

cis-form) whereas the part including **Thio-DMAzo** closed with 340 nm and 450 nm wavelength light irradiation (**Thio-DMAzo** isomerizes to *trans*-form). The regulation was also reversible and can be repeated many times simply by switching the photo-irradiation without any decrease of the cycling efficiency.

6-2 Introduction

Recently, DNA has been considered as not only as biomolecule but also as excellent nanomaterial by focused on its simple hybridization rule, as described in Chapter 1. For example, Yurke *et al.* reported DNA tweezers which can be opened and closed by adding DNA by using DNA hybridization as fuel (Figure 6-1).[1] They also succeeded in repeatedly regulation of open-close of DNA tweezers, however the DNA as fuel added additionally, so the regulation efficiency decreased after several times regulation because extra DNA duplex accumulated as waste products in the system. This drawback would not overcome as long as using DNA as fuel for driving the nanomachine.[2] On the other hand, as described in previous chapters, the DNA hybridization was photoregulated by introducing azobenzene derivatives into DNA via D-threoninol. Photo irradiation does not cause accumulating of by-product, so the dramatically improvement of repeatedly regulation. In the case of using only photo responsive DNA including **Azo**

derivatives which form duplex with visible light irradiation and dissociate duplex with UV light irradiation, photoregulation of DNA hybridization of specific part of DNA nanodevice is difficult. However, by using new type of photo responsive DNA including **Thio-DMAzo** which can form and dissociate duplex with other wavelength light compared with **Azo**, advanced type of DNA nanodevice would expect to be created.

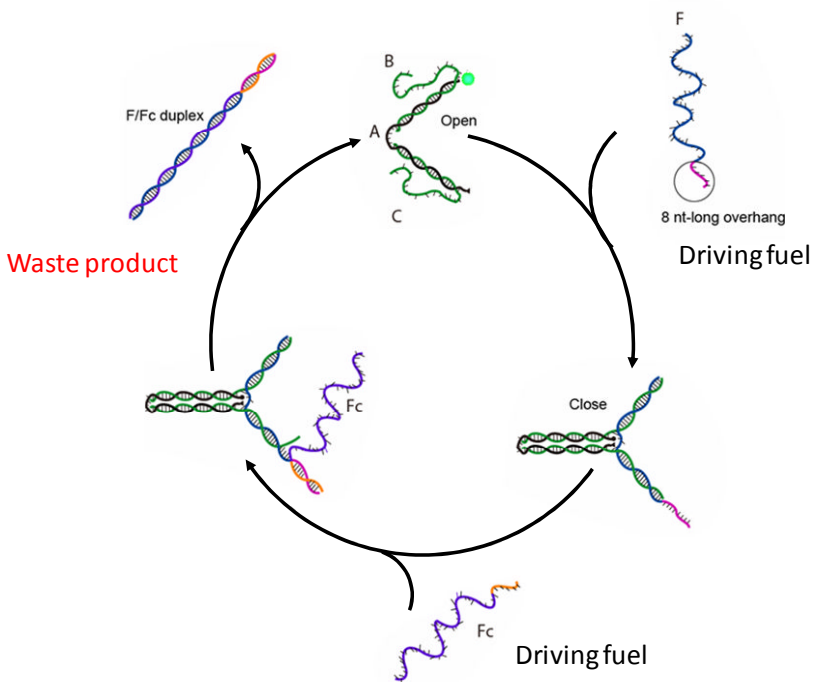

Figure 6-1. Scheme of DNA tweezers driven by DNA as fuel reported by Yurke *et al.* As shown in the upper right, waste product accumulates during successive opening and closing operation.

In this chapter, DNA nanodevice driven by light irradiation including **Azo** moieties and advanced type of photoregulation of DNA hybridization by using both **Azo** and **Thio-DMAzo** moieties were reported.

6-3 Results and Discussions

6-3-1 Photo responsive DNA tweezers

6-3-1-1 Molecular design of DNA tweezers

As shown in Figure 6-2, a photoresponsive DNA nanomachine composed of four strands (**A**, **B**, **C** and **F**) is designed based on the DNA-fueled tweezers reported by Yurke *et al.*[1] The working principle of the original DNA-fueled molecular tweezers is described in Figure 6-1: strand F is added to close the tweezers by partially hybridizing with strand **B** and **C**, leaving an 8 bases overhang. In order to open the closed tweezers, strand **F′** that is completely complementary to strand **F** is added. **F′** first hybridizes with the single-stranded overhang, followed by peeling of strand F from the DNA nanomachine through branch migration. For each operation cycle, **F** and **F′** are added, and **F**/**F′** duplex is produced as a waste. Obviously, more and more **F**/**F′** waste accumulates during successive opening and closing operation. Instead of opening the tweezers by adding strand **F′**, photo responsive DNA strand **F** ($\mathbf{F_{8x}}$ or $\mathbf{F_{12x}}$) that can be dissociated from the strands B and C by UV light irradiation (Figure 6-2). Here, the azobenzene moieties were tethered into DNA via D-threoninol as linker. It can be expected that photoisomerization of the multiple azobenzene moieties (**Azo**) to

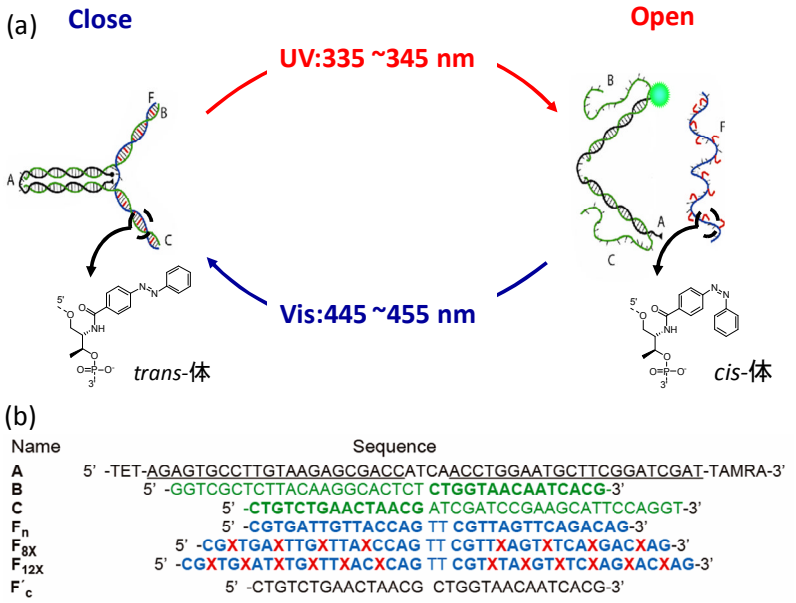

Figure 6-2. Schematic illustration of working principles of DNA nano-tweezers. (a) Photoresponsive tweezers involving non-substituted azobenzenes tethered on D-threoninol; (c) DNA sequences used in this study. Visible light irradiation (*trans*-form) closes the tweezers (left side of (b)), and UV light irradiation (*cis*-form) opens them (right side of (b)). The structures of azobenzene moiety (**X** residue) are also show in (b). Underlined letters in **A** indicate the sections that hybridize with **B** and **C**. Complementary sections between **F** ($\mathbf{F_n}$, $\mathbf{F_{8X}}$, and $\mathbf{F_{12X}}$) and **B**, **C** are shown in bold letters. $\mathbf{F_{8X}}$ and $\mathbf{F_{12X}}$ are the photoresponsive DNAs involving 8 and 12 azobenzene moieties, respectively. $\mathbf{F_n}$ is the native DNA without azobenzenes as the control sequence of $\mathbf{F_{8X}}$ and $\mathbf{F_{12X}}$. $\mathbf{F2_c}$ hybridizes to **F** and forms a duplex with a bulge of two thymidines.

non-planar photoisomerization of the multiple azobenzene moieties (**Azo**) to non-planar *cis*-form decreases greatly its hybridization ability and opens the tweezers (Chapter 5). This photoresponsive **F** can be simply recycled with visible light irradiation and the *cis*- to *trans* isomerization closes the tweezers again. So, the repetitive operation by simply switching the wavelength of the irradiation light can also be expected. For evaluating the efficiency of opening and closing operation through fluorescence resonance energy transfer (FRET), tetrachlorofluorescein (TET, as a fluorophore) and

carboxytetramethylrhodamine (TAMRA, as an acceptor) were attached at 5′- and 3′-end of A, respectively (Figure 6-1).[3] As the efficiency of resonant energy transfer increases abruptly with the decrease of distance between the donor and acceptor, opening and closing of the tweezers can be quantitatively monitored by measuring the fluorescence change of TET (emission at around 540 nm, excited at 514.5 nm).

As described in Chapter 5, an efficient photoregulation of DNA hybridization should be carried out at a temperature between the melting temperature (T_m) of the duplex involving *trans*-azobenzene moieties and that of the duplex involving *cis*-azobenzene moieties. If the temperature is too high, the duplex dissociates in both *trans*- and *cis*-form; if the temperature is too low, the duplex is formed in both cases. Here, the length of the single-stranded overhangs of **B** and **C** (when the tweezers are open) that are complementary to **F** was designed to be 15 bases (the corresponding parts of DNA-fueled "tweezers" reported by Yurke *et al*. are 24 bases), and two extra dTs were inserted in **F** at the middle position to lower the T_m. For efficient photoregulation of the opening and closing of DNA tweezers, as many as eight or twelve azobenzene residues were introduced into a 32 bases strand **F** (designated as $\mathbf{F}_{8x}$ and $\mathbf{F}_{12x}$). The photoresponsive DNA tweezers are expected to be operated at a proper temperature range of 40~60 ^{o}C, which is between the T_m of *cis*-form and *trans*-form. The sequences

in **A** were designed to hybridize with complementary sequences in **B** and **C** to form two 22 base-pairs stiff duplex tweezers that are stable enough at the operation temperature. The four-base single-stranded central region of **A** is used as the hinge of the tweezers.

Table 6-1. Melting temperature (T_m) of the parts of DNA tweezers.

	Tm / °C[a]		
Duplex	*trans*	*cis*	ΔT_m [b]
F_{8X}/F'_C	76.4	57.4	19.0
F_{12X}/F'_C	73.7	49.6	23.1
F_n/F_c	72.7		
A/(B,C)	78.7		

[a] Solution conditions [DNA] = 1.0 μM (or 0.5 μ for **A**/**B**,**C**), [NaCl] = 1.0 M ,pH 6.5 (50 mM Na_2HPO_4). [b] Change in T_m induced by *cis- trans* isomerization.

Firstly, the T_ms of $\mathbf{F_{8X}}$/$\mathbf{F2_c}$, $\mathbf{F_{12X}}$/$\mathbf{F2_c}$, and $\mathbf{F_n}$/$\mathbf{F2_c}$ duplexes (with a bulge of two dTs) were measured to evaluate the ability of $\mathbf{F_{8X}}$ and $\mathbf{F_{12X}}$ to photoregulate DNA hybridization (Table 6-1). Here, $\mathbf{F_{2c}}$ was used instead of the tweezers at opening state to avoid the influence from the hybridization of **A** and **B**, **C**, which has a T_m of 78.0 °C (Table 6-1). In both cases, the duplex involving *trans*-azobenzenes has a higher T_m than that of native duplex $\mathbf{F_n}$/$\mathbf{F_{2c}}$, indicating that introduction of as many as 12 azobenzene moieties did not influence the hybridization ability of the modified DNA.[4] From the difference in T_m between *trans*- and *cis*-form (ΔT_m), it can be concluded that $\mathbf{F_{12X}}$ (ΔT_m = 23.1 °C) has higher photoregulation ability than $\mathbf{F_{8X}}$. Therefore, $\mathbf{F_{12X}}$ was mainly used to construct the photoresponsive DNA tweezers.

6-3-1-2 Photoregulation of DNA Tweezers

The photoresponsive tweezers were prepared by mixing stoichiometric quantities of four strands, **A**, **B**, **C**, and **F** in a buffer (50 mM Na_2HPO_4, pH 6.5, 1.0 M NaCl) to a final concentration of 1.0 μM.[1] As shown in Figure 6-3, the fluorescence of the solution consisting of **A**, **B**, and **C** (in the absence of **F**) was the strongest (red lines, indicating that the tweezers were completely opened. When $\mathbf{F_n}$, the native DNA, was added at a temperature much lower than the T_m of the duplex formed from $\mathbf{F_n}$, **B** and **C**, the fluorescence became much lower (dot lines in Figure 6-3A and B), showing that the tweezers were closed. Here, a new peak at about 580 nm due to the FRET between TET and TAMRA appeared, indicating that the distance between TET and TAMRA became closer.[3] However, the fluorescence spectra did not change much at lower temperatures probably due to the low FRET efficiency between TET and TAMRA even if the tweezers were completely closed (data not shown).

The efficiency for the photoregulation of closing and opening of the tweezers with $\mathbf{F_{12X}}$ was estimated by measuring the change of fluorescence with the light irradiation at thermo-stable conditions. As shown in Figure 6-3B, for example, when the solution

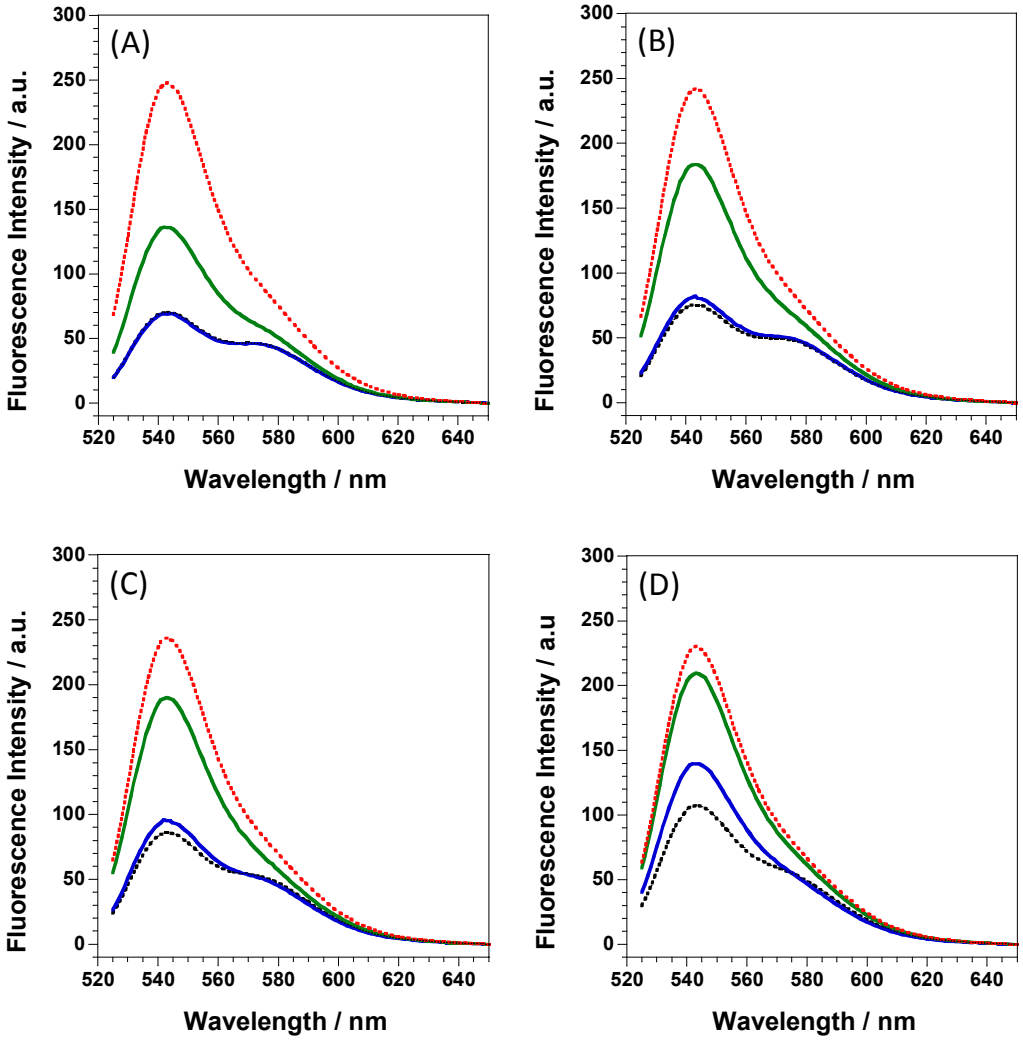

Figure 6-3. Closing and opening of the DNA tweezers involving $\mathbf{F_{12x}}$ with light irradiation at (A) 45 °C, (B) 50 °C, (C) 55 °C and (D) 60 °C, monitored by measuring fluorescence spectra. The tweezers are completely open when only strands A, B and C are present in the solution (red line). Upon the addition of strand $\mathbf{F_n}$, the fluorescence drops and the tweezers prefer to close (black line). The opening and closing are photoregulated to some extent with UV (green lines) and visible light (blue line) irradiation, respectively. Solution conditions [DNA] = 1.0 μM, [NaCl] = 1.0 M ,pH 6.5 (50 mM Na_2HPO_4).

consisting of **A**, **B**, **C** and $\mathbf{F_{12x}}$ was irradiated with visible light (440~460 nm) at 50 °C for 1 minute, the azobenzenes took *trans*-form (>95%), and its fluorescence spectra (blue lines) was very close to that of the solution consisting of **A**, **B**, **C** and $\mathbf{F_n}$ (closed

tweezers). On the other hand, when it was irradiated with UV light (330~350 nm) for 5 minutes, the spectra (green lines) became close to that of the opening tweezers consisting of only **A**, **B**, and **C** (Figure 6-3B). These results indicated that opening and closing of the tweezers were switched simply by light irradiation. Photoswitched opening and closing of the tweezers were also attained at other temperatures, although the photoregulation efficiency depended greatly on the operation temperature. The percentage of opening and closing states was calculated directly from the fluorescence intensity supposing that there is a linear correlation between fluorescence strength and the amount of tweezers of opening state. At 50 ^{o}C and 55 ^{o}C, about 70% of tweezers were opened after UV light irradiation, and more than 80% of tweezers were closed after visible light irradiation. At 45 ^{o}C, only about 40% of tweezers could be opened in the case of *cis*-form; at 60 ^{o}C, however, the tweezers could not close efficiently in the case of visible light irradiation. Accordingly, the most efficient photoregulation could be attained at 50-55 ^{o}C (Table 6-2).

Table 6-2. Contents of opening tweezers in the presence **F**$_{12x}$ after UV or visible light irradiation at various temperatures.

	The rate of the opening tweezers / %[a]		
Temperature / °C	UV	Vis	ΔUV-Vis[b]
45	38.7	2.0	36.6
50	67.0	9.7	57.3
55	73.3	17.6	55.6
60	87.3	45.2	42.1

[a] Solution conditions [DNA] = 1.0 μM (or 0.5 μ for **A**/**B**,**C**), [NaCl] = 1.0 M ,pH 6.5 (50 mM Na_2HPO_4). [b] Difference in contents of opening state between UV and visible light irradiation.

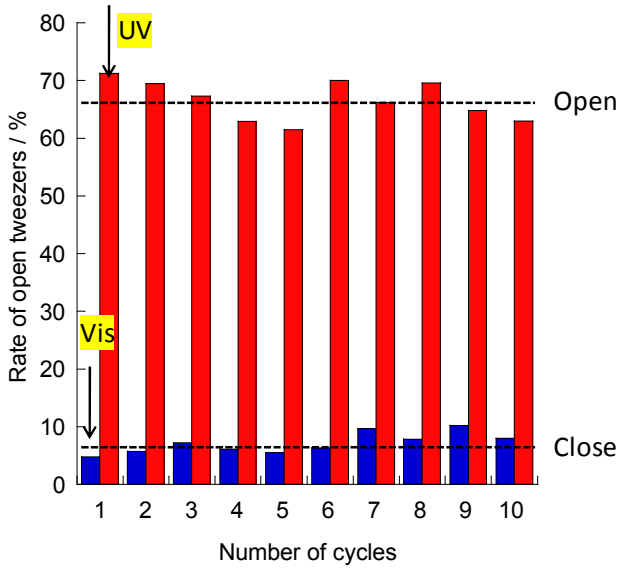

Figure 6-4. Repeated opening and closing of photoresponsive molecular tweezers at 50 °C by alternating irradiation with visible light for 1 min (blue bar) and UV light for 4 min (red bar). About 55% of tweezers were photoswitched to be open and closed in each cycle.

6-3-1-3 Repetitive Opening and Closing of the Photoresponsive DNA Tweezers with Light Irradiation

For the DNA nanomachine, one of the most important functions is whether it can operate successively without losing efficiency. The changes of fluorescence intensity were recorded while the photoresponsive tweezers were cycled ten times between the

opening and closing states by alternating irradiation with UV and visible light at 50 °C. The opening and closing efficiency were calculated from the fluorescence change and shown in Figure 6-4. For every cycle, about 90% of the tweezers were closed after visible light irradiation for 1 min, and about 65% of the tweezers were opened after UV light irradiation for 4 minutes. The cycling efficiency did not decrease at all after opening and closing of the tweezers for ten times. In this way, the photoresponsive tweezers constructed in this study are much better than the original DNA-fueled tweezers, whose cycling efficiency decreased by about 40% after 7 cycles due to the successive addition of DNA fuels and the production of waste duplex.[1] In the case of photo driven DNA tweezers, once the tweezers were constructed, the concentrations of all the DNAs remained stable during the operation because no extra DNAs were added.

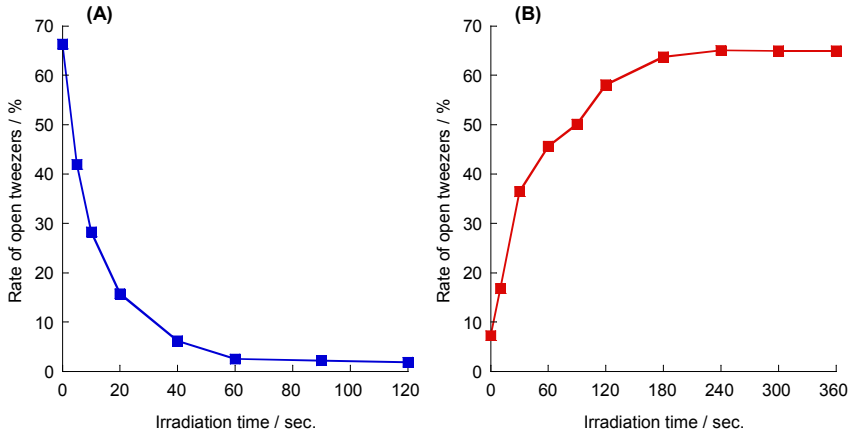

Figure 6-5. Dependences of regulation rates on irradiation times of (A) visible light and (B) UV light at 50 °C.

Therefore, the photoregulation efficiency does not change with the operation cycles as long as the DNAs involved are not destroyed.

Figure 6-5 showed the dependence of photoregulation of DNA tweezers on irradiation times at 50 ^{o}C. In the case of visible light irradiation, more than 90 % of tweezers were closed after one minute light irradiation (Figure 6-5A).On the other hand, in the case of UV light irradiation, after four minutes irradiation, the tweezers reached stationary states; about 65 % of tweezers were opened. The strong stacking interaction between *trans*-azobenzene and base pairs can be considered as one of the reasons for the time-consuming *trans*- to *cis*- photoisomerization.

Although a continuous irradiation with visible light for a long time (e.g. >30 min) was found to destroy the fluorophore TET (data not shown), no detectable decomposition of the introduced azobenzene residues was observed under the light irradiation conditions for photoregulating DNA tweezers. Thus, the opening and closing of photoresponsive tweezers are expected to be photoswitched for lots of cycles without decreasing the working efficiency. In conclusion, an efficient photon-fueled molecular machine that could be repeatedly operated was constructed.

6-3-2. Photo responsive DNA seesaw

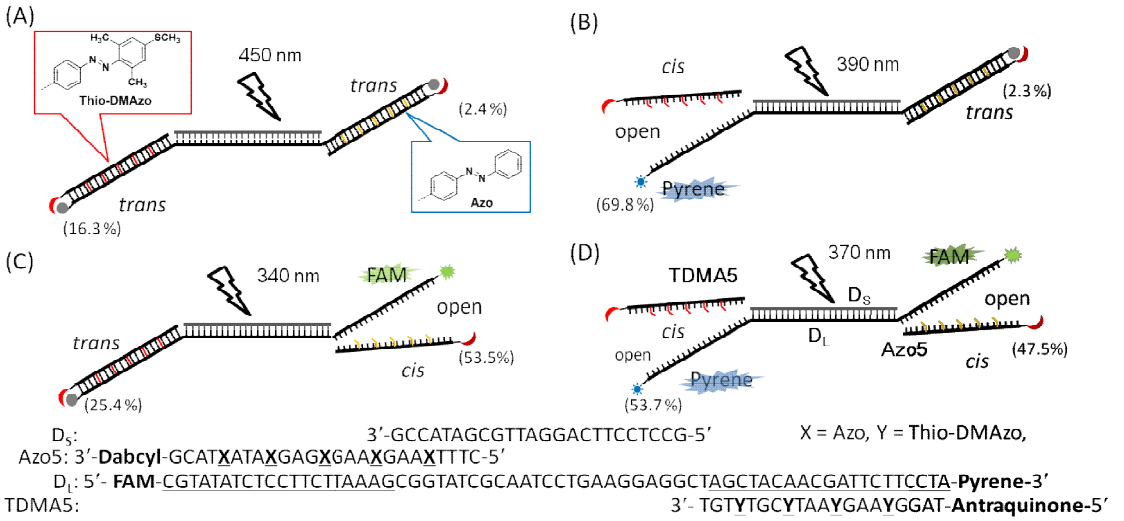

Figure 6-6. Schematic illustration of working principles and the sequences of DNA seesaw. Irradiated with 450 nm, 390 nm, 370 nm or 340 nm wavelength light, each part including **Thio-DMAzo** or **Azo,** the seesaw can be regulated independently. The form of **Thio-DMAzo** and **Azo** and the rates of open duplex calculated from the intensity of fluorescence (Figure 6-7) were also shown in each figure.

6-3-2-1 Molecular design of DNA seesaw

As described in Chapter 4, photoregulation of DNA hybridization with visible light by using methylthiolated azobenzene (**Thio-DMAzo**). In addition, **Thio-DMAzo** isomerizes to *cis*-form irradiated with 370 nm wavelength light which can isomerize **Azo** to *cis*-form and isomerize to *trans*-form irradiated 340 nm wavelength light which can isomerize isomerizes **Azo** to *cis*-form (Table 4-1 and 4-2 in Chapter 4). Therefore, by using **Thio-DMAzo** together with **Azo**, advanced type DNA nanomachine would be

expected to be created. Here, for demonstrating the possibility of advanced type of photo responsive DNA nanomachine, independently photoregulation of DNA duplex involving **Azo** or **Thio-DMAzo** was performed. Figure 6-6 showed the working principle and the sequences of DNA seesaw. **Azo** and **Thio-DMAzo** isomerize *trans*- and *cis*-form by several wavelength light like as follows: 1) with 450 nm light, both **Azo** and **Thio-DMAzo** isomerize to *trans*-form, 2) with 390 nm (or 400 nm) light, **Azo** isomerizes to *trans*-form whereas **Thio-DMAzo** isomerizes *cis*-form,[5] 3) with 370 nm light, both **Azo** and **Thio-DMAzo** isomerize to *cis*-form, and 4) with 340 nm light, **Azo** isomerizes to *cis*-form whereas **Thio-DMAzo** isomerizes to *trans*-form. Therefore, by selecting the irradiation light wavelength, arbitral regulation of DNA hybridization including either **Azo** or **Thio-DMAzo** would be expected as shown in Figure 6-6. In order to monitor the photoregulation of formation and dissociation of DNA duplex, fluorescence-quencher system was also used. At the 3′ end of $\mathbf{D_L}$, pyrene was attached and at the 5′ end of $\mathbf{D_L}$, FAM was attached as fluorophore. On the other hand, at the 3′ end of **Azo5** involving five **Azo** moieties, which could form duplex with 20 bases of 5′ end of $\mathbf{D_L}$, Dabcyl was attached as a quencher of FAM[3] and at the 5′ end of **TDMA5** involving five **Thio-DMAzo** moieties, which could form duplex with twenty bases of 3′ end of $\mathbf{D_L}$, antraquinone was attached as a quencher of pyrene.[6] The DNA strand $\mathbf{D_S}$

acts as spacer in order not to influence FAM and pyrene each others. Because of this design, the formation and dissociation of DNA duplex **D_L/Azo5** and **D_L/TDMA5** induced by isomerization of azobenzene moieties could be observed by the change of fluorescence intensities of FAM and pyrene.

Table 6-3. Melting temperature (T_m) of the each part of DNA seesaw.

	T_m / °C[a]		
duplex	*trans*	*cis*	ΔT_m[b]
D_L/Azo5	61.3	48.4[b]	12.9
D_L/TDMA5	59.8	~40[c]	~20

[a] Solution conditions: [**D_L**] = 0.07 μM, [**D_S**, **Azo5**, **TDMA5**] = 0.2 μM, [NaCl] = 100 mM, pH 8.0 (10 mM phosphate buffer). [b]Change in T_m induced by *cis-trans* isomerization. [c]340 nm light was irradiated for 10 minutes at 70 °C. [d] 390 nm light was irradiated for 10 minutes at 70 °C.

6-3-2-2 Photoregulation of DNA seesaw

As like as DNA tweezers, because the DNA seesaw also based on the DNA hybridization, the regulation should be carried out at a temperature between the melting temperature (T_m) of the duplex involving *trans*-azobenzene moieties and that of the duplex involving *cis*-azobenzene moieties. Table 6-3 showed the T_m of DNA duplex **D_L/Azo5** and **D_L/TDMA5** either azobenzene moieties took *trans*- or *cis*-form. In the case of **Azo** or **Thio-DMAzo** took *trans*-form, the T_m of duplexes were almost 60 °C. On the other hand, the T_ms of duplex in the case **Azo** moieties took *cis*-form were almost 48 °C whereas that of including **Thio-DMAzo** moieties was 40 °C. One of *cis*-**Thio-DMAzo** destabilized DNA duplex efficiently compared with *cis*-**Azo**, these

results were reasonable. From the results of T_m, DNA seesaw would be expected to be carried out form 45~55 °C for the efficient photoregulation. As the photoregulation of the seesaw carried out at 45 °C 50 °C and 55 °C, the most effective regulation was archived at 50 °C (Appendix Table 6-1).

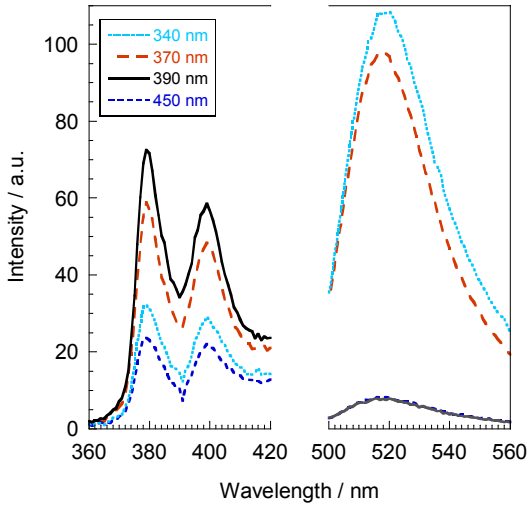

Figure 6-7. Change of fluorescence intensity of FAM (500- 560 nm) and pyrene (360- 420 nm) with light irradiation at 50 °C. The percentages of dissociated duplex calculated from these spectra were shown in Figure 6-6. Solution conditions: [$\mathbf{D_L}$] = 0.07 μM, [$\mathbf{D_S}$, **Azo5**, **TDMA5**] = 0.2 μM, [NaCl] = 100 mM, pH 8.0 (10 mM phosphate buffer). Each light irradiated for 15 minutes.

The change of fluorescence intensity at 50 °C was shown in Figure 6-7. As be expected, $\mathbf{D_L}$/**Azo5** part including **Azo** closed by irradiation of 390 nm and 450nm light (fluorescence intensity decreased), whereas it opened by irradiation of 340 nm or 370 nm light (fluorescence intensity increased). In addition, $\mathbf{D_L}$/**TDMA5** parts including **Thio-DMAzo** also showed expected results; irradiated by 340 nm or 450 nm light, the duplex formed (fluorescence intensity decreased) whereas the duplex dissociated by

irradiation of 370 nm or 390 nm light (fluorescence intensity increased). The rates of dissociated DNA duplex calculated from the fluorescence intensity were shown in Figure 6-6.[7] As shown in Figure 6-6, arbitrary regulations of DNA seesaw was archived by selecting the wavelength of irradiation light: 1) irradiated with 340 nm wavelength light, $\mathbf{D_L}$/**Azo5** opened and $\mathbf{D_L}$/**TDMA5** closed, 2) with 370 nm wavelength light, both $\mathbf{D_L}$/**Azo5** and $\mathbf{D_L}$/**TDMA5** opened, 3) with 390 nm light $\mathbf{D_L}$/**Azo5** closed and $\mathbf{D_L}$/**TDMA5** opened and 4) with 450 nm light, both $\mathbf{D_L}$/**Azo5** and $\mathbf{D_L}$/**TDMA5** closed.

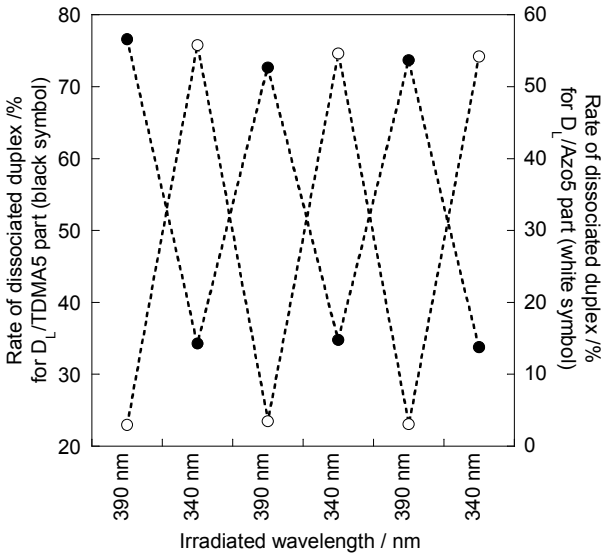

Figure 6-8. Symmetrically regulation of DNA seesaw irradiated by 340 nm and 390 nm light irradiation at 50 °C. Black symbol showed $\mathbf{D_L}$/**TDMA5** part and white symbol showed the $\mathbf{D_L}$/**Azo5** parts. Solution conditions: [$\mathbf{D_L}$] = 0.07 μM, [$\mathbf{D_S}$, **Azo5**, **TDMA5**] = 0.2 μM, [NaCl] = 100 mM, pH 8.0 (10 mM phosphate buffer). Each light irradiated for 10 minutes.

The repetitive regulation of DNA seesaw was also tried by irradiation of 340 nm and 390 nm wavelength light. Irradiation of theses wavelengths light, open and close of

each parts of DNA seesaw was regulated independently (Figure 6-8). In addition, this result indicated that DNA seesaw could regulate for several time without decrease of working efficiency.

As shown in Figure 6-6 or Figure 6-7, **D_L/TDMA5** part including *trans*-**Thio-DMAzo** was still open (irradiated with 340 nm or 450 nm light) compared with **D_L/Azo5** part including *trans*-**Azo**. This may be depending on the difference of T_m between **D_L/Azo5** and **D_L/TDMA5** (Table 6-3). Therefore, by designing the DNA sequence or the number of introducing azobenzene moieties, this problem would be solved.

6-4 Conclusions

(1) By using photo responsive DNA including **Azo** moieties, DNA tweezers driven by visible and UV light irradiation was created.

(2) About 55 % of DNA tweezers was regulated by light irradiation at 50 ^oC. In addition, between 45 ~ 60 ^oC, DNA tweezers could be regulated by light irradiation.

(3) The formation and dissociation of DNA duplexes involving **Azo** or **Thio-DMAzo** moieties can be regulated independently by selecting the irradiation light

in DNA seesaw. Advanced typed DNA nanomachine will be expected to be created.

(4) The working efficiencies both the photo responsive DNA tweezers and DNA seesaws did not decrease after several times regulation because light irradiation was not cause pollution in the system.

6-5 Experimental section

6-5-1 DNA tweezers

Materials The azobenzene-containing oligonucleotides were supplied by Tsukuba Oligo services Service Co., Ltd. (Tsukuba, Japan), and purified by R.P. HPLC. The oligonucleotides containing only native bases (strands **B**, **C**, and $\mathbf{F_n}$) and strand **A** modified with TET and TAMRA were supplied by Integrated DNA Technologies, Inc. (Coralville, USA). Oligonucleotides **B**, **C**, and $\mathbf{F_n}$ were used directly after desalting. Oligonucleotide **A** was purified by RP HPLC. Stock solutions of 25 μM in TE buffer (10 mm Tris pH 8.0, 1.0 mm EDTA) were prepared.

6-5-1-1 Fluorescence measurement

The photoresponsive tweezers were prepared by mixing stoichiometric quantities of four strands **A**, **B**, **C**, and **F** in SPSC buffer (50 mm Na_2HPO_4 pH 6.5, 1.0 M NaCl) to a final concentration of 1.0μM. The fluorescence spectra of TET were measured with a JASCO FP-6500 fluorescence spectrometer (JASCO, Tokyo, Japan) excited at 514.5 nm (3 nm bandwidth). For calculating the rate of opened tweezers, the fluorescence

intensity emitted at 543 nm was used. The intensity of TET was depending on the temperature, the data was divide by the intensity of strand **A** at same temperature for obtaining relative fluorescence intensity.

6-5-1-2 Photoirradiation

The irradiation was carried out with a xenon light source (MAX-301, Asahi Spectra Co., Ltd. Tokyo, Japan) equipped with an interference filter (half bandwidth 9 nm) centered at 341.5 nm for UV light irradiation and an interference filter (half bandwidth 9 nm) centered at 449.5 nm for visible light irradiation (90 $mWcm^2$). During irradiation, the cell containing the tweezers was put in a water bath to maintain a fixed temperature (± 2 ^oC). After irradiation, the cell was immediately moved into the fluorescence spectrometer that was kept at the same temperature to measure fluorescence. During the fluorescence measurements, further UV or visible light irradiation was not carried out.

6-5-1-3 T_m measurements

T_m values were determined from the maximum in the first derivative of the melting curve, which was obtained by measuring the absorbance at 260 nm with a JASCO V-530 UV-Vis spectrophotometer as a function of temperature. The temperature ramp was 1.0 °C/min. Both the heating and cooling curves were measured, and obtained T_m values agreed within 2.0 °C.

6-5-2 DNA seesaw

Materials: The DNA strand D_L including FAM and pyrene was prepared by ligated two DNA strand (**D_{FAM}** and **D_{pyrene}** in Figure 6-9). **D_{FAM}** was supplied by Integrated DNA Technologies, Inc. (Coralville, USA). **D_{pyrene}** including pyrene was synthesized on an automated DNA synthesizer (ABI-3400, Applied Biosystems) using conventional and pyrene-carrying phosphoramidite monomers. The DNA containing only native bases (**D_S** and **D_B** using for ligation) was supplied by Integrated DNA Technologies, Inc. (Coralville, IA. U.S.A.). The DNA containing **Azo** (DAzo5) was supplied by Tsukuba Oligo services CO., LTD. (Tsukuba, Japan), and purified by RP HPLC. The modified DNA containing **Thio-DMAzo** (**TDMA5**) was synthesized on an automated DNA synthesizer (ABI-3400, Applied Biosystems) using conventional and azobenzene-carrying phosphoramidite monomers and purified by RP HPLC.

MALDI-TOFMS for **TDMA5** with **Thio-DMAzo**: obsd. 8838 (calcd. for protonated form: 8841).

6-5-2-1 Synthesis of DNA strand D_L including FAM and pyrene

Because the DNA strand D_L including both FAM and pyrene was composed of 65 bases, it was impossible to synthesize all the D_L on automated DNA synthesize in one time. Therefore, D_L was prepared by ligatied two DNA strand as follows.

The phosphorylated of 5′-end of D_{pyrene} was performed as follows: 2.3×10^{-9} mol of D_L, 1 μ of T4PNK (NEB, Ipswich, Massachusetts, U.S.A) and 5 μl of ×10 Ligation buffer ( ) were putted in micro tube and satirized water was added until the total volume

became 50 μl. The mixture kept at 37 ^{o}C for 2 hours. After the reaction, the mixture kept at 75 ^{o}C for 10 minutes to deactivate the T4PNK. After that, the solution was used for ligation without further purification.

The ligation of D_{FAM} and D_{pyrene} was performed as follows: 2.3×10^{-9} mol of D_{FAM}, 3.45×10^{-9} mol of D_B was added to previous solution including D_{pyrene} and satirized water was also added until the total volume became 80 μl. The mixture kept at 90 ^{o}C for 5minutes, then cooled down for 37 ^{o}C slowly. In that mixture, 8 μl of T4 ligase (Invitrogen, Carlsbad, CA, U.S.A.), 8 μl of ×10 Ligation buffer and satirized was added until the total volume became 160 μl. The solution was kept 16 ^{o}C overnight.

The purification of D_L was performed as follows: In previous solution, 160 μl of phenol was added. Then the mixture was vortexed and separated by centrifugalization. The upper potion was corrected and 200 μl of chloroform was added. The mixture was vortexed and separated by centrifugalization, and the upper potion was corrected. Then, the solution was subjected to G-25 DNA Grade NAP column (GE Healthcare, Buckinghomshire, U.K.) and the filtrate was corrected. Finally, the solution was purified by R.P. HPLC.

6-5-2-2 Fluorescence measurement

Fluorescence spectra of FAM and pyrene were measured with a JASCO FP-6500 fluorescence spectrophotometer (JASCO, Tokyo, Japan). FAM was excited at 494 nm (bandwidth 3 mm) and the pyrene was exited at 345 nm (bandwidth 5 mm). The detected bandwidth was 3 nm and 5 nm, respectively. The photoisomerization was carried out for 15 minutes or 10 minute. Conditions of the sample Solution: $[\mathbf{D_L}] = 0.07$

μM, [$\mathbf{D_S}$, **Azo5**, **TDMA5**] = 0.2 μM, [NaCl] = 100 mM, pH 8.0 (10 mM phosphate buffer).

6-5-2-3 Photoisomerization of azobenzene

A xenon light source (MAX-301, Asahi Spectra Co.,Ltd. Tokyo, Japan) equipped with an interference filter was used for photoisomerization. The properties of interference filters were follows: 340 nm: (half bandwidth 9 nm) centered at 340.5 nm, 370 nm: (half bandwidth 12 nm) entered at 369.0 nm, 390 nm: (half bandwidth 10 nm) cantered at 390.0 nm, 400 nm: (half bandwidth 11 nm) entered at 398.5 nm, 450 nm: (half bandwidth 9 nm) centered at 449.5 nm.

6-5-2-4 T_m measurement

In order to obtain T_m, the fluorescence the fluorescence intensities at 520 nm (FAM, $\mathbf{D_L}$/**Azo5)** and 380 nm (pyrene, $\mathbf{D_L}$/**TDMA5**) were measured as a function of temperature. Because the intensity of FAM and pyrene itself depends on the temperature, the fluorescence intensities of DNA strand $\mathbf{D_L}$ (containing FAM and pyrene) at 520 nm and 380 nm were also measured as a function of temperature. Dividing the melting curves of DNA duplex by that of single-stranded D_C, relative melting curves of Duplex was obtained. The T_m values were determined from the maximum in the first derivative of the relative melting curve. The temperature ramp was 1.0 ˚C /min. The T_ms were obtained from cooling curves because *cis*-azobenzene thermally isomerized. *trans*-**Az**o and **Thio-DMAzo** were obtained by irradiation of 450 nm wavelength light for 10 minutes and keep the sample at high temperature for long time. *cis*-**Azo** was obtained by irradiating 340 nm light for 10 minutes at 70 ^oC and *cis*-**Thio-DMAzo** was obtained by

irradiating 400 nm light for 10 minutes at 70 ^{o}C.

6-5-2-5 Calculation of the rate of dissociated duplex

The rate of dissociated duplex was calculated from the fluorescence intensities at 520 nm (FAM, **D_L/Azo5)** and 380 nm (pyrene, **D_L/TDMA5**). The spectra at 80 ^{o}C and 20 ^{o}C of *trans*-azobenzene were used as standards of open and close states, respectively. The fluorescence intensity of both FAM and pyrene depends on temperature change, all the fluoresce intensities was divided by the fluorescence data at that temperature without quenchers. Azobenzenes, especially for **Azo**, was photoisomerized by excitation or fluorescence light, fixed wavelength measurement was carried out for symmetrically regulation of DNA seesaw. The result contained about 5 % error.

6-6 Notes and References

[1] B. Yurke, A. J. Turberfield, A. P. Mills Jr, F. C. Simmel, J. L. Neumann, *Nature*, **2000**, *406*, 605-608.

[2] Some group tried to remove the waste DNA duplex by modified the DNA with biotin. However, biotin labeling of DNA and regulation requires cumbersome handling. H. Yan, X. Zhiyong, Z. Shen, N. C. Seeman, *Nature*, **2002**, *415*, 62-65.

[3] S. A. E. Marras, F. R. Kramer, S. Tyagi, *Nucleic Acids Research*, **2002**, *30*, e122.

[4] As described in Chapter 5, introducing too many azobenzene moieties destabilize DNA duplex.

[5] Because **Thio-DMAzo** isomerizes to *cis*-form well irradiated by 390 nm wavelength light compared with by 400 nm, 390 nm light was used for regulation.

[6] H. Kashida, T. Takatsu, T. Fujii, K. Sekiguchi, X. G. Liang, K. Niwa, T. Takase, Y. Yoshida, H. Asanuma, *Angew. Chem. Int. Ed.*, **2009**, **48**, 7044 –7047.

[7] Note that because irradiation of light for ten minutes was not enough for isomerized azobenzene moieties to photo stationary states, the rate of dissociated duplex was depend on previous states. The detail data was shown in Appendix Table 6-2 and 6-3.

6-7 Appendixes

Appendix Table 6-1. Dependence of regulation efficiency of DNA seesaws on temperatures.

	The rate of dissociated DNA duplex / %[a]							
	450 nm[b]		400 nm[b]		370 nm[b]		340 nm[b]	
	D_L/Azo5	D_L/TDMA5	D_L/Azo5	D_L/TDMA5	D_L/Azo5	D_L/TDMA5	D_L/Azo5	D_L/TDMA5
45 °C	0.41	15.9	0.28	48.5	8.2	41.2	8.5	21.6
50 °C	1.5	30.1	1.1	79.4	39.5	70.6	66.8	38.0
55 °C	9.2	54.8	6.9	95.6	87.2	89.7	91.0	70.9

[a]The rate of dissociated DNA duplex was calculated from the intensity of pyrene measured by wave length scanning measurement. Solution conditions: [**D_L**] = 0.07 μM, [**D_S**, **Azo5**, **TDMA5**] = 0.2 μM, [NaCl] = 100 mM, pH 8.0 (10 mM phosphate buffer). [b]Each wavelength of light irradiated for 10 minutes. Note that the sample was different with other measurements (Appendix Table 6-2, Figure 6-7 or 6-8).

Appendix Table 6-2. Dependence of regulation efficiency of DNA seesaw on previous states at 50 °C: the **D_L/TDMA5** part including **Thio-DMAzo** moieties.

	The rate of dissociated DNA duplex / % [a]			
Previous State	450 nm[b]	390 nm[b]	370 nm[b]	340 nm[b]
A)		74.6	61.0	27.9
B)	18.9		58.5	26.6
C)	19.4	70.0		25.0
D)	18.2	74.8	54.0	

[a]The rate of dissociated DNA duplex was calculated from the intensity of pyrene measured by fixed wavelength measurement. Solution conditions: [**D_L**] = 0.07 μM, [**D_S**, **Azo5**, **TDMA5**] = 0.2 μM, [NaCl] = 100 mM, pH 8.0 (10 mM phosphate buffer). [b]Each wavelength of light irradiated for 10 minutes.

Appendix Table 6-3. Dependence of regulation efficiency of DNA seesaw on previous states at 50 °C: the **D_L**/**Azo5** part including **Azo** moieties.

	The rate of dissociated DNA duplex / % [a]			
Previous State	450 nm[b]	390 nm[b]	370 nm[b]	340 nm[b]
A)		2.2	46.8	58.3
B)	1.9		30.9	55.1
C)	1.6	4.2		54.7
D)	1.9	2.5	42.3	

[a]The rate of dissociated DNA duplex was calculated from the intensity of FAM measured by fixed wavelength measurement. Solution conditions: [**D_L**] = 0.07 μM, [**D_S**, **Azo5**, **TDMA5**] = 0.2 μM, [NaCl] = 100 mM, pH 8.0 (10 mM phosphate buffer). [b]Each wavelength of light irradiated for 10 minutes.

List of Publications

1. "Construction of photoresponsive RNA for photoswitching RNA hybridization."
   H. Ito, X.G. Liang, H.Nishioka, H. Asanuma
   Org. Biomol. Chem., **2010**, *8*, 5519-5524.

2. "Effect of the ortho modification of azobenzene on the photoregulatory efficiency of DNA hybridization and thermal stability of its cis-form."
   H. Nishioka, X.G. Liang, H. Asanuma
   Chem. Eur. J., **2010**, *16*, 2054-2062.

3. "An interstrand-wedged duplex composed of alternating DNA base pairs and covalently attached intercalators."
   X.G. Liang, H. Nishioka, T. Mochizuki, H.Asanuma
   J. Mater. Chem., **2010**, *20*, 575-581.

4. "Construction of Photon-Fueled DNA Nanomachines by Tethering Azobenzenes as Engines."
   X.G. Liang, H. Nishioka, N. Takenaka, H. Asanuma
   LNCS **2009**, *5347*, 21-32.

5. "Photoisomerization dynamics study on cis-azobenzene derivative using ultraviolet-to-visible tunable femtosecond pulses."
   N. Yamaguchi,; N. Nagasawa,; K. Igarashi, T.Sekikawa,; H. Nishioka, H. Asanuma, M. Yamashita
   Appl. Surf. Sci. **2009**, *255*, 9864-9868.

6. "Line up base pairs and intercalators one by one in a stable duplex."
   X. G. Liang, T. Mochizuki; H. Nishioka; H. Asanuma,
   Nucleic Acids Symp. Ser. **2009**, *53*, 189-190.

7. "A DNA Nanomachine Powered by Light Irradiation."
   H. Nishioka, X.G. Liang, N. Takenaka, H. Asanuma
   ChemBioChem, **2008**, *9*, 702-705.

8. "Molecular Design for Reversing the Photoswitching Mode of Turning ON and OFF DNA Hybridization"

X.G. Liang,; N. Takenaka, H. Nishioka, H. Asanuma,
Chem. Asian J., **2008**, *3*, 553-560.

9. "Light driven open/close operation of an azobenzene-modified DNA nano-pincette."
X.G. Liang, N. Takenaka, H. Nishioka, H. Asanuma
Nucleic Acids Symp. Ser. **2008**, *52*, 697-698.

10. "2',6'-Dimethylazobenzene as an efficient and thermo-stable photoregulator for the photoregulation of DNA hybridization."
H. Nishioka, X. G. Liang, H.Kashida, H. Asanuma,
Chem. Commun., **2007**, 4353-4356.

11. "Synthesis of Azobenzene-Tethered DNA for Reversible Photo-Regulation of DNA."
H. Asanuma,; X.G. Liang, H. Nishioka, D. Matsunaga, M. Z. Liu, and M. Komiyama
Nat. Protoc. **2007**, *2*, 203-212.

12. "Photoregulation of DNA hybridization by introducing an azobenzene: Molecular design for more stabilization of DNA duplex with cis-azobenzene than with its trans-form."
X. G. Liang, N. Takenaka, H. Nishioka, H. Asanuma
Nucleic Acids Symp. Ser. **2007**, *51*, 169-170.

13. "Development of photoresponsive RNA towards photoswitching of RNA functions."
H. Ito, H.Nishioka, X. G. Liang, H. Asanuma
Nucleic Acids Symp. Ser. **2007**, *51*, 171-172.

14. "Incorporation of Methyl Group on Azobenzene for the Effective Photo-Regulation of Hybridization and Suppression of Thermal Isomerization."
H. Nishioka, H. Kashida, M. Komiyama, X. G. Liang, H. Asanuma,
Nucleic Acids Symp. Ser. **2006**, *50*, 85-86.

List of Oral Presentations

1) Molecular design of azobenzene derivatives for reversible photoregulation of DNA functions with visible light
Hidenori Nishioka, Xingguo Liang, Hiroyuki Asanuma
59th Symposium on Macromolecules, *Sapporo, Japan*, September, 2010.

2) Improvement of thermal stability of *cis*-azobenzene by methylation at *ortho* positions and its mechanism
Hidenori Nishioka, Xingguo Liang, Hiroyuki Asanuma
The 90th Annual Meeting of Chemical Society of Japan, *Osaka, Japan*, March, 2010

3) Efficient Photo-Regulation of DNA Hybridization for Constructing Light-driven Nano Device
H. Nishioka, Xingguo Liang, Hiroyuki Asanuma,
Nagoya University Global COE in Chemistry Annual Symposium, Nagoya, Japan, June, 2009

Acknowledgment

The present article is a thesis for application of doctoral degree at the Department of Molecular Design and Engineering, Graduate School of Engineering, Nagoya University. All the study work was carried out under direction of Professor Hiroyuki Asanuma from April 2005 to March 2011.

I would like to express my deep appreciation and respect to Professor Hiroyuki Asanuma for his advice and guidance through this work. I also especially thank Associate Professor Xingguo Liang for his advice and valuable discussions to lead this research. Moreover, I would like to express thank to Assistant Professor Hiromu Kashida for his advice for this study. In addition, I would like to say thanks for co-worker Mr. Zhou Mengguang, Mr, Ryuji Wakuda Mr. Hiroshi Ito, Mr. Nobutaka Takenaka, Mr. Kenta Fujioka, Mr. Toshio Mochizuki, Mr. Teruchika Ishikawa and other members of Asanuma Laboratory for their contribution and advice for this study.

On accomplishing this thesis, Professor Takahiro Seki and Professor Kentarou Tanaka have given many helpful comments and suggestions. I would like to express my sincere thanks to them.

I am also greatly indebted to “Japan Society for Promotion of Science” for their financial support to me.

Finally, I would like to express my gratitude my family for there supports over both sides of discretion.